Book of Abstracts

Podium Session I

Friday, May 22nd, 12:15 – 1:30 PM

RELATIONSHIPS OF STRENGTH AND BALANCE TO TIBIAL LOAD DURING RUNNING IN HEALTHY PARTICIPANTS

Peach, MA, Rosario, L, and Becker, J
Department of Food Systems, Nutrition and Kinesiology
Montana State University, Bozeman, MT USA
Email: meganpeach406@gmail.com web: https://www.montana.edu/biomechanics/

INTRODUCTION

Tibial bone load has been implicated in the development of tibial bone stress injury.[1] However, estimating bone load in a clinical setting is challenging; therefore, surrogate measures of tibial bone load are necessary to identify runners who may be at risk for tibial bone stress injury. The purpose of this study was to investigate relationships between strength and balance assessments and tibial bone load during running in healthy participants.

METHODS

Forty-three recreational runners (22 F, 21 M, 23.80 ± 4.27 years, BMI 22.88 ± 2.70, 30.38 ± 19.36 km/week) ran at a self-selected pace on an instrumented treadmill for five minutes while kinematic and kinetic data were collected via motion capture. Following the run, clinical measures of ankle strength, assessed via hand-held dynamometry (HHD), single leg heel raise (SLHR) endurance, and dynamic balance, assessed via Y-balance test (YBAL), were performed.

Ankle joint angles, reaction forces, and moments were used as inputs to a musculoskeletal model which calculated tibial axial force as the sum of Achilles tendon and vertical ankle joint reaction forces. Additional tibial load variables included tibial force instantaneous loading rate (ILR), impulse, and cumulative load over one kilometer. Multiple linear regression was used to identify predictors of tibial load variables for the dominant limb from independent variables for strength, endurance, and dynamic balance.

RESULTS AND DISCUSSION

Descriptors of clinical measures are illustrated in Figure 1 while tibial load outcome variables' means and standard deviations are listed in Table 1. A model containing HHD-plantarflexion, HHD-dorsiflexion, SLHR, and YBAL was not predictive of tibial axial force ($F = 1.32$, $p = 0.28$, $R^2 = 0.03$), tibial ILR ($F = 1.32$, $p = 0.28$, $R^2 = 0.03$), impulse ($F = 0.67$, $p = 0.61$, $R^2 = 0.03$) nor cumulative load ($F = 1.04$, $p = 0.40$, $R^2 = 0.01$).

Table 1: Mean ± SD of Tibial Load Variables

Tibial axial force (BW)	8.40 ± 1.63
Tibial force ILR (BW/s)	109.61 ± 29.41
Tibial force impulse (BW/s)	1.17 ± 0.23
Tibial force cumulative load (BW/km)	1142.35 ± 285.97

Results suggest that clinical measures of strength, endurance, or dynamic balance should not be used to estimate tibial bone load. Tibial load during running may be influenced by additional factors such as gait mechanics and/or biomechanical modeling technique.

CONCLUSIONS

Clinical measures of strength, endurance, and dynamic balance are not predictors of tibial force variables during running in healthy recreational runners. Whether or not these variables distinguish between runners with and without tibial bone stress injury requires further investigation.

REFERENCES

1. Meardon MA, et al. *Clin Biomech* **30**, 895-902, 2015.

ACKNOWLEDGEMENTS

This study was funded by the National Center for Advancing Translational Sciences of the National Institutes of Health under award number 5TL1TR002318-09

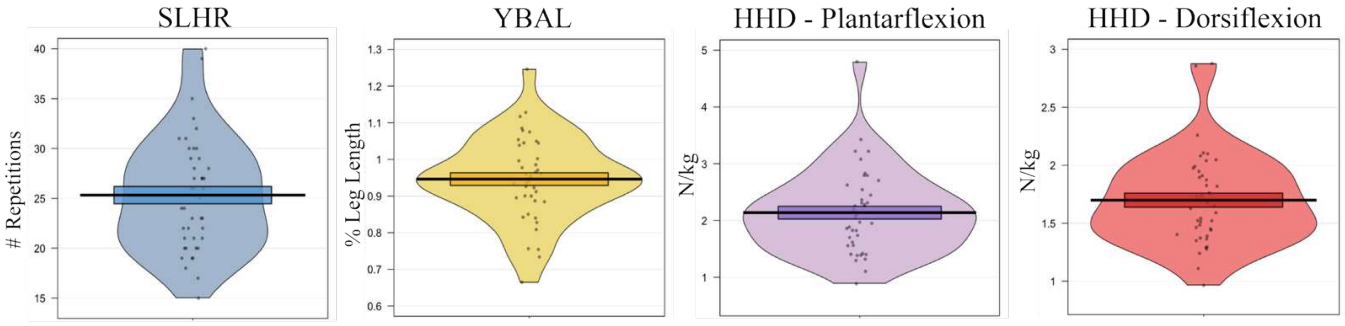

Figure 1: Pirate plots for independent variables illustrating individual data points and density distribution, mean and 95% CI band.

ECCENTRIC PLANTAR FLEXOR EXERCISE INDUCES REGION-DEPENDENT CHANGES IN ACHILLES TENDON BOUND WATER FRACTION

Forer JM[1,2], Smith J[3], Willett NJ[2], Hahn ME[1]
[1]Bowerman Sports Science Center, Dept. of Human Physiology, University of Oregon, Eugene, Oregon USA
[2]Knight Campus for Accelerating Scientific Impact, Dept. of Bioengineering, University of Oregon, Eugene, Oregon USA
[3]Robert and Beverly Lewis Center for Neuroimaging, University of Oregon, Eugene, Oregon USA
email: jforer@uoregon.edu

INTRODUCTION

Achilles tendinopathy presents with painful, long-lasting symptoms that negatively impact quality of life. While rehabilitative exercise is the primary recommended treatment, it only resolves the disease in 60-80% of patients, and the mechanisms by which loading improves tendon health are not fully understood [1]. In response to the morphological effects of exercise on Achilles tendons, it has been hypothesized that loading directly impacts fluid transport within and around the tendon [2]. This is especially relevant in cases of tendinopathy, where diseased Achilles tendons have demonstrated increased intratendinous fluid content compared to healthy controls, as measured with magnetic resonance imaging (MRI) [3]. While this connection between tendinopathy, mechanical loading therapy, and fluid transport has been discussed in the literature, no studies have empirically measured the effects of Achilles tendon loading on intratendinous fluid content. In this study we sought to investigate the effects of a clinically relevant eccentric plantar flexor exercise protocol on Achilles tendon fluid content using MRI. We hypothesized that intratendinous fluid content would decrease immediately after exercise as measured through transverse relaxation times (T2*) from ultrashort time to echo (UTE) MRI scans.

METHODS

Institutional Review Board approval and written, informed consent were obtained for this study. Healthy participants (N = 10, 5F/5M, age: 26.5±5.8 years, mass: 73.0±12.8 kg, height: 1.71±0.10 m) underwent MRI scan sessions immediately before (Pre), immediately after (Post), and 2 hours after (2Hr Post) completing an eccentric calf exercise protocol. The exercise protocol consisted of 50 straight leg and 50 bent-knee (20°) metronome guided unilateral heel drops with the forefoot placed on an elevated platform. For MRI scanning, fluid parameters were assessed by obtaining a UTE sequence on a 3T Skyra (Siemens) scanner. Achilles tendons were semi-automatically segmented using ITK-SNAP into insertion (INS), midsection (MID), and myotendinous junction (MTJ) regions using anatomical landmarks from a T1 scan. A voxel-wise biexponential decay curve was fit to normalized UTE intensity data over 7 echo times using MATLAB. In this biexponential model, the short ($T2^*_{Short}$) and long ($T2^*_{Long}$) components model the bound and unbound water in the tissue, respectively, while the fractional amplitude of the short component (F_{Short}) is considered an estimate of the bound water fraction. Statistical analyses were conducted using two-way repeated measures ANOVAs in Prism (GraphPad) with an alpha of 0.05.

RESULTS AND DISCUSSION

Results are shown in Table 1. Relaxation times ($T2^*_{Short}$ and $T2^*_{Long}$) both displayed a main effect of region ($p<0.05$) but not timepoint ($p>0.05$). $T2^*_{Short}$ was significantly higher in the INS compared to the MID and $T2^*_{Long}$ was significantly lower in the INS compared to the MTJ. Contrary to our hypothesis, we saw no change in T2* values immediately post exercise. Bound water fraction (F_{Short}) showed a significant interaction effect and a main effect of timepoint ($p<0.05$). These data indicate that exercise increases the proportion of bound water in the INS and the proportion of unbound water in the MTJ, with no change in the MID. These findings do not support the theory that eccentric exercise modifies tendon morphology through the exudation of intratendinous fluid, as we did not observe a difference in T2* directly after exercise. However, the changes identified in the bound water fraction (F_{Short}) do demonstrate that eccentric exercise is modifying the fluid microenvironment of the tendon by shifting the ratio of bound and unbound water within the INS and the MTJ.

CONCLUSIONS

Our quantification of MRI parameters after exercise do not demonstrate changes in intratendinous fluid content, but do show regional alterations in fluid compartmentalization. Further interpretation of these data and inclusion of tendinopathic tendons are needed to better understand how eccentric exercise impacts intratendinous fluid.

REFERENCES

1. Rees JD, et al. *Rheumatology* **47**, 1493-1497, 2008.
2. Grigg NL, et al. *Med & Sci in Sports & Exercise* **44**, 12, 2012.
3. Juras V, et al. *Eur Radiol* **23**, 2814-2822, 2013.

ACKNOWLEDGEMENTS

This work was supported by the Wu Tsai Human Performance Alliance and the Joe and Clara Tsai Foundation. MRI scans were operated by Alison Burggren and Vince Quesada and sequences were provided by Siemens.

Table 1: Transverse relaxation times and bound water fraction for voxel-wise biexponential fits organized by region and timepoint.

	$T2^*_{Short}$ [ms]			$T2^*_{Long}$ [ms]			F_{Short}		
Region	**Pre**	**Post**	**2Hr Post**	**Pre**	**Post**	**2Hr Post**	**Pre**	**Post**	**2Hr Post**
INS	0.253±0.195	0.243±0.167	0.266±0.205	6.21±2.46	6.28±1.57	7.03±3.77	0.716±0.048	0.739±0.034	0.746±0.054
MID	0.081±0.003	0.081±0.004	0.081±0.004	6.87±1.31	7.15±1.47	6.95±1.24	0.731±0.024	0.733±0.033	0.737±0.019
MTJ	0.129±0.094	0.148±0.135	0.146±0.117	9.16±2.97	9.16±3.00	9.04±1.63	0.762±0.020	0.747±0.024	0.769±0.026

INITIAL DEVELOPMENT OF A PROBABILISTIC METRIC OF RISKY BIOMECHANICS RELATED TO ANTERIOR CRUCIATE LIGAMENT INJURY RISK

Lynch, A[1]., Aflatounian, F[1]., Saxby, D[2]., Monfort, S[1].
[1]Montana State University, Bozeman, MT, USA [2]Griffith University, Queensland, Australia
email: alexandra.lynch@montana.edu

INTRODUCTION

Anterior cruciate ligament (ACL) injury risk factors are often assessed using single-limb drop jumps (SLDJ) with biomechanical variables averaged over several trials. However, many ACL tears appear to occur acutely rather than due to an accumulation. Thus, averaging performance across repeated trials may mask variability in performance and overlook less frequent but higher risk mechanics. The purposes of this study were to 1) develop a probabilistic metric [1] to characterize risky biomechanics (i.e. probability of injurious load (PoIL) [Fig.1A]) during SLDJ, and 2) determine how the number of jump landings in a dataset influence PoIL.

METHODS

Eight healthy participants (3 F/5 M, 23.3±3.3 years, 171.7±10.6 cm, 71.0±8.7 kg) performed reactive SLDJ. Body motions, ground reaction forces, and electromyograms (11 major lower-limb muscles) were collected. Calibrated electromyography-informed neuromusculoskeletal modeling was used to estimate muscle forces [2] and linked sequentially to a model of ACL loading to estimate force in the ACL (FACL) for each SLDJ [3]. Eight SLDJ landings per participant were analyzed. For each participant, a probability density function was calculated and PoIL [1] was estimated by integrating above a sex-, height-, and mass-adjusted estimate of ACL failure load (FINJ) [4]. PoIL was recalculated after removing 0-5 jumps and the resulting (log-transformed) PoIL estimates were compared using a mixed-effects model.

RESULTS AND DISCUSSION

PoIL estimates varied by participant [Fig.1C] and were influenced by the number of jumps used in their estimation ($p=0.024$). Significant pairwise differences existed between n8-n4 ($d = 0.693$, $p = 0.025$) and n8-n3 ($d = 0.630$, $p = 0.021$). The results indicate that PoIL varied across the number of jumps used in its estimation, with the highest number of trials (8) not yet establishing an effect size asymptote [Fig.1B].

PoIL was calculated for SLDJ landings, which aims to reflect relative risk (i.e., higher is riskier), incorporating mean and variance measures relative to ACL failure strength. Notably, PoIL is not a direct probability of sustaining an injury and the clinical utility of this metric must still be established. This study provides initial development of PoIL as a tool for assessing ACL injury risk. Ongoing efforts will explore higher numbers of trials (>8), with effects expected to stabilize as more trials and participants are included.

CONCLUSIONS

These results indicate that more trials are necessary to estimate PoIL robustly. Future efforts should focus on increasing number of trials included in the calculation of this probabilistic metric.

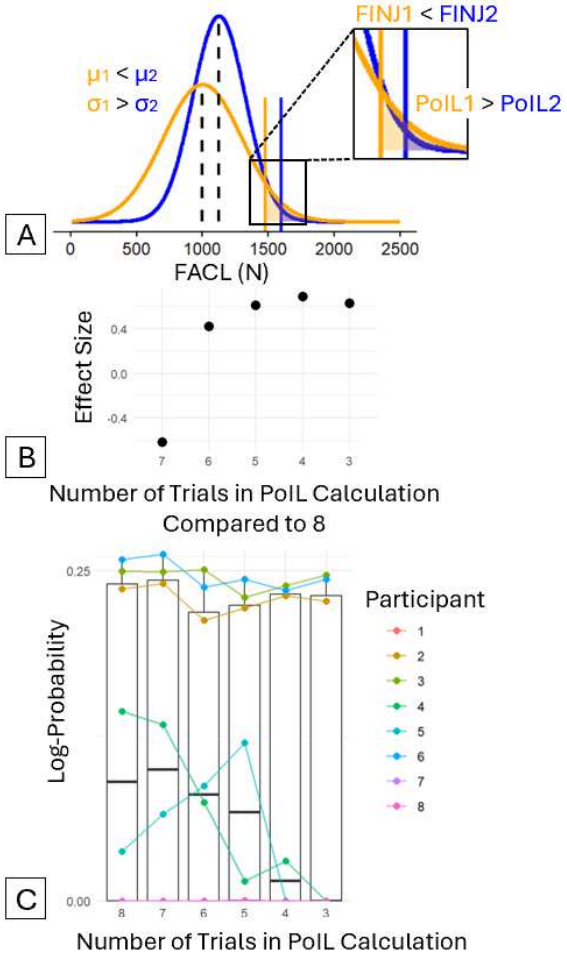

Figure 1: A) Example probability density functions (PDF) are calculated from the mean (μ_1, μ_2) and standard deviation (σ_1, σ_2) of FACL for two participants. Probabilities of injury (PoIL1, PoIL2) are found by integrating the PDFs above ACL failure strengths (FINJ1, FINJ2). Despite $\mu_2 > \mu_1$, PoIL1 > PoIL2 because of greater variability and ACL failure strength, illustrating a pitfall of using mean FACL alone. B) Effect sizes on log-transformed data between n8 and all other trials were calculated using paired Cohen's d. C) Log-probability plot of raw PoIL values on a log-scale. Minimum PoIL values for Participants 1, 7, and 8 approach 0.

REFERENCES

[1] Kazanski, *J. Biomech.*, (2022).
[2] Pizzolato, *J. Biomech.*, (2015).
[3] Nasseri, A., Med. Sci. Sports Exerc., (2021).
[4] Hashemi, *J. Orthop.* (2011).

ACKNOWLEDGEMENTS

Supported by MSU NACOE TEER and MSU NRT seed grants.

Evaluating the Impact of Camera Motion on Single-Camera Biomechanics Estimates of Knee Angle

Dumont, S[1], Arora, I[1],and Kuo, C[1]
[1]School of Biomedical Engineering, University of British Columbia, Vancouver, BC CAN
email: sarah.dumont@ubc.ca web: https://humbl.sbme.ubc.ca/

INTRODUCTION

This study is motivated by return-to-sport assessments which is a critical milestone where ACL-reconstruction patients undergo biomechanical evaluation to determine their readiness for activity. Currently, there is no standardized method to determine when a patient is ready for this formal evaluation; markerless tracking offers a way to remotely gauge readiness before a participant ever enters the lab. Advancements in computer vision have led to the development of pose estimation technologies, such as World-Grounded Human Motion Recovery via Gravity-View Coordinates (GVHMR) [1]. The markerless tracking system utilizes a single camera to generate 3D joint positions, presenting a potential solution for remote assessment to address the limitations of the marker-based gold standard. From a cell phone video alone, it is possible to obtain kinematic data anytime, anywhere, potentially providing a more accessible tool for biomechanical analysis. However, before implementing this technology, it is critical to determine the practical constraints and recording conditions required to ensure accurate, meaningful data outputs. Specifically, this study aims to determine if a stationary camera is an important constraint to enforce during out-of-lab data collection.

METHODS

Five participants (22±1.7 yrs; 3F) performed movements relevant to return-to-sport assessment, including the triple crossover hop and 45° cut. Participants were recorded simultaneously with two Motorola 5G smartphones. Video was captured at Full HD resolution (1080p) at a frame rate of 30Hz using the devices' 50 MP (f/1.8) primary camera sensors. One camera was affixed stationary to a tripod positioned approximately 45° relative to the participant. The second camera was handheld by the researcher and moved laterally following the participant. Camera movement was classified as low, medium, or high speed, with each condition repeated three times. The 'Low' condition involved the researcher holding the camera as still as possible, while 'Medium' and 'High' conditions introduced increasing levels of lateral camera movement. All videos were processed using GVHMR, which provides an output of 126 landmarks coming from the SMPL-X body models and the corresponding x,y,z positions [2]. The hip, knee and ankle markers were used to extract the knee joint angles through a process of data filtering with a low-pass second-order Butterworth filter 5Hz, interpolation, and knee angle computation via the dot product. The joint angles serve as an appropriate method of comparison between the stationary and moving camera outputs.

RESULTS AND DISCUSSION

The root mean square error (RMSE) of the knee angles was calculated relative to its corresponding stationary camera recording. A Kruskal-Wallis test indicated significant differences in RMSE across movement levels ($p < 0.001$). Post-hoc Stepdown Dunn's tests showed:

- Low vs. Medium: $p = 0.0007102$
- Low vs. High: $p = 0.000002597$
- Medium vs. High: $p = 0.1886$

Only comparisons involving the low movement condition reached statistical significance, showing that introducing movement increases error significantly, while increased movement speed has less of an effect. Despite this, the overall average RMSE across all trials and conditions was 1.9°, indicating good accuracy of GVHMR.

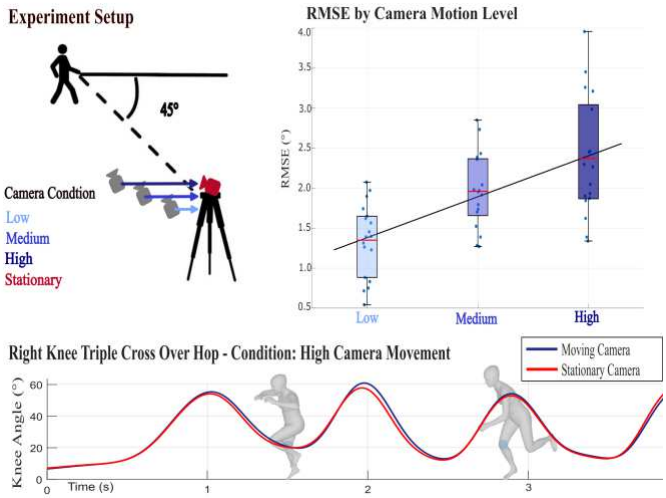

Figure 1: Experimental workflow, including camera configuration, RMSE results by movement condition, and GVHMR kinematic output.

CONCLUSION

These results demonstrate the viability of out-of-lab data collection, as the system remains accurate despite camera motion. This will make data collection easier to use for nontechnical users who may not have access to specialized equipment, widening the range of applications. The next steps for this project are to take data collection out of the controlled lab environment and into the hands of users. This will allow for biomechanical data to be captured throughout the entire progression of an individual's injury rehabilitation, providing a clearer indication of readiness for formal return-to-sport assessments.

REFERENCES

1. Shen Z. (2024). SIGGRAPH.
2. Pavlakos G. (2019). CVPR.

Mediolateral Ground Reaction Force Impulse Reflects Frontal-Plane Center of Mass Control during Load Carriage

Kim Y*, Freemyer B*, Stickley C*:
*University of Hawai‘i at Mānoa, Honolulu, HI
email: ytkim@hawaii.edu

INTRODUCTION

Military personnel demonstrate a high prevalence of post-traumatic knee osteoarthritis[1], particularly following anterior cruciate ligament or meniscal injury. Load carriage tasks, such as ruck marching, further increase frontal knee joint loading and may accelerate cartilage degeneration.[2] Previous studies suggest that changes in the lateral position of the center of mass (COM) during load carriage may influence frontal knee loading.[3] Mitigating mediolateral ground reaction force impulse (ML impulse) may represent a frontal-plane balance strategy during gait that reflects control of mediolateral COM motion. However, the biomechanical mechanisms between COM modulation and frontal-plane knee loading remain unclear. Therefore, the purpose of this study was to examine the extent to which COM displacement and frontal plane knee kinetics predicts ML GRF impulse during walking in either simulated ruck marching (load carriage) or normal gait (no load carriage).

METHODS

A total of nineteen Reserve Officers' Training Corps (ROTC) cadets participated in this study (14 males, 5 females, 24.4 yo ± 4.3, 177.8 cm± 11.8, 74.7 kg± 14.3). Subjects performed walking of 4 meters across an embedded force plate toward the positive y-axis with and without a 35lb load. Subjects finished three trials on both limbs. The kinematic and kinetic data of the hip, knee, and ankle joints were collected using a three-dimensional motion capture system (Vicon, Colorado, USA). Visual 3D (Germantown, MD) was used to process and reduce data. Two multiple linear regressions were computed to evaluate associations between ML impulse with COM, KAM rate, and KAM impulse during both no load carriage (NLC) and load carriage (LC) gait.

RESULTS AND DISCUSSION

Under load carriage, ML impulse was predicted by ($R^2 = 0.61$, $p = 0.002$) mediolateral COM displacement ($\beta = 0.56$, $p = 0.007$). KAM rate ($\beta = -0.14$, $p = 0.481$) and KAM impulse ($\beta = -0.27$, $p = 0.170$) were not associated with ML impulse and were negatively correlated. These findings indicate that greater mediolateral COM displacement during load carriage was accompanied by larger ML impulse, suggesting that ML impulse may reflect a compensatory frontal-plane balance strategy. However, frontal-plane knee loading variables were not associated with ML impulse. During the no load condition, the regression model was not significant ($R^2 = 0.36$, $p = 0.112$), and no significant associations were observed between ML impulse, mediolateral COM displacement ($\beta = 0.42$, $p = 0.091$), and frontal knee loading variables: KAM rate ($\beta = -0.22$, $p = 0.400$) and KAM impulse ($\beta = 0.43$, $p = 0.096$).

Table 1. Multiple regression results for ML impulse in NLC and LC conditions.

Condition	Predictors	β	p-value	R^2
No Load	COM displacement	0.42	0.091	0.36
	KAM rate	-0.22	0.400	
	KAM impulse	0.43	0.096	
Load Carriage*	COM displacement	0.56	0.007	0.61
	KAM rate	-0.14	0.481	
	KAM impulse	-0.27	0.170	
*=significant p<0.05				

CONCLUSIONS

These findings suggest that ML impulse during load carriage is more related to mediolateral COM sway, rather than frontal-plane knee loading. This indicates that frontal-plane balance strategies may play a key role in regulating ML impulse under load, whereas no biomechanical factor was observed during unloaded gait.

REFERENCES

1.Radzak KN, Sefton JM, Timmons MK, Lopp R, Stickley CD, Lam KC. Musculoskeletal Injury in Reserve Officers' Training Corps: A Report From the Athletic Training Practice-Based Research Network. *Orthop J Sports Med*. 2020;8(9):2325967120948951. doi:10.1177/2325967120948951
2.Drew MD, Krammer SM, Brown TN. Effects of prolonged walking with body borne load on knee adduction biomechanics. *Gait Posture*. 2021;84:192-197. doi:10.1016/j.gaitpost.2020.12.004
3.Mündermann A, Dyrby CO, Andriacchi TP. Secondary gait changes in patients with medial compartment knee osteoarthritis: Increased load at the ankle, knee, and hip during walking. *Arthritis Rheum*. 2005;52(9):2835-2844. doi:10.1002/art.21262

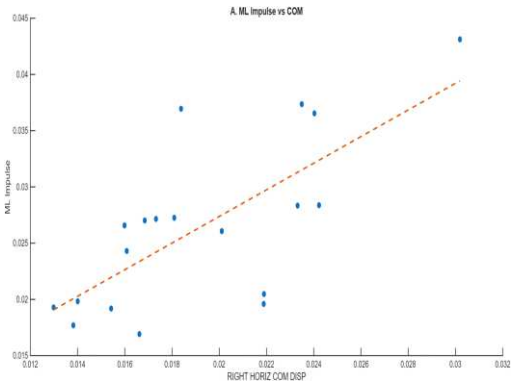

Figure 1. Relationship between ML GRF impulse and mediolateral COM displacement during load carriage. Mediolateral COM displacement was the only significant predictor of ML impulse in the multiple regression model ($\beta = 0.56$, $p = 0.007$).

Podium Session II

Friday, May 22nd, 3:45 – 5:00 PM

IMU Misalignment Correction and Calibration Methods for Telemedicine Segmental Symmetry Analysis

Redmond J.R., Banghart C., Pew C.A.
Department of Mechanical and Industrial Engineering
Montana State University, Bozeman, MT USA
email: joesph.redmond@montana.edu

INTRODUCTION

Inertial Measurement Units (IMUs) provide a low-cost option for accessible gait analysis. For clinicians, IMUs can provide an objective measure of gait asymmetry using sagittal plane gyroscopes [1]. For patients in remote regions, IMUs could be self-placed for a virtual visit to forgo travel to the clinic. IMU alignment to anatomical segments is critical for accurate measures. While an experimental protocol partially constrained IMU self-placed misalignment, longitudinal axis rotation persisted, producing artificial asymmetry in readings. We hypothesize a algorithmic calibration can mitigate effects of misalignment on asymmetry score repeatability.

METHODS

Four IMUs were self-placed by participants using a removable pin aligning the vertical axis of thigh and shank sensors. Participants were recorded treadmill walking. Optical motion capture (MoCap) quantified sensor misalignment. Placement was done twice to evaluate repeatability. IMUs misalignment was corrected using 3 methods: 1) An ideal correction computed using MoCap, 2) A 3-axis magnitude, 3) Optimized correction, orienting maximum gyroscope variance between the thigh and shank to one axis, assuming hinge-like knee behavior [2]. Asymmetry scores were computed by average Euclidian difference of sequential sagittal gyroscope cycles on the left and right sensor [1]. Method inter-trial variance was compared using Pitman-Morgan tests.

RESULTS AND DISCUSSION

MoCap generated Shank asymmetry scores on 9 Healthy Controls (6F; 53±19yrs.) produced a Minimal Detectable Change (MDC) of 2.55 points exceeded by 4% of repeated trials. Uncorrected IMU had higher variance than MoCap (Variance Ratio=3.7; p=0.001); 30% MDC exceedance. Ideally Corrected IMU was statistically the same as Mocap (Ratio=1.4; p=0.263); 15% MDC exceedance. A 3-axis magnitude showed increased variance (Ratio=2.13; p=0.038); 18% MDC exceedance. Optimized corrections had marginally equivalent variance (Ratio=1.9; p=0.056); 11% MDC exceedance.

Realigning IMUs using a MoCap-dependent correction improves score variability under repeated conditions to match MoCap. Optimization did not depend on MoCap; while corrections were not exact, score variance improved over no correction. Axis alignment is likely dependent on gait characteristics, with asymmetrical gait causing asymmetrical alignment. However, score deficiencies due to calibration error are related to asymmetry rather than random due to placement.

CONCLUSIONS

Additional analysis will evaluate thigh data, quantify misplacement impacts on intra-trial scoring error relative to MoCap, and discuss acceptable margins of misalignment for score reliability.

REFERENCES

1. Sheila Clements et al. *Clinical Biomechanics* 2020.
2. Thomas Seel et al. *IEEE CCA* 2012.

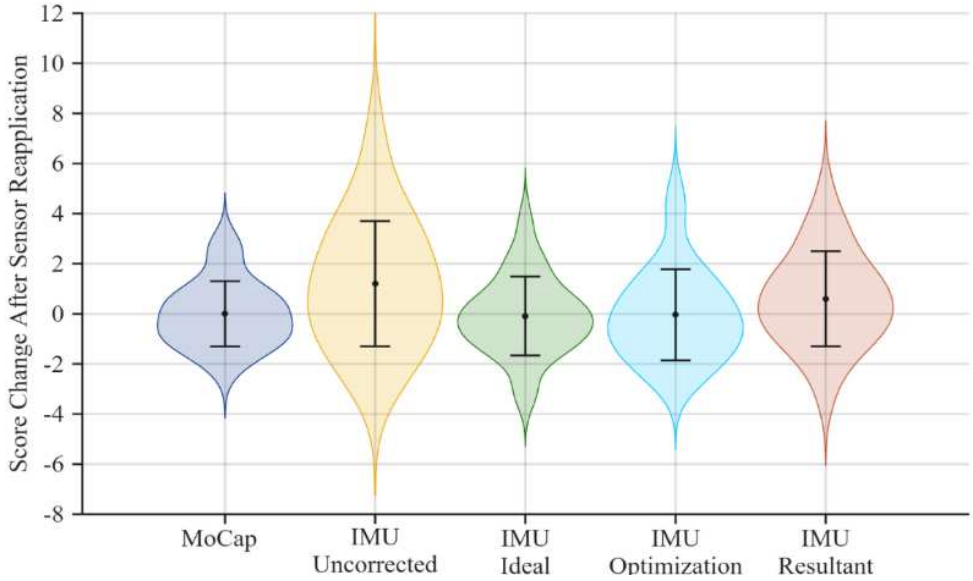

Figure 1: Violin plot of score changes in repeated trails with 2 different self-placements, compared between Mocap and methods of correcting IMU misalignment (Mean ± 1 Std. Dev.)

Automated Labeling of Muscle Contractions from HDsEMG in Dynamic Exercises

Thompson, J[1], Douglas, F[1], Pei, M[1], Gould, G[1] and Kuo C[1]
School of [1]Biomedical Engineering, University of British Columbia, Vancouver, BC CAN
email: jjthompson124@gmail.com web: https://humbl.sbme.ubc.ca

INTRODUCTION

Stroke remains the third leading cause of global disability, necessitating long-term neuromuscular rehabilitation [1]. Physiotherapists use sEMG as it is a non-invasive method to observe neuromotor activity. Monitoring the muscle contractions, and watching the resulting movements are used to evaluate neuromotor pathways [1]. The voltage amplitudes during muscle contraction guide the recommended exercises for rehabilitation programs. While surface electromyography (sEMG) serves as a valuable, non-invasive tool for monitoring neuromotor recovery, its widespread clinical adoption is severely hindered by inter-session variability [2]. Minor translational or rotational shifts in electrode placement can significantly alter signal properties, precluding reliable longitudinal assessments.

To address this, we have developed an algorithm to quantify High-Density sEMG (HDsEMG) sensor displacement on isometric muscle contractions. However, to make this algorithm viable for clinical use, we are adapting this algorithm to analyze muscle contractions during dynamic activities. This first requires automated identification of muscle contractions utilizing targeted signal filtering and energy operators.

METHODS

Data were collected from 10 healthy participants using a 64-channel HDsEMG array (8×8 grid, 1 cm spacing) placed over four lower-limb muscles (gastrocnemius, tibialis anterior, semitendinosus, and tensor fasciae latae) according to SENIAM guidelines [3]. To establish a ground-truth positional reference, markers were applied to the array corners and localized using a 3D surface scanner (Structure Sensor Pro). Participants executed isometric contractions, sit-to-stand movements, and touch-and-go trials. To simulate inter-session variability, the array was then physically displaced on the same muscle (up to ±4.25 cm translation and ±30° rotation). The new location was 3D-scanned to record the exact spatial shift, and the dynamic exercise protocol was repeated.

After processing the HDsEMG data with an 8th order butterworth bandpass filter with cutoff frequencies of 20 Hz, and 450 Hz, a notch filter at 60 Hz was also implemented to remove any powerline interference. Lastly, any open channels were removed from analysis. To automate data processing, the Teager-Kaiser Energy Operator (TKEO) was applied to detect rapid amplitude and frequency changes, effectively isolating distinct muscle contractions [4]. The TKEO results were then rescaled between 0 and 1 for each channel, to remove the dependence on the peak amplitude of the signal. Three times the median TKEO value for each trial was used as the threshold to identify a contraction. These isolated segments were subsequently processed through a sensor shift algorithm to quantify electrode displacement.

RESULTS AND DISCUSSION

Our automated contraction algorithm used in conjunction with the array displacement algorithm estimated displacements within 1cm 18.18% of the time, compared with 17.31% of the time for manually labeled contractions (Figure 1). The performance using automatically labeled contractions was not significantly different from manual segmentation, indicating that automatic labels provide a similar quality of results, and are feasible for use with the sensor displacement algorithm.

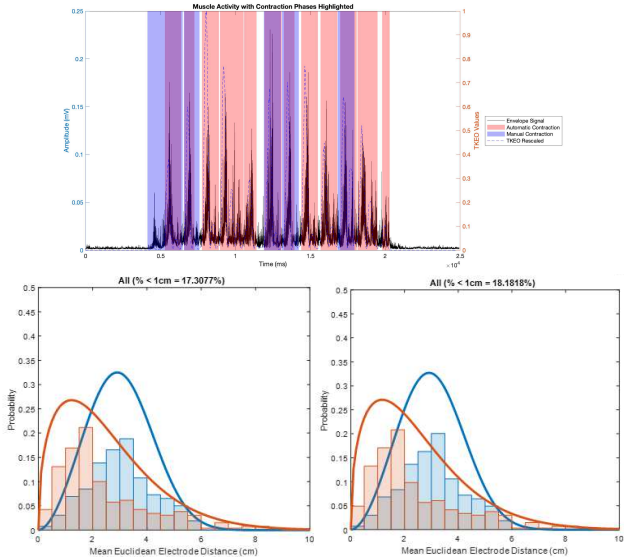

Figure 1: Top – Signal Envelope Plotted with TKEO values. Automatic labels were shown in red, and Bottom - Comparison of shift prediction results with manual contraction labeling (left) and automatic contraction detection (right), histograms showing the distribution of mean Euclidean distances to the ground truth for the origin assumption (blue) and shift algorithm outputs (orange). Solid lines represent Weibull distributions fit to the data.

CONCLUSIONS

This methodology provides a repeatable, quantitative framework for automatically labelling HDsEMG data, addressing the time-consuming process of manually labelling EMG contraction data. Therefore, this automated muscle contraction algorithm will allow us to improve HDsEMG consistency, enabling clinical utilization for stroke rehabilitation.

REFERENCES

1. Feigin VL, et al. *Int J Stroke* **20**, 132-144, 2025.
2. Douglas F, et al. *IEEE Trans Instrum Meas* **74,** 1-11, 2025.
3. Hermens HJ, et al. *J Electromyogr Kinesiol* **10**, 361-374, 2000.
4. O'Leary TJ, et al. *Eur J Appl Physiol* **110,** 1067-1074, 2010.

ACHILLES TENDON FORCE DURING UPHILL RUNNING IN HIGH PERFORMING RUNNERS

Madden, T and Pew, C
Department of Mechanical and Industrial Engineering
email: ThomasMadden4@montana.edu, web: https://www.montana.edu/biomechanics/

INTRODUCTION

Achilles tendon (AT) overuse injuries occur frequently in runners as a result of accumulated damage during cyclic loading. Understanding how different running conditions (speeds and grades) affect AT force is crucial to the health and performance of runners. AT force increases with running speed and grade independently [1,2]. However, increasing grade at constant speed does not reflect real-world scenarios in which runners adjust their speed while running uphill to maintain intensity [3]. It remains unclear how per-step and cumulative weighted AT force, reflecting the nonlinear relationship between peak stress/strain and rate of damage accumulation [4], change across speed-grade combinations reflecting real-world training scenarios in high performing distance runners. Therefore, the purpose of this study was to examine the effects of running speed and grade at grade-adjusted speed on per-step and cumulative weighted AT force in high performing distance runners. We hypothesized that 1) increasing speed would increase per-step and cumulative weighted AT force and 2) increasing grade at adjusted speed would not affect AT forces.

METHODS

Participants included 8 (4F, 22 ± 3y) high performing distance runners (10k < 39min for women/32min for men or equivalent in the last year). An initial visit established each participant's speed at lactate threshold (LT) before a second visit consisting of biomechanical testing. In this visit, we collected 3D markerless motion capture data (Qualisys, Goteborg, Sweden and Theia, Kingston, ON) as participants ran on a force-instrumented treadmill (Treadmetrix, Park City, UT) at 70% and 95% LT at each grade: 0°, 3°, and 6°. Grade-adjusted speeds maintained predicted metabolic power across grades, based on a graded running model [5]. Peak AT force per step was estimated via inverse dynamics and musculoskeletal modeling. Cumulative weighted peak force ($CWPF$) per minute (Eq. 1) was computed using stride rate (n), peak force per step (F), and an empirically determined weighting factor [4,6].

$$CWPF = nF^{9.3} \quad (1)$$

Mixed effects models tested effects of speed and grade on per-step and cumulative weighted AT force. In the case of significant grade effects, pairwise comparisons evaluated between-grade differences.

RESULTS AND DISCUSSION

Speed and grade showed significant ($p < 0.001$) main and interaction effects on per-step and cumulative weighted AT force (Fig. 1). Increasing speed from 70% to 95% LT increased per-step AT force by 1.04 body weight (BW) (20%) and increased cumulative weighted AT force by 1.74 BW/min$^{1/9.3}$ (21%) on average at 0° grade, consistent with our hypothesis and previous results [1,2]. Contrary to our hypothesis, grade showed inverse relationships with per-step and cumulative weighted AT force, with greater effects at higher speed (Fig. 1).

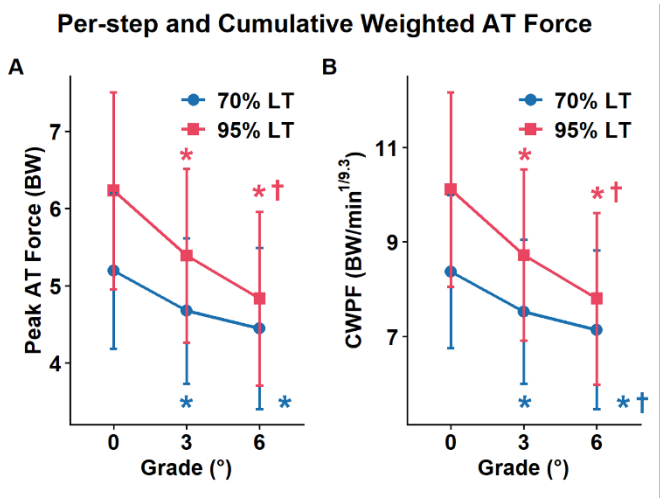

Figure 1: (A) Per-step and **(B)** cumulative weighted peak AT force (CWPF) across speeds and grades (mean ± standard deviation). CWPF is raised to the power of 1/9.3 to give units in BW/min$^{1/9.3}$. Pairwise comparisons at each speed revealed between-grade differences: *significant difference from 0° ($p < 0.01$); †significant difference from 3° ($p < 0.05$).

Increasing grade from 0° to 3° decreased per-step AT force by 0.52-0.84 BW (10-13%) and decreased cumulative weighted AT force by 0.85-1.39 BW/min$^{1/9.3}$ (10-14%) on average, suggesting that even low (3°) grades can meaningfully reduce AT force relative to level ground when running at fixed metabolic power. This contrasts with previous results at fixed absolute speed, showing increased AT force with increased grade [2]. The effect of speed may outweigh the effect of grade such that decreasing speed to maintain intensity on uphill grades ultimately reduces AT forces relative to level ground.

CONCLUSIONS

Per-step and cumulative weighted AT force relate directly to speed and inversely to grade at constant predicted metabolic power. Training on low-moderate uphill grades at the same metabolic power as level ground may reduce per-step and cumulative weighted AT force in high performing runners.

REFERENCES

1. Starbuck C, et al. *Scand J Med Sci Sports* **31**, 1657-1665, 2021.
2. Van Hooren B, et al. *Scand J Med Sci Sports* **34**, 2024.
3. Townshend AD, et al. *Med Sci Sports Exerc* **42**, 160-169, 2010.
4. Edwards WB. *Exerc Sport Sci Rev* **46**, 224-231, 2018.
5. Looney DP, et al. *Eur J Appl Physiol* **126**, 1621-1633, 2025.
6. Wren TAL, et al. *Ann Biomed Eng* **31**, 710-717.

ACKNOWLEDGEMENTS

This research is funded by World Athletics/ACSM. We thank the Montana State University Cross Country/Track and Field team and others for their participation.

Visual Onset Determination of Rate of Torque Development: A Level of Agreement Study

Dios, C[1], DeRosia, KD[2], Mulligan, CMS[1], and Johnson, ST[1]
[1]College of Health, School of Exercise, Sport, and Health Sciences, Oregon State University, Corvallis, OR, USA
[2]College of Nursing & Health Sciences, Seattle University, Seattle, WA
Email: diosc@oregonstate.edu

INTRODUCTION

Consistently identifying onset of torque production is vital for accurate analysis of rate of torque development (RTD). Previous research suggests that visual identification of the torque onset is the gold standard approach in minimally filtered signals from low-noise dynamometers [1], but a similar determination has not been made with high noise dynamometers that require filtering [2]. The purpose of this study was to assess the inter-rater level of agreement in visual onset identification of torque production in a high noise dynamometer.

METHODS

A total of 200 RTD trials from 47 participants were analyzed. The participants performed an isometric contraction of the knee extensors while seated on a Biodex System 3 dynamometer (Biodex Medical Systems, Inc., Shirley, NY, USA). They were instructed to contract "as hard and fast as possible."

A custom computer software program (LabVIEW; National Instruments, Corp.; Austin, TX, USA) was used to filter the raw voltage signal using a low-pass, 4th order Butterworth filter with a cutoff frequency of 10 Hz. The first 500 ms of the trial were averaged and subtracted from the signal to correct for limb weight. Trials that contained an initial countermovement were excluded from data processing. Two experienced investigators (CD, KD) independently identified the onsets using a systematic approach [2]. First, the torque-time curve was plotted in LabVIEW with the x-axis scaled to 500 ms and y-axis to 1 Nm centered around the apparent onset. A vertical cursor was placed at the minima of the last trough before the signal deflected from baseline; the torque-time curve was then re-scaled to an x-axis of 25 ms and a y-axis of 0.5 Nm. The vertical cursor was adjusted to the minima before the signal deflected away from baseline and this time point was recorded. Five trials were excluded due to the presence of a initial countermovement and one trial was excluded due to a presumed data entry error.

The onsets were analyzed for level of agreement by finding the inter-rater mean difference, standard deviations of the difference, mean absolute difference, and a Bland-Altman analysis with confidence intervals (Figure 1). Due to the time prior to contraction onset not being standardized between trials, traditional methods of reliability (e.g. ICCs) were unsuitable. To account for the high-noise signal, a predefined 2 ms clinically significant window was established as an acceptable limit of difference between raters.

RESULTS AND DISCUSSION

The results of this study demonstrate good agreement between raters as the mean inter-rater difference was 0.67 ms. The mean absolute difference was 2.07 ms (SD ± 12.74 ms). Of the analyzed trials, 97.5% fell within the 2 ms window. Five trials were greater than the 95% limits of agreement. Upon further inspection these trials all had high baseline noise. There is ambiguity in determining a visual onset in instances of increased noise; these contexts should be further evaluated to improve the standardized approach to account for them.

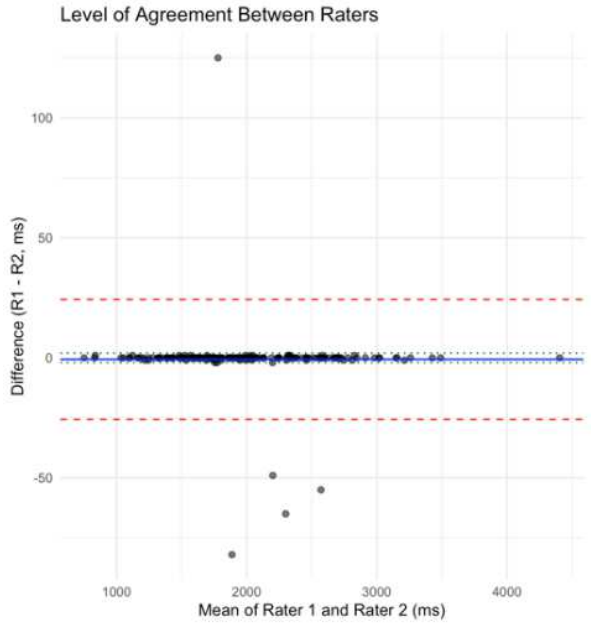

Figure 1: Bland–Altman plot illustrating agreement between raters. The solid line represents the mean difference (bias), and the dashed lines represent the 95% limits of agreement. The dotted lines indicate the predefined acceptable limits of ±2 ms, representing the clinically significant limits.

CONCLUSIONS

Visual onset determination of RTD in a high noise dynamometer demonstrates good inter-rater agreement. However, the variability in onset determination is influenced by signal noise, even with filtering. Visual onset determination may therefore be appropriate for most trials, but noisy signals likely require additional decision rules before this approach can be recommended without reservation.

REFERENCES

1. Maffiuletti, N. et al. European Journal of Applied Physiology, 116, 2016.
2. Tillin, N., et al. Journal of Electromyography and Kinesiology, 23, 2013

ACKNOWLEDGEMENTS

Funded through the John C. Erkkila, M.D., Endowment for Health and Human Performance

THE INFLUENCE OF LIFESTYLE, PHYSICAL ACTIVITY LEVEL, AND ANTHROPOMETRIC FACTORS ON PLANTAR FASCIA THICKNESS

Teixeira, B[1], MacMichael, P[1], Krumpl, L[1]
[1]Department of Kinesiology and Educational Psychology
Washington State University, Pullman, WA, USA
email: bruno.teixeira@wsu.edu

INTRODUCTION

The plantar fascia (PF) works as a passive, viscoelastic ligamentous structure that supports the foot arch, shares load and contributes to stable gait. An increase in PF thickness (PFT) is considered a marker of tissue deterioration [1] and linked to injury, such as plantar fasciitis, but could also represent a physiological adaptation to loading [2]. Plantar fasciitis is a common PF injury, accounting for approximately 15% of foot pathology in the general population [3]. Mass, plantarflexion range of motion, and loading mechanics are among the identified risk factors in physically active individuals [4]. However, most evidence comes from cross-sectional studies, making it unclear whether these factors precede or result from pathology. Therefore, examining these relationships in healthy adults may clarify whether systemic or morphological factors are the primary drivers of fascial adaptation. The purpose of this study is to investigate how anthropometric characteristics, physical activity (PA) volume, foot length (FL), and sedentary behavior influence PFT in healthy adults.

METHODS

Sixteen healthy adults (171.7 ± 9.6 cm; 72.8 ± 12.6 kg; 23.6 ± 5.5 yrs) participated in this study so far. Inclusion criteria required participants to be between 18-65 years old with no history of foot surgery. Participants were instructed to avoid high intensity, or heavy load exercise for 24 hours prior to data collection to avoid PF compression due to mechanical loading. After obtaining consent, participants' mass (kg), height (cm), and standing FL (cm) were measured. Participants then completed the Global Physical Activity Questionnaire and a Health & Lifestyle Questionnaire. To assess PFT, participants lay prone on a treatment table, with both feet in a neutral, relaxed position. Then, three bilateral B-mode ultrasound images (Versana Active, GE) were collected 2cm from the calcaneal insertion. PFT was defined as the perpendicular distance (mm) between the superficial and deep borders of the fascia. Data was collected by a single investigator with 8 years of ultrasound experience. The mean of three bilateral measurements was utilized for statistical analysis. PA volume was calculated by summing the product of days, minutes, and MET-intensity values (8 METs for vigorous, 4 METs for moderate) across the work, transport, and recreational domains (MET-min/week). An independent t-test was conducted to assess potential bilateral differences in PFT. Pearson correlation coefficients (r) were used to assess the relationships between PFT and BMI, PA volume, daily sitting, and FL. Alpha was set at 0.05. Statistical analyses were completed in R (v. 4.4.0).

RESULTS AND DISCUSSION

Left (3.1 ± 0.26 mm) and right (3.06 ± 0.22 mm) PFT were not significantly different (p = 0.63); therefore, the mean bilateral PFT (3.1 ± 0.2 mm) was used for all analyses. Preliminary analyses indicate a significant positive correlation between PFT and FL (r = 0.52, p = 0.04) (Figure 1). In contrast, no significant correlation was found between PFT and BMI (24.7 ± 3.7 kg/m²) (r = 0.25, p = 0.35). Similarly, weak correlations were observed between PFT and PA volume (6952.5 ± 3723.1 METmin/week) (r = 0.16) and daily sitting time (296.2 ± 118.4 min) (r = -0.15).

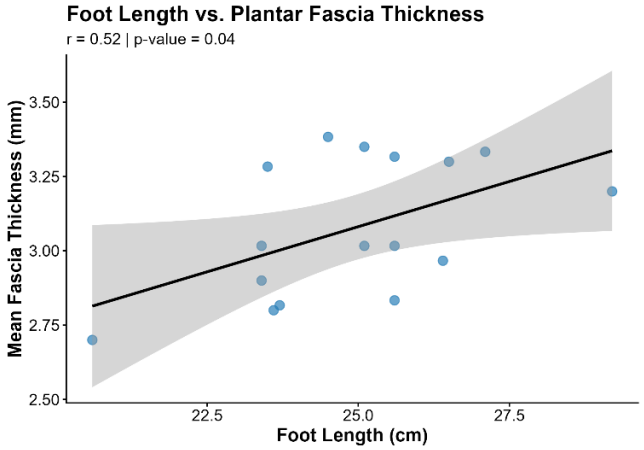

Figure 1. Relationship between foot length (cm) and mean plantar fascia thickness (mm) in healthy adults (n=16). Shaded area represents 95% CI.

These findings suggest that neither height-weight ratio nor lifestyle behaviors are primary determinants of PFT in healthy adults. The significant association between FL and PFT indicates that mechanical factors, specifically the mechanical level arm of the foot, may drive fascial adaptation more than the systemic loading variables. This is consistent with the windlass mechanism, where longer feet generate greater tensile demands on the PF during the propulsive phase of gait [5,6].

CONCLUSIONS

Foot length emerged as the principal variable correlated to PFT, while BMI, PA volume, and sitting time showed no significant associations. These preliminary findings suggest that FL, through its role as a mechanical lever, may be a primary driver of PF adaptation in healthy adults. Data collection is ongoing, so expanded analysis will clarify these relationships later.

REFERENCES

1. Chen H, et al. *J Orthop Sports Phys Ther* 43, 727–734, 2013.
2. López Ripado O, et al. *J Bodyw Mov Ther* 2025.
3. Koc TA, et al. *J Orthop Sports Phys Ther* 53, CPG1–CPG39, 2023.
4. Hamstra-Wright KL, et al. *Sports Health* 13, 296–303, 2021.
5. Caravaggi P, et al. *J Exp Biol* 212, 2491–2499, 2009.
6. Wearing SC, et al. *Sports Med* 36, 585–611, 2006.

Podium Session III

Saturday, May 23rd, 9:35 – 10:50 AM

ASSESSMENT OF DE NOVO MOTOR LEARNING USING VIRTUAL REALITY

Roduin, E[1], Whittier, T[1]
[1]Department of Food Systems, Nutrition and Kinesiology
Montana State University, Bozeman, MT USA
Email: emilyroduin@montana.edu

INTRODUCTION

Motor learning involves experience-dependent changes in performance and underlies skill acquisition across rehabilitation and sport [1]. While traditional laboratory models often rely on simplified adaptation tasks, de novo motor learning requires the formation of entirely new sensorimotor mappings and coordination strategies [2]. Present in many everyday activities, such as riding a bicycle, this type of learning is essential in human life, but has proven difficult to assess in a research setting. Due to its immersive and customizable qualities, virtual reality (VR) offers a controlled yet ecologically valid platform for studying complex motor behavior [3,4].

The purpose of this study was to design a de novo motor learning assessment that is both internally valid and ecologically relevant. It was hypothesized that through training, participants would show improvements in accuracy, movement time, and bimanual coordination while learning a bimanual object transport task. Additionally, retention of these improvements across visits and with increased cognitive demands will indicate the internal validity and ecological relevance of the VR-based de novo motor learning task.

METHODS

Eleven healthy young adults (3 females, M_{age} = 23.02 ± 1.81 years) completed VR training protocol involving two study visits and using the HTC Vive Pro 2 headset and controllers. Participants controlled a virtual cursor by moving both arms in a novel, non-intuitive mapping. In this altered mapping, cursor right-left motion is controlled by the Y-axis movements of the left controller, while cursor up-down and forward-backward motion were controlled by the right controller's Z- and X-axes movements, respectively. During participants' first research visit, after receiving explicit instructions of the altered mapping, they each completed ten learning blocks consisting of sixty targets each. To assess attentional requirements of the VR task, in between the fifth and sixth learning block, participants performed a dual-task block involving a serial-sevens subtraction assessment performed concurrently with the VR task. Participants returned two weeks later (M_{days} = 14.6 ± 0.9 days after first visit) for their second visit, during which five additional blocks of sixty targets were performed to assess retention followed by an additional dual-task condition block.

Normalized path length, movement time, trial-to-trial variability, and bimanual control metrics were calculated and averaged for each block.

Data were processed in MATLAB R2023a. Learning during visit 1 (Blocks 1–10) was analyzed using mixed-effects models with block as a fixed effect and participant as a random effect. Linear, quadratic, and log-transformed models were compared using Akaike Information Criterion (AIC) to determine best fit. Retention between visits (Block 10, visit 1 vs. Block 5, visit 2) and dual-task differences were evaluated using paired t-tests. Statistical significance was set at $\alpha = 0.05$.

RESULTS AND DISCUSSION

Model comparison using AIC indicated that a log-transformed model provided the best fit for normalized path length (AIC_{Linear}: 404.41, $AIC_{Quadratic}$: 391.31, AIC_{Log}: 298.38). Average normalized path length decreased (β = -0.067, SE = 0.025, p = 0.009), corresponding to a 6.7% improvement in cursor path length across each block (Figure 1). Performance was retained at visit 2, with moderate (yet not significant) difference between the final block of visit 1 and the final retention block ($t(10) = 2.27$, $p = 0.05$). Dual-task performance improved from visit 1 to visit 2 ($t(10) = -4.04$, $p = 0.002$).

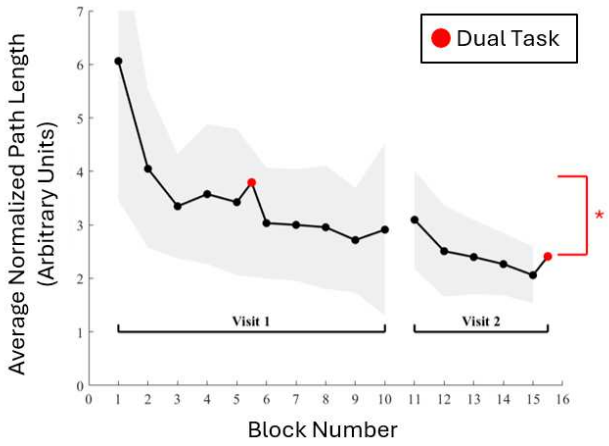

Figure 1. Average normalized path length (± SD) (Arbitrary Units) across training blocks (1–10), retention blocks, and dual-task blocks. Decreasing values indicate improved movement efficiency.

★ p = 0.002.

These findings indicate that participants successfully formed a new control policy for their novel bimanual mapping, consistent with prior work on de novo learning [2].

CONCLUSIONS

Together, these findings support the use of this VR task as a valid method for studying de novo motor learning. The task provides an internally controlled yet ecologically relevant method for examining complex motor skill acquisition. This approach may be useful for future investigations of de novo motor learning mechanisms and further applications into rehabilitation and training.

REFERENCES

1. Krakauer, J-W, et al. *Comprehensive Physiology*, 613-633, 2019.
2. Haith, A-M et al. *Journal of Neurophysiology* **128**, 982-993, 2022.
3. Levin, M-F et al. *Physical Therapy* **95**, 415-425, 2015.
4. Lohse, K-R et al. *Plos One* **9**, e93318, 2014.

OFFSET VISION IN VIRTUAL REALITY ALTERS LIMB SYMMETRY DURING A BILATERAL TASK

Taylor J Wilson[1] & Andy Karduna
University of Oregon, Eugene, Oregon, US
Email: [1]twilson8@uoregon.edu

INTRODUCTION

Virtual reality (VR) is increasingly used in research due to its ability to manipulate environments and sensory feedback [1]. Our lab has utilized VR to evaluate the effects of joint accuracy when given incorrect/offset vision during a joint position sense (JPS) task. For example, participants were required to go to 90° shoulder flexion with one arm, relax, then replicate this with accurate vision (AV) and offset vision (OV; +8° shoulder flexion from real world angle). When given OV of their hand, participants tended to undershoot the target and thus rely on incorrect vision [2]. While this is promising in the effects of using incorrect vision to alter joint target tasks, we are unsure if participants would rely on the altered visual stimuli while completing a moving bilateral limb symmetry task.

The purpose of this study was to evaluate the effects of OV on the right hand and AV of the left hand, during a bilateral out and back reaching task in virtual reality. We hypothesize that OV of the right hand will increase limb asymmetry compared to AV of the right hand, when given AV left hand.

METHODS

Twenty healthy participants (13F/7M, 25.3 ± 6.6 yrs (mean ± std)) were recruited from the University of Oregon (UO) campus. Participants were excluded if they had experienced chronic upper body pain in the past three weeks, upper limb injury in the past year, history of neurological disorder(s), or uncorrected impaired vision. All participants read and signed the informed consent, approved by the UO IRB.

Participants were outfitted with an HTC VIVE VR headset with over-the-ear headphones. A wrist brace was fitted on both lower arms, as well as an arm strap on their upper arms (halfway between the acromion process and the lateral epicondyle) to secure the HTC VIVE trackers (0.36 kg). Auditory cues were delivered through over-the-ear headphones. A simple three-dimensional visual environment (white walls and floor) with the participant's hand positions were presented (Figure 1A). Wrist and upper arm positions were determined using the inertial measurement unit (IMU) output from the VIVE trackers, recording kinematic data for both arms.

Table 1: Block definitions and parameters

	Left Hand		Right Hand	
Block	Proprioception	Vision	Proprioception	Vision
WUAV_100	Yes	Yes	Yes	Accurate
VPAV_000	Yes	Yes	Yes	Accurate
VPOV_050	Yes	Yes	Yes	Offset 5cm
VPOV_075	Yes	Yes	Yes	Offset 7.5cm
VPOV_100	Yes	Yes	Yes	Offset 10cm

Participants were told to keep limb symmetry while moving in the middle 80% of movement trajectory, between 90° elbow flexion to full extension, a total of ten times. Participants completed this type of movement for a total of five blocks under different visual conditions for the left and right hand. Table 1 includes the available sensory information for each hand, defined for the warmup block and main experiment blocks of AV and during the OV conditions at 5cm, 7.5cm and 10cm in the forward direction. A visual example of a 10cm offset is given in Figure 1A, where the participant's hands are symmetrical in the real world, but appear asymmetric in VR.

To determine the effect of offset vision on limb symmetry, limb asymmetry (LA) was calculated at the 10th trial at the end point of 80% full elbow extension and compared across blocks. A one-way RM ANOVA was used to compare LA during the AV block against each OV block. Post-hoc analyses and effect sizes were calculated when necessary.

RESULTS

The RM ANOVA compared the participant average LA during VPAV_000 against the participant average LA during the VPOV blocks, which showed a significant effect of block on LA ($p < .001$, $\eta^2 = 0.28$). Holm-corrected post-hoc tests revealed significant differences in all six block contrasts (all $p < .01$, Cohen's $d = 0.69–1.61$), with larger asymmetry as VPOV offsets increased. Interestingly, the amount of offset did not directly correlate with a one-to-one increase in LA - while a visual offset of 10cm was given in one block, the difference in LA from VPOV_100 to VPAV_000 was only 3.8cm on average. Medians and IQR for are shown in Figure 1B.

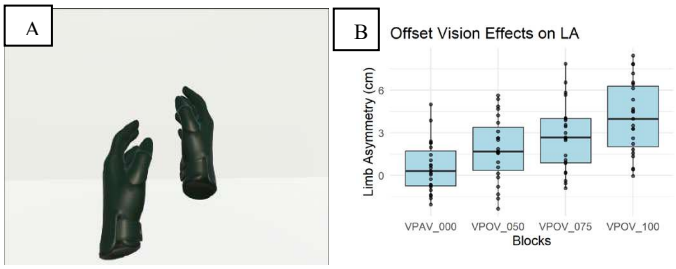

Figure 1: A. Hands during VPOV_100. While the hands are symmetric in the real world, the right hand is 10cm forward in VR **B.** Medians and interquartile range (IQR) of limb asymmetry of each block.

DISCUSSION

In line with our hypothesis, offset vision of the right hand in virtual reality increased limb asymmetry, with differences in LA increasing in a step wise fashion between all visual conditions. It appears that even with a proprioceptive reference frame from two limbs, vision still impacts motor behaviors during this specific task. However, the increase in LA was not equal to the amount of offset given. Therefore, the increased proprioceptive input from both arms during a moving task appears to limit the visual stimuli's effect on motor behavior.

The results presented are part of a larger study, which found that offset vision of the right-hand influences LA to a different extent depending on the sensory information available of the left hand (only vision or only proprioception). Future studies in our lab are looking to replicate this task, along with a bilateral target task, to both young and geriatric populations to determine age related effects on sensory reliance in virtual reality.

REFERENCES

[1] Linge AD, et al. *J Multidiscip Healthc* **17**, 5138-49, 2024.
[2] Spitzley K & Karduna A. *J Motor Beh* **54**(1), 92-101, 2022.

UNILATERAL PLYOMETRIC BIOMECHANICS FOLLOWING ECCENTRIC QUADRICEPS MUSCLE DAMAGE

Rinehart A[1, 2], Denton, AN[1,3], Dreyer, HC[2], and Hahn, ME[1, 2]
[1]Bowerman Sports Science Center, [2]Department of Human Physiology, University of Oregon, Eugene, OR USA
[3]Knight Campus for Accelerating Scientific Impact, Department of Bioengineering, University of Oregon, Eugene, OR USA
Email: aidenrin@uoregon.edu

INTRODUCTION

Eccentric muscle damage (EMD) exercise can promote greater adaptations in strength, muscle mass, and neuromuscular control than traditional concentric-focused exercise [1]. However, short-term EMD recovery creates acute force reductions and neuromuscular control alterations [1, 2]. The recovery period in lower limb muscles following EMD, particularly the quadriceps, can be extensive [3]. Understanding the timeline of functional recovery is critical for applying EMD effectively in lower limb rehabilitation and strength training. Previous compensatory profiles for quadriceps muscle fatigue, a related model of acute force reduction, suggested greater negative mechanical power at the ankle joint during plyometric landings [4, 5]. This pilot study aimed to identify the lower limb mechanics of unilateral plyometric performance during braking and propulsion phases after quadriceps EMD across the subsequent recovery period. We hypothesized that positive and negative work and power at the knee joint during unilateral plyometrics would be attenuated immediately post-EMD, accompanied by compensatory increases in positive and negative work and power at the ankle and hip joints.

METHODS

Six healthy, untrained participants (1M/5F, 20.7±0.8 yr, 60.6±7.9 kg, 168.1±6.1 cm) provided informed consent as part of a larger study. Participants performed maximal unilateral eccentric contractions (3x20 - 30°/s & 3x20 - 180°/s) augmented by continuous electrical stimulation (300 µs single-pulse, 35 Hz, 100 mA), after which the knee was immobilized for 72 hours using a knee brace, and crutches to maintain non-weight bearing. Data were collected seven days prior to EMD (Baseline), seven days post-EMD (7D), and fourteen days post-EMD (14D). Participants performed three trials of a unilateral triple hop for distance (left leg only). A 10-camera motion capture system (Motion Analysis Corp., 200 Hz) and four force platforms (Kistler, 1000 Hz) were used to collect marker displacements and ground reaction forces, respectively. The braking and propulsion phases of the penultimate stance from the trial with the largest horizontal displacement were isolated and included for further analysis. Joint work and peak power for the ankle, knee, and hip joints were calculated using standard inverse dynamics in Visual 3D (HAS-Motion). One-way repeated measures ANOVAs with a Bonferroni correction were used to evaluate condition effects ($\alpha = 0.05$).

RESULTS AND DISCUSSION

There were no significant differences across visits for jump distance ($p = 0.87$), or mechanical work ($p > 0.29$) and power ($p > 0.38$) across joints. At 7D post-EMD, trends indicated less negative work at the ankle (-5.4%) and knee (-18.4%), but greater negative work at the hip (4.0%) during the braking phase (Figure 1a). Concurrently, there was less positive work across the ankle (-6.8%), knee (-8.3%), and hip (-38.7%) during the propulsive phase (Figure 1a) at 7D post-EMD. At 14D post-EMD, positive ankle and knee work showed substantial recovery, negative ankle and knee work demonstrated moderate recovery, and both positive and negative hip work exhibited minimal recovery relative to baseline. Negative power showed similar directional trends at 7D post-EMD, with lower ankle (-2.2%) and knee (-6.2%) values but greater hip power (6.3%), whereas positive power was slightly reduced at the ankle (-1.2%), but greater negative power at the knee (4.6%) and hip (4.1%) (Figure 1b). 14D post-EMD, negative and positive peak mechanical power were greater across all joints relative to baseline, except for negative ankle power. Greater relative hip contributions to negative work during braking suggest increased reliance on the hip to absorb energy post-EMD, but this represented only a modest redistribution. The knee contributed most of the negative work, whereas the ankle was responsible for the majority of positive work and power, as well as negative power. Although positive mechanical power increased across all joints post-EMD, this apparent improvement in joint-level power production did not translate to better jumping performance.

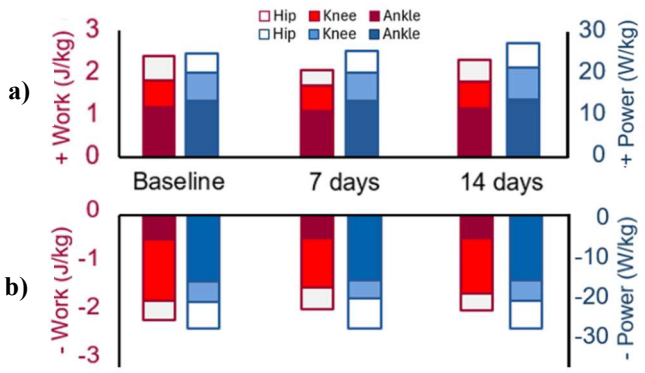

Figure 1: Mean positive (a) and negative (b) mechanical work (red) and peak power (blue) during unilateral horizontal jump braking and propulsion at baseline, 7D, and 14D after EMD.

CONCLUSION

The findings indicate that unilateral plyometric performance did not benefit from greater joint power production post-EMD, and participants continued to rely on a predominantly ankle-driven strategy despite early reductions in ankle work and power. Larger samples from trained populations may clarify whether these redistribution patterns persist or differ in sport-specific contexts.

REFERENCES

1. Hody S et al. *Front Physiol*, **10**, 536, 2019.
2. Proske U & Morgan DL. *J Physiol*, 537, 333–345, 2001.
3. Serrão FV et al. *Braz J Med Biol Res*, **36**, 781–786, 2003.
4. Chen C et al. *Sensors*, **24**, 6712, 2024.
5. Weinhandl JT et al *J Appl Biomech*, **27**, 108-115, 2011.

Kinematic Differences Across Development Levels in Elite Biathletes

Livingood, E., Burgess, I., Peach, M., Becker, J.
Food Systems, Nutrition and Kinesiology
Montana State University, Bozeman, MT USA
email: ethanlivingood@montana.edu, web: https://www.montana.edu/biomechanics

INTRODUCTION

Athletes at different stages of development differ in physiological capacity, technical skill, and coordination in Nordic skiing and biathlon. Understanding how these developmental differences are expressed in movement mechanics may help identify technique characteristics associated with progression toward higher levels of performance [1-3]. Despite the importance of skiing performance to overall biathlon success, few studies have examined whether or how these differences manifest in whole body skate skiing technique. Therefore, the purpose of this study was to compare whole-body kinematics during V2 skate skiing between junior (JN), development (D), and national team (NT) biathletes.

METHODS

Fourteen national team (NT; 8 male/6 female, age: 27.6 ± 3.9 y), nine development level (D; 6 male/3 female, age: 25.1 ± 3.9 y), and nine junior level (JN; 4 male/5 female, age: 18.0 ± 1.0 y) biathletes participated in this study. Athletes performed race-intensity roller skiing using the V2 skating technique on a ski treadmill while whole-body kinematics were recorded using markerless motion capture. A 12-segment biomechanical model was used to calculate joint angles at the shoulder, elbow, trunk, hip, knee, and ankle. Individual skiing cycles were identified as pole plant to pole plant on the right side and normalized to 100% of the movement cycle, allowing joint kinematic waveforms to be compared across groups. Statistical Parametric Mapping (SPM1D) was used to assess temporal differences in joint kinematics between JN, DEV, and NT athletes across the full skiing cycle [4].

RESULTS AND DISCUSSION

SPM identified several significant between-group differences across the skiing cycle (all clusters $p < 0.05$, Figure 1). Compared with D and NT athletes, JN athletes demonstrated greater sagittal and lateral trunk flexion prior to pole plant, greater elbow flexion during poling, less hip flexion during the ski-to-ski transition, and reduced hip abduction during the return phase of the cycle.

These findings indicate that athlete development level is reflected in distinct movement strategies during key phases of V2 skate skiing. Greater elbow flexion during poling may reflect less effective force transmission through the poles, while reduced hip abduction during the return phase may indicate reduced lateral balance control. Collectively, these results suggest that progression across development levels is characterized by improved postural control, coordination, and technical execution.

CONCLUSIONS

Athlete development level influences movement patterns during V2 skate skiing, with JN athletes exhibiting distinct kinematic characteristics compared to D and NT athletes. These findings improve understanding of how developmental differences are expressed in skate skiing and may help identify technique targets to support progression toward higher levels of biathlon performance.

REFERENCES

[1]Laaksonen et al. Front Physiol, 9, 796, 2018.
[2]Luchsinger et al. Front Sports Act Living, 1, 60, 2019.
[3]Holmberg. Scand J Med Sci Sports, 25, 100–109, 2015.
[4]Pataky. Comput Methods Biomech Biomed Engin,15,2012.

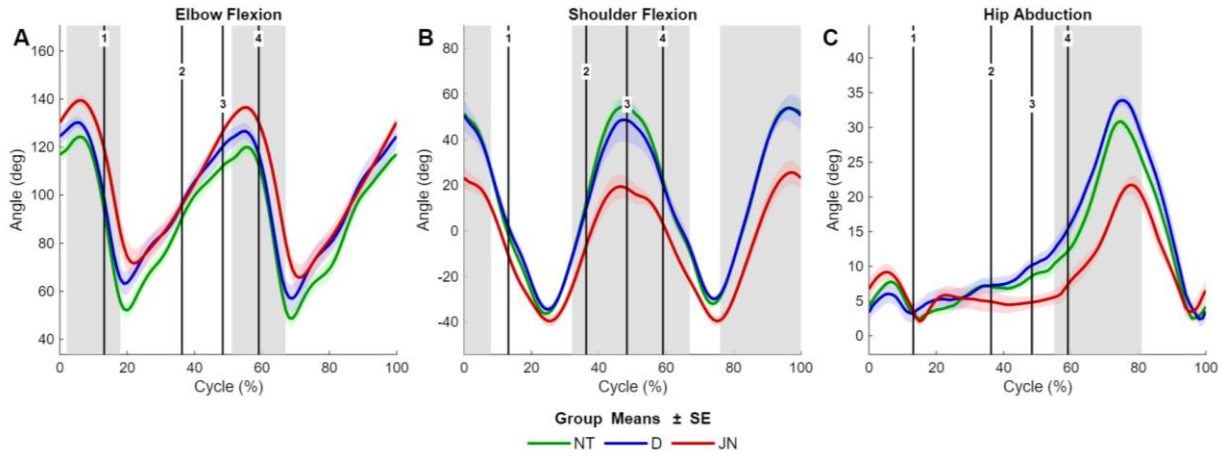

Figure 1. Group mean waveforms for elbow flexion (A), shoulder flexion (B), and hip abduction (C) across the normalized V2 skate skiing cycle in NT, D, and JN biathletes. Shaded regions indicate portions of the cycle with significant between-group differences identified using Statistical Parametric Mapping (SPM1D, $\alpha = 0.05$). Vertical event markers denote: 1) right pole off, 2) right leg peak force, 3) left ski contact, and 4) left ski peak force. The skiing cycle was normalized from right pole plant to the subsequent right pole plant.

The Relationship Between Countermovement Jump Height and Competitive Collegiate Female Swimming Performance

Lewis, AE[1], Krumpl, L[1]
[1]Department of Kinesiology and Educational Psychology
Washington State University, Pullman, WA USA
email: addyson.lewis@wsu.edu

INTRODUCTION

Swimming is a unique sport, combining explosive and aerobic power across a variety of distances and styles. Despite the mechanical and physiological differences in distance and style, all swimming competitions involve explosive start and change of direction movements. Thus, strength and power training play a vital role in preparing swimmers for their competitions. A commonly used indicator for lower extremity strength and power is the countermovement jump (CMJ). CMJs have been utilized to determine athlete readiness, and neuromuscular performance in collegiate basketball players [1]. While other factors may contribute to a college athlete's readiness (sleep, stress, workload, etc.) [2], the use of pre-competition power testing has shown to be a promising addition to athlete monitoring [1]. However, data on CMJ height and its influence on competition performance is missing in collegiate female swimmers, despite females making up 53.4% of the competitive swimming population in the United States [3]. Therefore, the purpose of this study was to determine if CMJ can be used to predict collegiate female swimmer performance.

METHODS

CMJ data were collected as part of the team's strength and conditioning program, and swim meet performance data were retrospectively obtained from team records for the 2024-2025 collegiate swim season. Twenty-six female athletes contributed data for this study. All data were de-identified, and demographic data was omitted to maintain confidentiality. Integrated into a strength training session, athletes recorded three CMJs on force plates (VALD) three times per week. Overall team mean CMJ height (cm) was calculated for each week of the season. For seasonal comparisons, CMJ values from the first and final weeks of Fall and Spring were analyzed. In addition, CMJ height of weeks immediately preceding a swim meet (n=8) were paired with team performance outcomes. These specific CMJ values were standardized using z-scores, calculated as the difference between weekly team mean CMJ height and the seasonal mean, divided by the corresponding standard deviation. Swim meet success (SMS) was defined as the total number of personal bests and seasonal bests achieved during each meet. Changes in CMJ across season and time were assessed using a two-way repeated measures ANOVA. Any main or interaction effects were followed up by post-hoc analyses following Bonferroni corrections. CMJ height and SMS relationships were evaluated using Spearman's rank-order correlation. Statistical analyses were completed via JASP (v.0.95.4), and statistical significance was set at $p < 0.05$.

RESULTS AND DISCUSSION

Analyses revealed a significant main effect of time ($p < 0.001$) and a significant interaction between time and season ($p = 0.024$). Post-hoc analyses revealed a significant increase in CMJ height throughout the Fall season ($p < 0.001$). Though CMJ height was greater at the beginning of, and peaked at the end of Spring season, these changes were not statistically significant ($p > 0.05$). The increase in CMJ height observed throughout the season is likely attributed to training adaptations. This suggests performance and readiness monitoring opportunities using CMJ height across the season. In addition, correlation analysis revealed a strong, positive relationship between CMJ performance and SMS ($\rho = 0.6$, $p = 0.11$). The two most successful meets of the season were recorded following the team's CMJ season highs. This indicates that CMJ height may provide reasonable data for coaches and athletes to suggest competition readiness and performance outcomes. Mean (± SE) CMJ height and SMS across seasons are displayed in Figure 1.

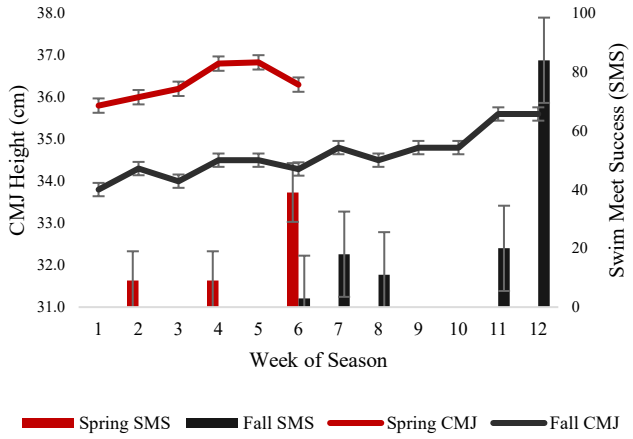

Figure 1. Mean (± SE) CMJ height (lines) and SMS (bars) data across the season (black = Fall; red = Spring).

CONCLUSIONS

CMJ height may be used as an indicator for swim performance and general power development across a competitive season in Division I collegiate female swimmers. A normalized weekly increase in CMJ resulted in overall greater SMS. Most importantly, peak seasonal CMJ height aligned with the best swim results seen in the championship meets at the end of both seasons.

REFERENCES

1. Murr, S et al. *Am J Sports Sc* 2023, ***11*** (1), 33-40.
2. Taber, CB et al. *Sci Reports* 2024, ***14*** (1), *1162.*
3. USA Swimming, M*embership Demographics Report* 2024

ACKNOWLEDGEMENTS

We thank Washington State University Strength and Conditioning, and specifically Coach Evelyn Grimm, for providing the CMJ height data.

Podium Session IV

Saturday, May 23rd, 11:15 AM – 12:30 PM

Preseason Functional Assessments May Not Predict Technical Ski Performance in Elite Biathletes

Koskela, M, Becker, J
Department of Food Systems, Nutrition and Kinesiology
Montana State University, Bozeman, MT USA
email: james.becker4@montana.edu, web: https://www.montana.edu/biomechanics

INTRODUCTION

While functional assessments are commonly used to evaluate injury risk in high level athletes, their utility for providing insight into athletic performance is less clear [1]. This might be especially relevant for technical sports where precise execution of movement skills is critical for performance. In such contexts, physical limitations identified during movement screens may constrain sport-specific movements thereby inhibiting performance [2].

Nordic skiing is one such technical sport requiring coordination and synchronization of whole-body movement. Although movement screens may not predict injury risk in Nordic skiers [3,4], their ability to provide performance insights is unclear. Therefore, the purpose of this study was to determine whether components of the Elite Athlete Health Profile (EAHP) movement screen used by the United States Olympic and Paralympic Committee (USOPC) are related to biomechanical variables associated with skiing performance in elite biathletes.

METHODS

Thirteen U.S. national team biathletes (7M, 6F, age: 27.3 $\pm$ 4.0 years, height: 175.3 $\pm$ 6.8 cm, body mass: 69.5 $\pm$ 6.9 kg) completed the EAHP administered by a certified athletic trainer. The EAHP consisted of a battery of assessments evaluating overall health and performance; from these, the Y-Balance Test (YBT), hip abduction strength (HAB), ankle dorsiflexion range of motion (AROM), and shoulder internal (IROM) and external (EROM) range of motion were selected as measures with potential relevance to ski technique. Participants then skied on a treadmill at race pace while kinematics of whole body, poles, and skis were recorded using a 16-camera hybrid motion capture system.

YBT reach distances and HAB were used as functional measures of balance and strength. On-ski balance was quantified as a composite score derived from the standardized mean COM-ankle inclination during gliding and the step-out distance at initial ski contact. Linear regression was used to evaluate whether YBT reach distances and HAB predicted on-ski balance.

Similar approaches were used to evaluate whether AROM predicted forward body position on the ski, quantified as a composite score derived from standardized mean ankle–shoulder planar angle during gliding and ankle dorsiflexion at weight acceptance, and whether shoulder IROM and EROM predicted poling range of motion, quantified using standardized surrogates of pole angle at plant and shoulder range of motion during poling.

RESULTS AND DISCUSSION

Observed verse expected plots for all three regressions are shown in Figure 1. YBT and HAB were not significant predictors of balance on the ski (R^2 = .303, p = .219). AROM did predict whether athletes obtained a forward position on the ski (R^2 = .486, p < .001). Finally, Shoulder IROM and EROM were not predictors of poling range of motion (R^2 = .134, p = .339).

CONCLUSIONS

While AROM predicted whether athletes obtained a forward position on the ski, other EAHP assessments did not predict technical ski performance outcomes. If an improvement in forward lean technique during skiing is necessary, assessing AROM could guide training outcomes. Further investigation into other functional assessments is needed to determine if there are tests that could be more beneficial to include in the EAHP to predict performance outcomes.

REFERENCES

1. Chimera, N. et al. *World J Orthopedics*, *7*(4), 202–217, 2016.
2. Hatchett, A., et al. *Sports 5*(2), 37, 2017.
3. Björklund, G., et al. *J Human Kinetics* **60,** 9-18, 2017.
4. Worth, S., et al. Int. J. Sport Phys Ther, 14(2), 237-252, 2019.

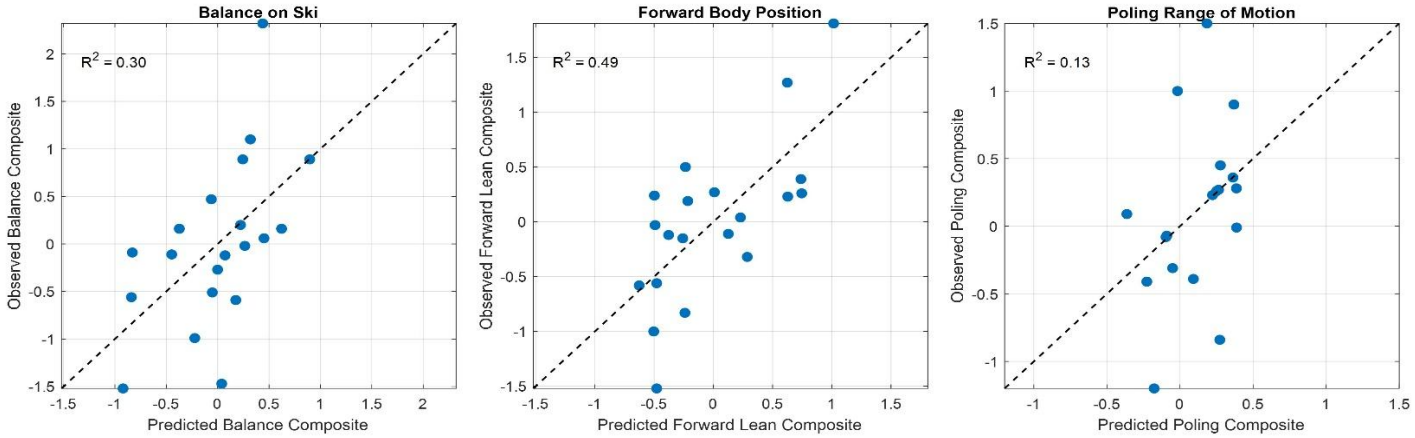

Figure 1. Plots of observed vs. expected outcomes of composite scores for each ski performance variable.

ACL RECONSTRUCTION AND KNEE OSTEOARTHRITIS INFLUENCE FRONTAL PLANE JERK BIOMECHANICS IN THE TIME AND FREQUENCY DOMAIN

Nicholas L. Hunt[1*] and Tyler N. Brown[1]
[1]Boise State University, Boise, ID, USA
*Corresponding author's email: nichunt@u.boisestate.edu

INTRODUCTION

Following ACL injury and reconstruction (ACL-R), altered neuromuscular function may accelerate knee osteoarthritis (OA) development [1]. Assessing knee jerk, or the third time derivative of knee joint angle, following ACL-R and OA may provide valuable insight into underlying gait neuromuscular control and joint loading that may contribute to long-term joint disease. Jerk cost and fluctuation analysis in the time and frequency domain may effectively assess smoothness of knee joint motion and provide a biomechanical measure of dynamic joint neuromuscular control. We hypothesize that ACL-R and radiographic knee OA individuals will exhibit "jerkier" knee motion with increased frontal plane fluctuations compared to healthy controls particularly during early stance.

METHODS

Four cohorts (1: 14 ACL-R, 2: 9 radiographic knee OA and 3: 14 healthy controls) had knee biomechanics quantified during a 10-m self-selected walk. During each walk, synchronous 3D marker trajectories and GRF data were collected using ten high-speed optical cameras and a single force platform. Marker and GRF data were lowpass filtered (12 Hz, 4th order Butterworth) and processed in Visual3D to obtain knee joint biomechanics.

Using filtered marker data, frontal plane jerk was calculated as the third time derivative of stance phase (0% to 100%) knee abduction-adduction angle, while jerk cost was determined as the area under the logarithmically transformed jerk-time curve according to [2]. Then, peak, minimum, and range (peak minus min) of stance phase frontal plane jerk as well as jerk cost during weight acceptance (initial contact to peak knee flexion angle) and stance phase (0% to 100%) were quantified.

For fluctuation analysis, the jerk-time curve was submitted to a fast-Fourier transform to obtain the signal power spectral density (PSD). From the obtained PSD, mean, median, and peak power frequency (PPF) as well as total power of the signal were calculated. Mean frequency is the weighted average frequency of the signal, median frequency splits the area under the PSD curve into two equal parts, PPF was determined as the frequency with the highest power, and total power is the area under the PSD curve. Magnitude of fluctuations were calculated as the coefficient of variance (CV, ∂/μ) of the jerk-time curve.

Jerk measures from the time and frequency domain were submitted to a non-parametric Kruskal-Wallis H test to assess cohort (ACL-R, OA, and control) differences.

RESULTS AND DISCUSSION

In partial agreeance with our hypothesis, we found significant cohort differences for time and frequency domain jerk measures. Specifically in the time domain, the ACLR and OA cohorts exhibited greater jerk range than the control cohort (p=0.002 and p=0.035), while the OA cohort exhibited significantly greater peak jerk compared to the control cohort (p=0.019). Greater peak and range of jerk in the clinical cohorts may indicate jerkier knee motion with more abrupt changes in knee positioning than they older adult controls. Further, no significant difference was observed between any cohort for frontal plane jerk cost during weight acceptance and full stance (p=0.124 and p=0.107). Despite the large increase in peak and range of jerk, insignificant differences in jerk cost suggest clinical cohorts adopt compensatory biomechanics to mitigate jerk across stance which may influence knee joint loading.

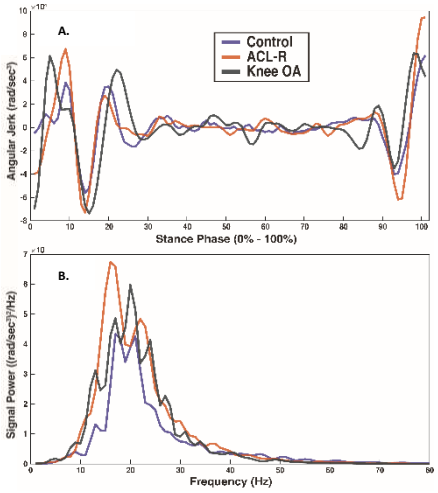

Figure 1: Depicts stance phase (0% to 100%) sagittal and frontal plane angular jerk (A) and power spectral density (B) for each cohort.

In the frequency domain, the ACLR and OA cohorts exhibited significantly smaller mean frequency than the control cohort (p=0.014 and p=0.042), and significantly smaller peak power frequency than the controls (p=0.043 and p=0.029, respectively). Although the reduction in fluctuation frequency in the jerk waveform suggest the ACLR and OA cohorts restrict gait to stabilize the joint and protect from further injury, future research is necessary to understand the relationship between fluctuation content and neuromuscular control during gait.

CONCLUSIONS

These results provide valuable insight on neuromuscular control in individuals with ACL-R and OA during walking. These individuals may exhibit harmful "jerkier" knee biomechanics and concurrently restrict frontal plane knee motion to protect the joint from further injury. Altered frontal plane jerk may indicate altered neuromuscular control and contribute to cartilage loading that elicits knee OA development or progression. Thus, clinicians need to include rehabilitation that targets smoothness of knee motion to facilitate better neuromuscular control in ACL-R and OA populations.

REFERENCES

[1] Tayfur et al. (2021), *Sports Medicine* 51.
[2] Krammer et al. (2018), *Gait & Posture* 84.

ACKNOWLEDGMENTS

NIH NIA (R15AG059655) and NIGMS (2U54GM104944, P20GM109095, P20GM148321) supported this work.

MARATHON TRAINING EFFECTS ON TIBIAL DENSITY AND STRENGTH IN A NOVICE POPULATION

Hugard, S[1], Kindl, Z[1], Hahn, ME[1]
[1]Bowerman Sports Science Center, Department of Human Physiology, University of Oregon, Eugene OR USA
Email: hugard@uoregon.edu

INTRODUCTION

Load-bearing bone continuously adapts to changes in mechanical demands. For this reason, weight-bearing exercise is recommended as a strategy for increasing bone strength and preventing osteoporosis. Running is one of the most popular forms of weight-bearing exercise globally. However, the efficacy of running as an exercise intervention for increasing bone strength has yet to be prospectively evaluated using high-resolution peripheral quantitative computed tomography (HR-pQCT). HR-pQCT is considered the gold standard for evaluating the effects of a pharmaceutical or mechanical intervention on bone strength. Therefore, the primary objective of this study is to perform an HR-pQCT investigation of the time course and magnitude of tibial bone density and strength adaptations in response to marathon training. We hypothesize that there will be a positive correlation between marathon training time and increased tibial density and strength.

METHODS

Novice recreational marathon runners aged 18-30 (n=8, 2M/6F) performed 16 weeks of standardized marathon training. This is a preliminary subset of an ongoing study with a projected sample size of 28. Dual-energy x-ray absorptiometry (DXA) scans were performed at baseline. Participants with an areal bone mineral density (aBMD) ≤ −2.0 SD relative to population averages were excluded. HR-pQCT (Xtreme CT II, Scanco CH) scans of the distal tibial metaphysis were collected at baseline and every 2-4 weeks throughout training. Changes in total volumetric bone mineral density (Tt.vBMD) were quantified with the manufacturer-supplied software. Changes in compressive failure load and stiffness were estimated using manufacturer-provided microfinite element analysis software. Linear mixed-effects models were performed in R Studio (Posit, Boston MA) to assess the effect of marathon training time on bone density and strength metrics. A linear regression analysis was performed to assess the relationship between baseline DXA leg region aBMD and change in Tt.vBMD measured by HR-pQCT after 16 weeks of marathon training.

RESULTS AND DISCUSSION

Preliminary results showed a non-significant trend of increased Tt.vBMD with marathon training time ($p = 0.07$). Notably, Tt.vBMD decreased at week 14 for most participants (Figure 1a) before recovering at week 16. This decrease in Tt.vBMD at week 14 may indicate training overload in the preceding weeks. After 16 weeks of training, the average increase in Tt.VBMD was 0.8%, and the maximum individual increase was 2.7%. This is notable as every 1% increase in peak BMD is estimated to delay osteoporosis onset by more than 1 year [2]. Failure load ($p = 0.10$), and stiffness ($p=0.10$) were not significantly associated with marathon training time. Change in Tt.vBMD after 16 weeks of marathon training was found to be significantly negatively correlated with baseline leg region aBMD (Figure 1b). This result indicates that individuals with less leg region bone mineral density at baseline had greater increases in tibial bone density in response to marathon training.

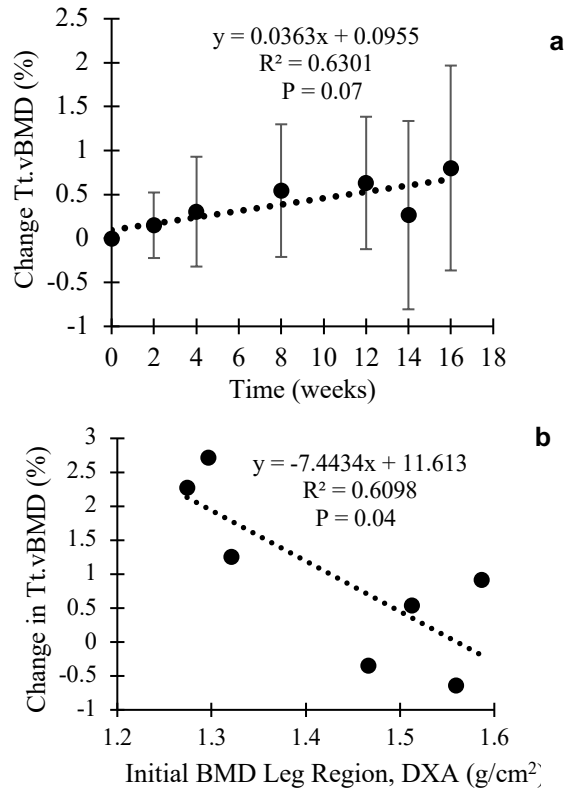

Figure 1: (a) Change in tibial metaphyseal bone mineral density vs. marathon training time (n=8). (b) Baseline areal bone mineral density vs 16-wk change in total volumetric bone mineral density (n=7).

CONCLUSIONS

Preliminary results indicate a non-significant positive trend between marathon training time and tibial Tt.vBMD. Additionally, a significant negative correlation was found between change in tibial density and initial leg region aBMD. This result suggests that marathon training may be most effective at increasing Tt.vBMD in individuals with lower baseline bone mineral density. Additional data collection is ongoing to further investigate these preliminary findings.

REFERENCES

[1] N. Mikolajewicz et al. J Bone Miner Res, 2019
[2] C. Hernandez et al. Osteoporosis Int, 2003

ACKNOWLEDGEMENTS

This work was supported by the Wu Tsai Human Performance Alliance and the Joe and Clara Tsai Foundation

Multivariate Analysis Predicting Ski Speed in Elite Biathletes

Isaac Burgess, Ethan Livingood, Brandon Cabaniss, James Becker
Department of Food Systems, Nutrition and Kinesiology, Montana State University, Bozeman, USA
email: isaacburgess@montana.edu

INTRODUCTION

Physiological performance measures from laboratory testing predict between 50-60% of the variance in ski speed during biathlon competitions [1]. While numerous studies have shown gross-biomechanical measures such as cycle length and rate influence ski speed [2], it is unclear whether kinematic and kinetic markers of ski technique measured in laboratory assessments also predict ski speed in races. Therefore, the purpose of this study was to evaluate whether laboratory based biomechanical assessments of ski technique predicts ski speed in elite biathletes.

METHODS

Elite-biathletes from the U.S. National (N; n=9), Development (D; n=6), and Junior National (J; n=8) teams (12M/11F, 24±5years) skied on a rollerski treadmill at race intensity. Kinematics were captured with motion capture while forces applied to the ski were measured using plantar-pressure insoles. Biomechanical variables which are important for achieving high ski speeds during V2 skating were then calculated including: anterior-posterior center of mass - ankle angle of the pole at plant (θAP), step out distance (dstep) and V-angle (Vθ) at ski contact, mean mediolateral center of mass - ankle inclination angle (θML) and mean asymmetry in mediolateral plantar pressure (ASI) while gliding, peak knee angular velocity (ωknee) while preloading the ski, and peak force applied to the ski (Fpeak) while pushing. Between 4-6 weeks following biomechanical assessment all athletes competed in a biathlon sprint competition on matching rollerskis, where average ski speed was measured.

Variables significantly correlated with ski speed were entered into a principal component analysis [3]. Variables loading onto each principal component were standardized and averaged to create surrogate scores representing each underlying factor [4]. Surrogate scores were then entered a multiple regression to evaluate their ability to predict ski speed.

RESULTS AND DISCUSSION

Table 1. PCA with varimax rotation of biomechanical variables correlated with ski speed (n = 440).

Factors	Pressure Balance (*P*)	Stacked Skiing (*S*)	Force Production (*F*)
Eigenvalue	3.506	1.754	1.167
% of Variance	43.8	21.9	14.6
ASI_{MAX}	0.952		
ASI_{UNLOAD}	0.908		
ASI_{AVG}	0.853		
θML_{MAX}		0.889	
dstep		0.879	
θML_{AVG}		0.876	
Fpeak			0.889
ωknee			0.679

Note. MAX – maximal value during gliding, UNLOAD – value at peak force unloading (glide-to-push transition), AVG – average value across gliding

Three principal components were extracted, accounting for 80.3% of the total variance in the data (Table 1). Based on variable loading patterns they were interpreted as Factor 1 representing pressure distribution underfoot; factor 2 representing stacking the body over the gliding ski; and factor 3 representing efficient preloading of the ski and applying force during the push. Surrogate variables accurately captured their respective factors (R^2 > 0.95). Multiple regression analysis showed that 50.2% of the variance in competition ski speed was explained by pressure balance, stacked skiing, and force production ($F_{3,19}$=6.38, p=0.004; Figure 1).

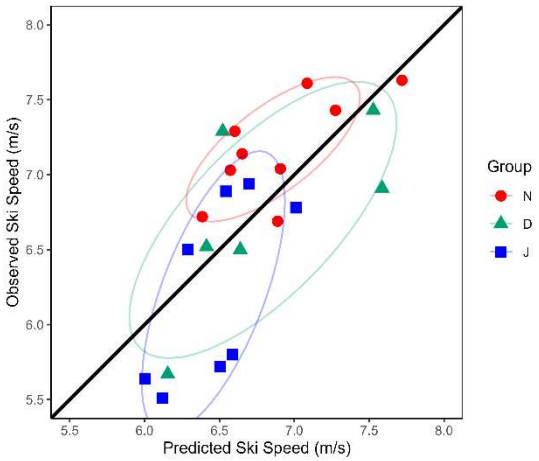

Figure 1. Multiple regression model performance for predicting mean ski speed. Groups of athletes are shown with 1-SD confidence ellipse. Model Eq: *Ski Speed = 6.7 – 0.3*P – 0.1*S + 0.4*F*

These results suggest an even pressure distribution across the foot, stacked body alignment over the ski, and greater preloading and pushing are important for maximizing ski speed during biathlon competitions. These may be indicative of faster skiers using a body positioning which allows for more propulsive forces as well as more effective use of the stretch shortening cycle in leg muscles for greater force production. These are also areas which can be targeted for coaching interventions, and should improve as athletes progress across development levels (Figure 1).

CONCLUSIONS

These findings suggest even pressure under the foot, balancing over the ski, and preloading and pushing are key factors for achieving high ski speeds in competition environments. Future studies should confirm whether these same factors also predict ski speed on variable surfaces like snow.

REFERENCES

[1] Laaksonen et al. Front Sports Act Living. 2020 Aug 5;2.
[2] Zoppirolli et al. J Sports Sci. 2020; 38, 2127-2148.
[3] Köykkä et al. Scand J Med Sci Sports. 2022;32(2):414–23.
[4] Ramsey & Schafer. The Statistical Sleuth 3rd ed. 2013

EFFECT OF TWO WARMUPS ON DEADLIFT AND COUNTERMOVEMENT JUMP PERFORMANCE: A POST ACTIVATION POTENTIATION STUDY

Schlittler, SE[1], Hanchey, J[1], and Bailey, JP[2]
[1]Department of Movement Sciences
University of Idaho, Moscow, ID, USA
Email: sschlittler@uidaho.edu

INTRODUCTION

Post-activation potentiation (PAP) refers to the short-term enhancement of muscular performance following a high-intensity, non-fatiguing contraction. This effect is thought to occur through mechanisms such as phosphorylation of myosin regulatory light chains, which increase calcium sensitivity, and enhanced neural drive resulting in greater motor unit recruitment. When appropriately balanced with fatigue, PAP may transiently improve force and power production during subsequent explosive tasks. Previous research has demonstrated that isometric contractions can elicit PAP and enhance performance outcomes. The purpose of this study was to assess the effects of different warm-up protocols, including isometric pulls, on strength and power performance. Strength was evaluated via peak force production in the deadlift, while power was assessed using countermovement jump (CMJ) performance. It was hypothesized that isometric pulls would increase propulsive reactive strength index (RSI) during the CMJ, as well as increase jump impulse at takeoff and increased jump height.

METHODS

Nine recreationally active college aged males [Age (years): 20.33(1.22), Height (m): 1.77(0.10), Mass (kg): 86.58(7.50), and 3RM Load (kg): 163.81(19.18)] participated in three sessions. Session 1 (S1) started with a self-selected warmup and included a 3-repetition maximum (3RM) test. The load achieved in S1 was used to estimate 1RM (e1RM) and subsequent loads for the other sessions. For sessions 2 (S2) and 3 (S3), the participants performed an assigned dynamic warmup including ten air squats, ten goblet squats with a self-selected kettlebell weight, eight hip hinges (same kettle bell or body weight), and 10 banded pull-throughs. S2 and S3 session specific warm-up conditions (conventional deadlift [1 set of three repetitions at 75%, 83%, and 90% of e1RM] and an isometric mid-thigh pull [3 max effort 5 second pulls with bar at the midthigh position]) were counterbalanced. Prior to the session specific warm-up, participants performed a series of 2 countermovement jumps (CMJ) for a baseline measure. Immediately following the session specific warm-up, they performed a second set of 2 CMJ followed by 3 deadlift repetitions at 93% e1RM. Participants were allowed 45-90 seconds of rest between the load assignments. CMJ performance was assessed with calculated jump height (m), jump impulse (Ns), reactive strength index (m/s), and the potential influence of the warm-ups were analyzed using multiple 2 by 2 (Warm-up by time) ANOVAs.

RESULTS

The effects of session and time on jump height, reactive strength index (RSI), and impulse were examined using a 2 × 2 repeated-measures ANOVA. A significant main effect of time was observed for jump height [$F(1, 8) = 8.66$, $p = .019$, $\eta p^2 = .52$], with higher values post compared to pre. No significant main effect of session [$F(1, 8) = 1.45$, $p = .263$, $\eta p^2 = .15$] or session × time interaction [$F(1, 8) = 4.07$, $p = .078$, $\eta p^2 = .34$] was observed for jump height. No significant main effects or interactions were found for RSI (session: $F(1, 8) = 0.01$, $p = .947$; time: $F(1, 8) = 1.45$, $p = .263$; interaction: $F(1, 8) = 0.47$, $p = .514$) or impulse (session: $F(1, 8) = 0.57$, $p = .470$; time: $F(1, 8) = 0.01$, $p = .941$; interaction: $F(1, 8) = 1.02$, $p = .341$). These findings indicate that jump height improved over time, while reactive strength and impulse remained unchanged.

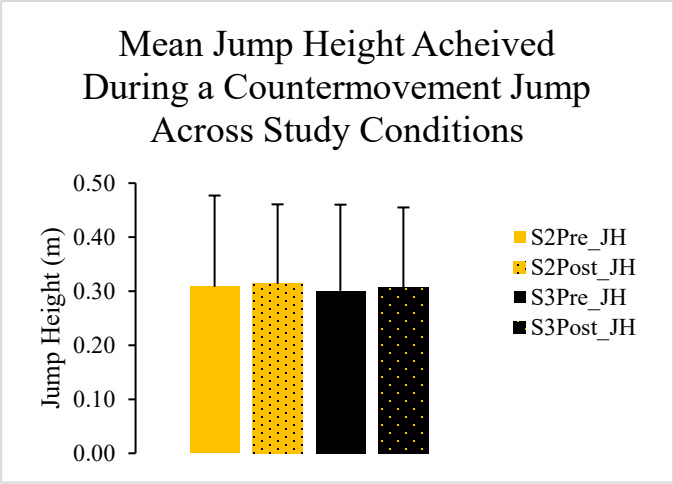

Figure 1: Mean jump height (m) achieved across participants for the four times assessed. Standard deviation for each mean is represented by error bars.

CONCLUSIONS

Jump height significantly increased from pre to post, while reactive strength index and impulse showed no significant changes. No session or interaction effects were observed for any variable. This suggests that improvements in jump performance were not driven by changes in reactive strength or impulse and may instead reflect other neuromuscular or technical factors.

REFERENCES

1. Hodgson M, et al. *Sports Med.* **35**(7), 585-595, 2005.
2. Prieske O, et al. *Sports Med.* **50**, 1559-1565, 2020.
3. Tillin NA, and Bishop D. *Sports Med.* **39**(2), 147-166, 2009.
4. Arabatzi F, et al. *Pediatr. Exerc. Sci.* **26**, 187-194, 2014.
5. Blazevich AJ, and Babault N. *Front. Physiol.* **10**:1359, 2019.

ACKNOWLEDGEMENTS

We would like to thank the ISMMAL team for all of their hard work and dedication.

Podium Session V

Saturday, May 23rd, 2:25 – 3:40 PM

EFFECT OF VOLITIONAL HEAD TURNS ON DYNAMIC STABILITY DURING WALKING TURNS

Aderonmu, JA, Curtze, C
Department of Food Systems, Nutrition, and Kinesiology
Montana State University, Bozeman, MT USA
email: joseph.aderonmu@montana.edu

INTRODUCTION

During daily locomotion, humans frequently perform volitional head turns to explore their environment. Turning involves a coordinated "top-down" sequence of head, trunk, and pelvis reorientation until the body is aligned in a new heading direction [1]. Volitional head turns directed opposite the heading direction (head turns) can occur during turning and deviate from this sequence. These head turns introduce additional vestibular demands on the postural control system [2] in addition to ongoing turning requirements. Yet the effect of head turns on dynamic stability during turning remains unexamined.

In this study, we aim to quantify the effect of head turns on dynamic stability during turning. We assess dynamic stability using the margin of stability (MoS), a measure of instantaneous mechanical stability [3]. We hypothesize that mediolateral (ML) MoS will become more positive on the inside limb and less positive on the outside limb during turning with head turns compared to turning without head turns.

METHODS

Twenty healthy young adults (age: 26.7 ± 3.89 years; 10 females) completed 90° walking turns (left and right) and straight-ahead walking under laboratory conditions. Trials were performed with and without head turns at both self-selected normal and fast walking speeds (42 randomized trials). Participants walked through an initial gate and, for turning trials, proceeded into a second gate requiring a 90° turn. During trials with head turns, participants rotated their heads opposite to their direction of travel to identify a shape displayed in the contralateral visual field. During straight-ahead walking trials, head turns were directed either left or right, as instructed, to identify a displayed shape.

Whole-body kinematics were recorded at 100 Hz, processed in Visual3D, and filtered with a 4th-order dual-pass Butterworth filter (6 Hz cutoff). CoM and marker positions were exported to MATLAB (R2025a) and transformed into a pelvis-fixed reference frame to account for changes in body heading relative to the global reference frame during turning [4]. The extrapolated CoM (XcoM) was computed as the CoM position with its velocity scaled by the eigenfrequency of the inverted pendulum [2]. Mediolateral MoS was calculated as the difference between the XcoM and the maximum ML extents of a piecewise base of support boundary constructed from metatarsal and calcaneus markers. Linear mixed effects models examined the effects of head turns (No Head Turn/Head Turn), walking speed (Normal/Fast), and Stepping limb (Inside/Outside) on ML MoS ($\alpha = 0.05$).

RESULTS AND DISCUSSION

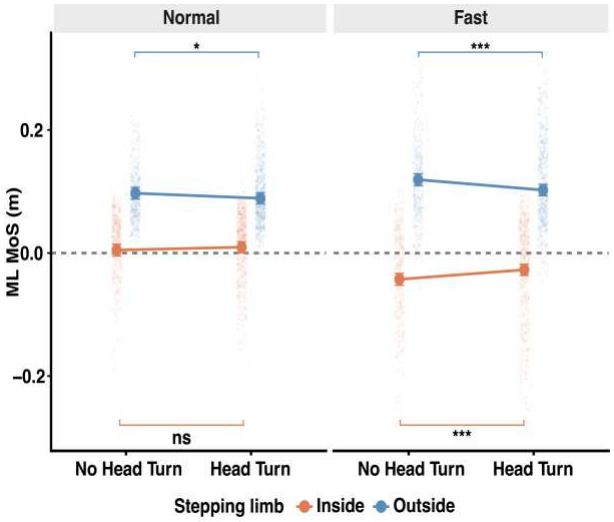

Figure 1: Head turns alter mediolateral margin of stability (ML MoS) during walking turns. Mediolateral MoS was less positive at both normal and fast walking speed for the outside limb, but more positive only during the fast walking speed on the inside limb. * $p < 0.05$, *** $p < 0.001$, ns: not significant.

With head turns, ML MoS became more positive on the inside limb, but only at fast walking speed ($p < 0.001$, Figure 1). In contrast, ML MoS became less positive on the outside limb at both normal and fast walking speeds ($p < 0.05$). A negative ML MoS indicates that the extrapolated center of mass exceeds the lateral boundary of the base of support, reflecting a transient instability that facilitates change in direction. Our results suggest that, at fast walking speeds, head turns reduced the controlled instability required to initiate turning on the inside limb. On the outside limb, head turns reduced the lateral stability available to guide the turning trajectory across both speeds.

CONCLUSION

Head turns performed during turning imposed measurable alterations in ML stability control. These alterations may provide a sensitive measure of functional decline in populations with impaired sensorimotor integration, such as older adults and individuals with neurological disease.

REFERENCES

1. Grasso R. et al. *Neuroreport*, **26**;7(6):1170-4, 1996.
2. Marchetti et al. *Phys. Ther,* 88(5):640-51. 2008
3. Hof AL et al. *J. Bmech,* **38**(1):1-8, 2005.
4. Ho TK et al. *J. Bmech* **151:**111544, 2023.

DEVELOPMENT OF A COMPUTATIONAL MATTRESS MODEL FOR MOTHER-INFANT BEDSHARING

Lee, D[1], Wortmann, O[1], McCartney M[1], Wilson C[1], Fitzpatrick C[1], Quinlan, KP[2], Lowell, G[2], Mannen, E[1]
[1]Boise State University, Boise ID; [2]Rush University Children's Hospital, Chicago, IL
Email: dawsonlee@u.boisestate.edu, web: https://www.boisestate.edu/coen-babi/

INTRODUCTION

Sixty percent of sudden infant deaths from 2011 to 2020 occurred when the infant shared a sleep space with another person [1]. However, the mechanisms behind the bedsharing hazard remain unexplored from a biomechanics lens. We need to better understand how mechanical factors within the sleep space influence an infant's ability to move into hazardous positions that increase risk of suffocation. To avoid risking injury during in vivo studies, a finite element simulation is needed. The purpose of this study is to develop a finite element (FE) model that will allow for greater precision in identifying the specific factors that affect infant safety during bedsharing.

METHODS

Physical data collection was utilized as the baseline of the FE model to showcase the complex reactions seen in mattress deformation. Known point loads from 0 to 70 newtons were placed onto a mattress using a weighted rod in 10 newton increments (Figure 1). This range of forces allows tests for static and dynamic forces in the sleep space. Deformation at and around the load was measured with an 8 camera Qualisys motion capture system with sub-0.5mm accuracy. Linear interpolation between tested areas was used to design a computer model composed of one-inch squares on the mattress.

To determine accuracy, the deformation of a simple dispersed load was measured by laying a 25lb (111 N) 11 in, round plate across the mattress surface. The weight was then recorded using the same Qualisys system This known distributed deformation was then used to calibrate the measured point loads and will be used to rebuild more complex anatomical designs for parents and infants.

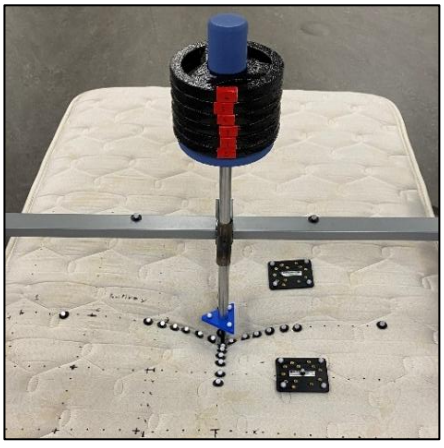

Figure 1: Weighted rod applying 70N of force to mattress with motion capture markers

RESULTS AND DISCUSSION

Point load estimates showed an average error of 2.87 mm with a standard deviation of 1.42 mm. Using the computational model, deformations can be estimated by overlaying weighted objects across the model grid (Figure 2). With this method of determining deformations, specific mother infant pairs can be modeled computationally, and safety risks can be assessed.

By accurately measuring the deformation of mattresses by complex forces, a better understanding of bedsharing risks can be studied. Deformations decrease the muscular force required for rollover in infants, meaning that understanding how a mattress deforms or creates inclined microenvironments, can better inform how hazardous inclines are created by bedsharing. With a computational solution, many simulations can be conducted, and a large amount of information can be gathered without conducting potentially dangerous and costly in-person testing. This will better inform parents of potential hazards within the bedsharing space.

Ten collections will be conducted to provide a wide variety of surfaces to utilize in the FE model. This will allow testing between new and older mattresses as well as air mattresses.

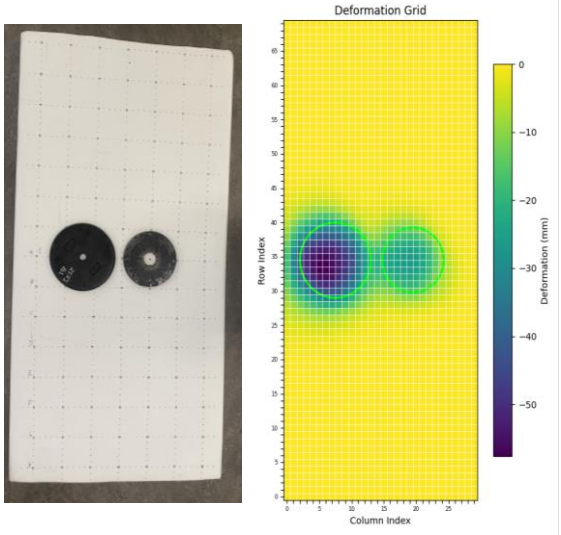

Figure 2: Physical load compared to simulated deformation

REFERENCES

[1] Lambert *et al*, Pediatrics, 2024

ACKNOWLEDGEMENTS

This research is supported by the American SIDS Institute. EMM owns Mannen Bio, LLC, an expert and engineering consulting company.

THE RELATIONSHIP BETWEEN BREATHING BIOMECHANICS AND BODY POSITION IN INFANTS

Olvera, H[1], Wilson, C[1], Carroll, J[2], Whitaker, B[2], Fitzpatrick, C[1], Mannen, E[1]
[1]Department of Mechanical and Biomedical Engineering, Boise State University, Boise, ID, USA
[2]Arkansas Children's Research Institute, Little Rock, AR, USA
email: HollyOlvera@u.BoiseState.edu

INTRODUCTION

Infants in the US spend ~ 5.7 hours per day in seated products like bouncers, rockers, and swings [1,2]. These products often place infants in higher head-neck flexion and slouched trunk positions – postures which can increase the risk of respiratory-related problems and positional asphyxiation. Previous research has not explored respiratory mechanics in relation to trunk posture for healthy non-sedated infants. Therefore, the purpose of this study aims to evaluate relative torso expansion in a 45° thoracic flexion environment compared to a flat surface.

METHODS

Five healthy full-term infants (2F/3M) participated in the IRB-approved longitudinal study. Infants completed three laboratory sessions (1-2, 3-4, and 5-6 months old). Infants were placed supine in two conditions: 0° flat (baseline) and 45° thoracic flexion. An eight-camera Qualisys motion capture system collected positional data of 23 retroreflective markers (Figure 1). A Medtronic Capnostream 35 Portable Monitor recorded respiratory rate and a Masimo Rad 97 Pulse Oximeter recorded heart rate simultaneously for each condition. Each condition was collected for 2-5 minutes of calm breathing. Marker data was segmented into individual breaths using MATLAB, where the peaks were identified as the inhale (larger torso expansion) and troughs were identified as the exhale (smaller torso expansion). Percent change of torso expansion was calculated between the peak and trough of each cycle. Two-tailed t-tests were used to compare results from the flat surface vs. 45° thoracic flexion across each age bin ($p<0.05$).

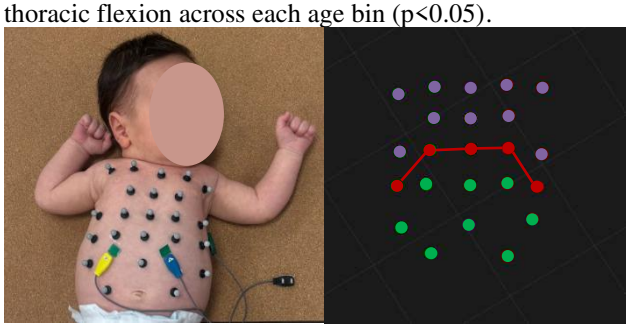

Figure 1: Unique marker placement on an infant participant (left). Designated marker regions for calculations, purple: chest, red: rib cage, and green: abdomen (right).

RESULTS AND DISCUSSION

Our preliminary findings suggest that posture may influence relative torso expansion (Figure 2). When lying flat, infants demonstrated greater ability to expand their torso while breathing (~8-12% change). In contrast, when placed at 45° thoracic flexion, infants demonstrated consistently smaller torso expansion (~3-7% change). Larger changes represent larger displacement of the torso per breath, whereas smaller changes represent reduced torso expansion. Descriptive statistics for respiratory rate and heart rate across each age bin and position are shown in Table 1, yet no clear trends were identified due to the n=5 sample size.

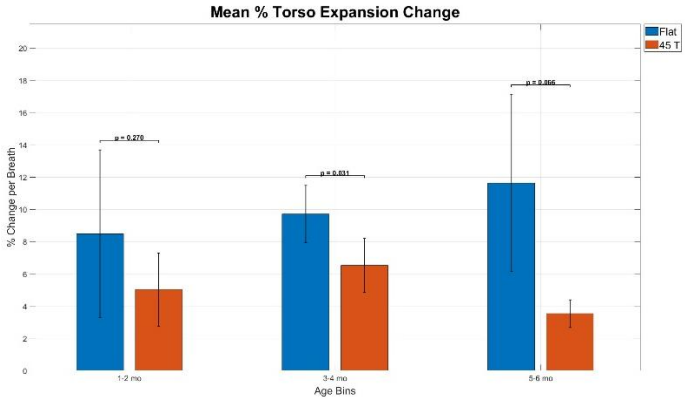

Figure 2: Comparison of the mean percent change of torso expansion for infants in the flat and 45° thoracic flexion (45T) conditions.

Table 1: Mean and standard deviations of the recorded respiratory rates (RR) and heart rates (HR) by age group (1-2 months, 3-4 months, 5-6 months) and condition (flat vs. 45° thoracic).

Age Group	Condition	RR (breaths/min)	HR (beats/min)
1-2 mo	Flat	48.4 ± 5.8	152.8 ± 7.6
1-2 mo	45 T	43.4 ± 10.6	137.6 ± 8.4
3-4 mo	Flat	51.7 ± 9.2	140.3 ± 4.8
3-4 mo	45 T	52.3 ± 12.9	142.3 ± 3.2
5-6 mo	Flat	44.5 ± 8.0	144.6 ± 13.4
5-6 mo	45 T	49.2 ± 5.8	134.1 ± 14.9

CONCLUSIONS

Our findings demonstrate that trunk posture may influence breathing mechanics in early infancy. Infants in a slouched trunk position exhibited reduced torso expansion as compared to flat laying infants. This reduction in thoracic expansion may negatively impact respiratory efficiency as infants are primarily belly breathers. Our future work includes processing data for the next 25 infants who have completed the study, exploring other tested postures, and comparing longitudinal data.

REFERENCES

1. Little et al. (2019), *Inf Beh & Dev*. 2. Callahan et al. (1997), *Arc Peds & Ado Med*.

ACKNOWLEDGEMENTS

This research is supported by the NICHD, NIH Grant No, 1R01HD113921. EMM owns Mannen Bio, LLC, an engineering and expert consulting company.

MOTHER-INFANT MOVEMENT AND INTERACTION DURING BEDSHARING

Benavidez, Y[1], Beasley, L[1], McCartney, M[1], Wilson, C[1], Quinlan, KP[2], Lowell, G[2], Mannen, E[1]
[1]Mechanical & Biomedical Engineering, Boise State University, Boise ID; [2]Rush University Children's Hospital, Chicago IL
email: yafabenavidez@u.boisestate.edu

INTRODUCTION

Sharing a sleep-surface (i.e. co-sleeping or bedsharing) nearly triples the risk of sleep-related Sudden Unexpected Infant Death [1]. Airway obstruction or chest compression from soft bedding, wedging, overlay, or a combination of these can lead to suffocation in a bedsharing environment [2]. However, there is little biomechanical understanding of bedsharing and limited research on the bedsharing environment overall. This study seeks ways to quantify biomechanical data obtained from video of mother-infant dyads during bedsharing, and investigate potential relationships between airway risks to the infant and biomechanics unique to bedsharing.

METHODS

Three mother-infant dyads were recorded using a single night-vision camera (Phasm Cam) during bedsharing in their own home for two nights. Infants were aged 1.0-2.9 months for the first, and 3.0-4.9 months for the second collection. A calibration grid (checkerboard pattern) was used to define a 2D-plane on the sleep surface. Videos were reviewed to mark instances of observed airway risks including facial occlusion by soft bedding, overlay, or sleep-surface, and overlay on the chest or neck. Methods in Python and OpenCV were developed to create visual maps representing spatial body positions over time, and calculate bedspace occupied by the dyads, and mother-infant overlap.

RESULTS AND DISCUSSION

Each dyad presented unique bedsharing habits. Total bedspace occupied by mother and infant throughout the night are shown in Figure 1. Positional maps shown in Figure 2 reveal various movement patterns, and mother-infant relative locations. Mother-infant contact and exposure to airway risks in Table 1 further establish variability. Mothers 1 and 2 slept with their infants in close proximity, and mother 3 placed their infant in an in-bed sleeper. Dyads 1 and 2 were in contact most of the night, and had a greater percent of overlapping bedspace.

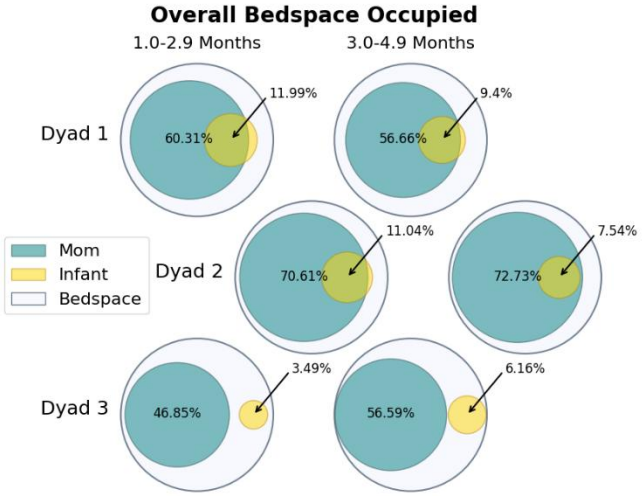

Figure 1: Area of bedspace occupied by mother and infant over full night of bedsharing, and relative overall bedspace.

CONCLUSIONS

A novel method of evaluating mother-infant biomechanics during bedsharing was developed and evaluated with three participants of a larger study on the biomechanics of bedsharing. Greater overlapping bedspace as determined by the position maps may increase suffocation risks, however potential factors contributing to airway risks during bedsharing are not exclusive to those presented here requiring further analysis. Future work will increase sample size, and analyze further biomechanical factors such as mattress firmness and rolling.

REFERENCES

1. Moon et al., Pediatrics 150, 2022
2. Lambert E, et al. Pediatrics 153, 2024

ACKNOWLEDGEMENTS

Supported by the American SIDS Institute. EMM owns Mannen Bio, LLC, an engineering and expert consulting company.

Table 1: Duration of contact and possible exposure to airway risks as percent of time spent bedsharing.

	Dyad 1		Dyad 2		Dyad 3	
Infant Age Months	**2.9**	**4.2**	**1.7**	**3.6**	**1.0**	**3.4**
Contact	>99.9	99.3	79.2	95.9	<0.1	<0.1
Airway Risk	20.4	19.5	2.9	0.3	0.1	<0.1

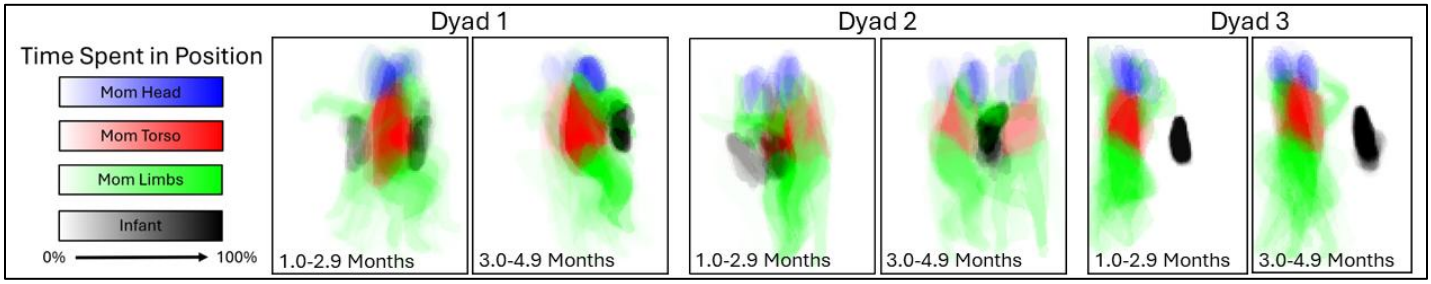

Figure 2: Maps showing dyad spatial positions while bedsharing. Darker colors represent longer time spent in a given space.

DOES PREFONTRAL CORTEX ACTIVATION PREDICT DECISION-MAKING PERFORMANCE ON A REACTIVE JUMP LANDING TASK?

Aflatounian, F[1], Lynch, A[1], Becker, J[2], Hutchison, K[3], Pew, C[1], and Monfort, S[1]
Departments of [1]Mechanical and Industrial Engineering and [2]Food Systems, Nutrition and Kinesiology, [3]Psychology
Montana State University, Bozeman, MT USA
email: fatemehaflatounian@montana.edu

INTRODUCTION

Anterior cruciate ligament (ACL) injuries happen often without contact in sport and are frequently linked to interruptions in cognitive–motor control during unanticipated movements [1]. Although biomechanical risk factors have been widely studied, growing evidence suggests neural processes underlying visuomotor coordination and attention control as risk factors. Functional near-infrared spectroscopy (fNIRS) enables non-invasive measurement of cortical activation during dynamic tasks. This study examined whether prefrontal cortex activation (PFC) during an attention control task relates to decision-making performance through unanticipated jump-landings associated with ACL injury risk

METHODS

Thirty-one healthy recreational athletes (15F/16M; 23.1±2.6years) completed a computerized attention-control battery [2] while wearing an fNIRS cap targeting Brodmann areas (BA) 46 and 9. Neural activation (t-statistics) was derived using an autoregressive iterative reweighted least squares general linear model with short-separation channel regressors. Participants performed unanticipated conditions that included a simple task (Simple) of landing on the limb towards an image on one side of the screen, and a complex task (Complex) of landing on the limb towards a picture of the basketball or away from a simulated opponent. Failed trials involved incorrect cue responses and landing on the wrong limb(s). Failed trial percentage (Failed%) was calculated for each cognitive condition. Pearson correlations tested associations between fNIRS activation and Failed%.

RESULTS AND DISCUSSION

PFC in BA46 and BA9 showed no significant correlations with Failed% in either challenging condition ($p > 0.05$, Figure 1). Small-to-moderate effect sizes ($|r| \approx 0.3$) suggested a nonsignificant trend toward fewer failed landings with greater prefrontal activation.

PFC measured during isolated cognitive testing was not associated with decision-making accuracy during dynamic jump-landings, suggesting that landing errors were not explained by baseline cognitive activation. Instead, failures likely reflected task-specific cognitive–motor demands during reactive movement. This aligns with behavioral work showing that attention-control tests typically demonstrate only small–moderate associations with task accuracy ($r \approx 0.20–0.40$), underscoring the challenge of capturing cognitive variability through isolated tasks alone. Future work should incorporate real-time neural measures and refined task designs to better characterize rapid cognitive load fluctuations preceding movement error.

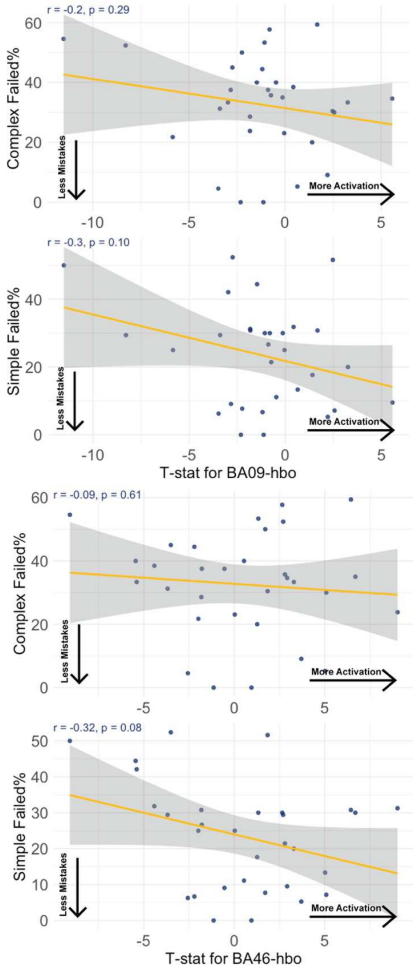

Figure 1: Scatterplots of T-stats for BA9 (up) and BA46 (down) and Failed% of simple and complex jump-landing

CONCLUSIONS

Prefrontal cortex activation measured during an isolated attention-control task was not significantly associated with failed decision-making during unanticipated jump-landings. These findings suggest that ACL injury–related landing errors are likely driven by cognitive–motor demands that occur during the dynamic task itself rather than baseline cognitive activation measured at rest.

REFERENCES

1. L. Chia, et al. *Sports Med* **52**, 2447-2467, 2022
2. Burgoyne, et al. *J Exp Psychol Gen* **152 (8)**, 2369–2402, 2023

ACKNOWLEDGEMENTS

This research was supported by the MSU NACOE TEER grant and MSU NRT seed grant. We would also like to thank Luke Juergensen, Max Johnsen and Sophie Stemler for their help in collecting data.

Poster Session A

Friday, May 22nd 5:10 – 6:10 PM

EFFECT OF RUNNING SPEED AND FATIGUE ON VERTICAL CENTER OF MASS DISPLACEMENT

Eastin, A[1], Hugard, S[1], Hahn, M[1],
Bowerman Sports Science Center, Department of Human Physiology, University of Oregon, Eugene, OR USA
email: aeastin@uoregon.edu

INTRODUCTION

Through training, individuals may be able to change mechanical characteristics to reach their optimal running form [1]. Previous research has shown that greater vertical center of mass (COM) displacement during running is associated with reduced efficiency and increased bone stress injury risk in collegiate runners [2]. Therefore, monitoring and modifying COM displacement during training may serve as a practical strategy to improve running efficiency and potentially reduce injury risk. Understanding how running conditions such as speed and fatigue influence COM displacement may provide insight into biomechanical changes that occur during prolonged running and their potential implications for injury risk and running efficiency. Therefore, the goal of this work is to determine if vertical COM displacement is affected by different speed and fatigue conditions during running.

METHODS

Recreational runners (n=6; 1 F, age 18-30) performed 3 running trials at high and low speed and fatigue conditions (Table 1). Reflective markers were placed on each participant's trunk and lower extremities, using a common marker set. Marker position data were collected at 200 Hz using an eight-camera motion capture system (Motion Analysis Corp., Rohnert Park, CA). Participants ran at 80% of their speed at lactate turnpoint (LTP) for the low-speed conditions, and at 105% LTP for the high-speed condition. A fatigued state was achieved by having participants run to volitional exhaustion at 105% LTP before performing the low-speed, high-fatigue trial. Marker position data were collected at minute eight for 30 seconds during each trial. An inverse dynamics model was used to calculate running kinematics and kinetics. Whole body COM was estimated as the pelvis center. Displacement of the COM was calculated as the difference between the vertical maximum and minimum COM position at each step and was averaged over the 30 seconds of data collected for each trial in MATLAB (Mathworks, Natick MA). Two paired t-tests were performed to assess whether average vertical COM displacement differed with changes in speed or fatigue. Trials 1 and 2 were compared to assess the effects of speed on vertical COM displacement, and trials 1 and 3 were compared to assess the effects of fatigue (Table 1).

RESULTS AND DISCUSSION

Trials run at the low-speed condition showed a higher average COM displacement compared to the high-speed trial. A significant difference in vertical COM displacement was found between high and low speed trials (p=0.003) performed under low-fatigue conditions (Figure 1). No significant difference in vertical COM displacement was found between low- and high-fatigue states (p=0.631) performed at the same relative intensity (80% of LTP) (Figure 1). These findings suggest that running speed has a greater influence on vertical COM displacement than fatigue during running.

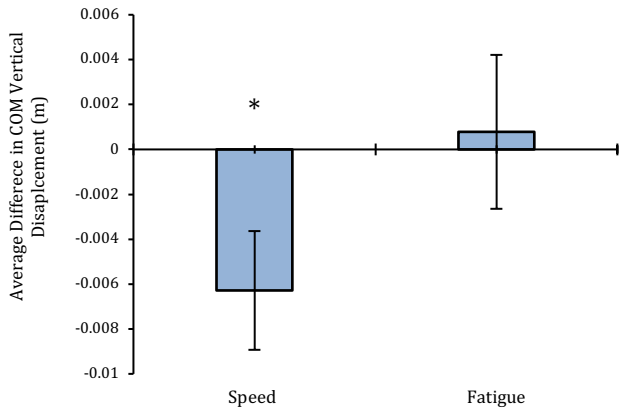

Figure 1: Average COM vertical displacement differences between high and low speed and fatigue trials. * p <0.05

CONCLUSIONS

Vertical COM displacement was found to be significantly different between high- and low-speed conditions, but not between fatigue conditions. These findings indicate that studies which evaluate COM displacement during running should control for speed conditions. Additionally, this work indicates that vertical COM displacement may be reduced by having athletes run at higher speeds.

REFERENCES

1. Anderson T. 1996. *Sports Medicine*. 22(2):76–89.
2. Joachim et al. 2023. *J Orthop Sports Phys Ther.* 53(12):761–768.

ACKNOWLEDGEMENTS

This work was supported by the Wu Tsai Human Performance Alliance and the Joe and Clara Tsai Foundation.

Table 1: Average COM displacement over each running condition

Running Speed and Fatigue Conditions	COM Displacement (m)	Normalized to Height (%)
Trial 1: Low Speed, Low Fatigue	0.11 ± 0.0071	5.84 ± 0.48
Trial 2: High Speed, Low Fatigue	0.099 ± 0.0086	5.50 ± 0.57
Trial 3: Low Speed, High Fatigue	0.11 ± 0.0053	5.90 ± 0.52

ARE FAILED DECISIONS ASSOCIATED WITH INCREASED KNEE LOADING UNDER COMPLEX COGNITIVE DEMANDS?

Aflatounian, F[1], Becker, J[2], Hutchison, K[3], Pew CA[1], and Monfort, S[1]
Departments of [1]Mechanical and Industrial Engineering and [2]Food Systems, Nutrition and Kinesiology, [3]Psychology
Montana State University, Bozeman, MT USA
email: fatemehaflatounian@montana.edu

INTRODUCTION

Anterior cruciate ligament (ACL) injuries often occur during unplanned cutting/landing movements [1]. Cognitively challenging jumping protocols aim to evaluate biomechanics during these scenarios by requiring participants to react to directional cues, which often produce failed or unbalanced landings. These imperfect trials are typically discarded, yet they may reveal meaningful deficits in muscle activation, joint stability, and dynamic postural control [2]. This study examines whether knee biomechanics of unbalanced and successful jump landings vary with failure rate in response to challenging decision-making demands.

METHODS

Forty-one active recreational athletes (17F/24M; 23.7±3.7yrs) completed drop-landing tasks recorded with markerless motion capture (100Hz) and force plates (1000Hz). Three conditions were tested: Baseline (anticipated direction), Simple (reactive single leg landing toward a basketball image displayed on one side of the screen), and Complex (reactive landing toward a basketball image or away from a simulated opponent). Trials were classified as successful, unbalanced, or failed. Unbalanced trials involved correct cue responses but inability to maintain balance for two seconds. Failed trials involved incorrect cue responses but landing on the wrong limb(s). Failed trial percentage (Failed%) was calculated for each cognitive condition. Kinematic/kinetic data were processed in Theia3D/Visual3D. Primary outcomes included changes between successful and unbalanced trials for peak knee flexion angle (ΔpKFA), peak knee abduction angle (ΔpKAbA), and peak knee abduction moment (ΔpKAbM), and their Pearson/Spearman correlations with Failed% (α=0.05).

RESULTS AND DISCUSSION

For ΔpKFA and ΔpKAbA, no significant correlations were observed (Table 1). ΔpKAbM showed no association in the Simple condition; however, in the Complex condition, higher failure rates were associated with greater ΔpKAbM (ρ=-0.4,p=0.01; Figure-1).

Differences in kinematic outcomes between successful and unbalanced landings were not associated with failure rate. However, under higher cognitive load, athletes with higher failure rates demonstrated riskier responses during unbalanced landings, which may indicate gross deficits in coordinating neuromuscular responses to directional stimuli. This result highlights the potential bias that may be introduced if isolating pKAbM estimates to only typically considered 'successful' trials (i.e., those with higher failure rates show greater deterioration in biomechanics for unbalanced trials that are often omitted). These findings support incorporating cognitively demanding tasks and unbalanced trials to reveal ACL-relevant neuromechanical vulnerabilities.

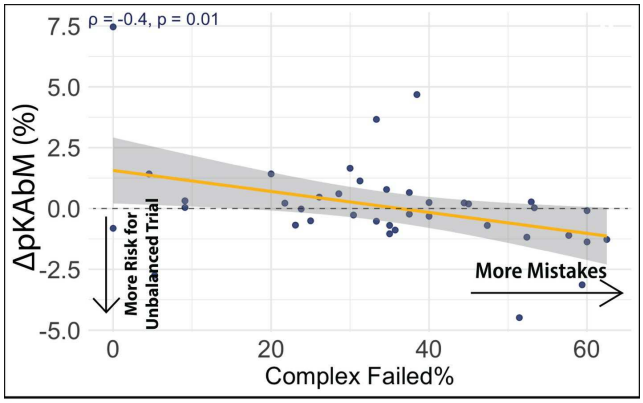

Figure 1: (A) Relationship between complex-task failure percentage and change in knee abduction moment (ΔpKAbM = Successful – Unbalanced variables, ρ = -0.4, p = 0.01).

CONCLUSIONS

Unbalanced landings under cognitive load may expose high-risk knee mechanics that are missed when only successful trials are analyzed. Including these trials can improve ACL injury-risk assessment and better reflect real-world sport demands.

REFERENCES

1. L. Chia, et al. *Sports Med* **52**, 2447-2467, 2022
2. E. A. Wikstrom, et al. *Scand J Med Sci Sports* **18**, 55-67, 2008

ACKNOWLEDGEMENTS

This research was supported by the MSU NACOE TEER grant and MSU NRT seed grant. We would also like to thank Luke Juergensen, Max Johnsen and Sophie Stemler for their help in collecting data.

Table 1: Correlations Between Success-Unbalanced Differences and Failed-Trial Percentage

Outcome Variables	Condition	Correlation	P-value
ΔpKFA [°]	**Simple Failed%**	0.186	0.271
	Complex Failed%	0.027	0.870
ΔpKAbA [°]	**Simple Failed%**	0.265	0.113
	Complex Failed%	0.171	0.297
ΔpKAbM [%BW-HT]	**Simple Failed%**	-0.047	0.271
	Complex Failed%	0.403*	0.011

*Spearman correlation used due to non-normal distribution.

INVESTIGATING THE RELATIONSHIP BETWEEN A STRENGTH AND POWER LOWER BODY ASSESSMENT AND MAXIMAL PITCHING VELOCITY

L. Collett, S.E. Schlittler, H. Adetunji, & J.P. Bailey
Department of Movement Sciences
University of Idaho, Moscow, ID

INTRODUCTION

Baseball pitching is a dynamic, complex skill that relies on efficient, powerful movement throughout the body (1). Previous research has shown that forces generated by the lower body are transferred up the kinetic chain and aid in accelerating the arm and ball (2). In addition to performance effects, lower-body weakness or inefficient energy transfer can increase injury risk (3). The role of the lower body in pitching can be divided into the drive (rear) leg and the lead (front) leg (4). The purpose of this project is to investigate the relationship between propulsive performance on a battery of lower-body assessments and maximal pitching velocity.

Hypothesis:

Peak propulsive impulse of the drive leg, measured during the ULMJ, BBJ, and UCMJ will demonstrate a strong positive correlation to pitching velocity.

METHODS

Twenty-four males (18.0±3.6 years old, 1.81±0.07 m, 77.4±14.1 kg) with 8.7±3.0 years of baseball experience and some pitching experience participated in this study. Following a warm-up, participants performed five pitches to identify their maximal pitching velocity (MPV) measured via radar gun. They then performed a battery of lower-body assessments used by a local baseball coach to assess strength and power mechanics:

- Isometric Mid-Thigh Pull (IMTP): Peak Ground Reaction Force (GRF) (N), Mean GRF (N)
- Bilateral Broad Jump (BBJ): Jump Distance (m), Propulsive Concentric RFD (N/s), Propulsive Impulse (Nm)
- Unilateral Lateral to Medial Jump (ULMJ): Jump Distance (m), Propulsive Concentric RFD (N/s), Propulsive Impulse (Nm)
- Unilateral Countermovement Jump (UCMJ): Jump Height (m), Propulsive Concentric RFD (N/s), Propulsive Impulse (Nm)

Multiple regression analyses were conducted with pitch velocity as the outcome variable. General linear models were also run to examine differences between limbs.

RESULTS AND DISCUSSION

Models including performance related kinetic variables (e.g., RFD, RSI, impulse) were not significant ($p > .05$). However, bilateral broad jump (BBJ) distance significantly predicted pitching velocity ($R^2 = .479$, $p = .001$) and remained the only significant independent predictor in the final model ($\beta = .678$, $p = .003$). Repeated-measures GLMs on the unilateral countermovement jumps (UCMJ) indicated no significant limb differences for most variables ($p > .05$), with the exception of reactive strength index (RSI), which demonstrated a significant asymmetry ($p = .019$).

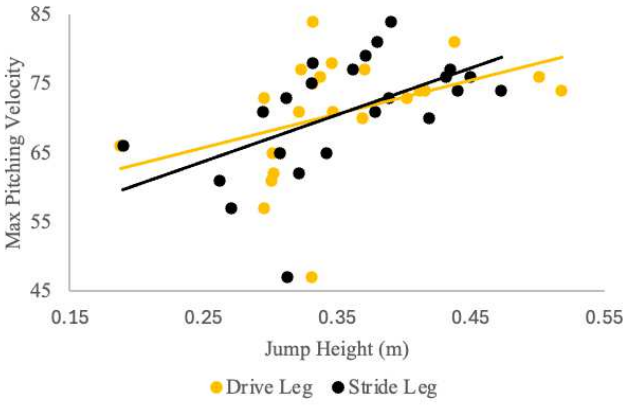

Figure 1: Drive and Stride Leg Unilateral Countermovement Jump Heights and Maximal Pitching Velocity

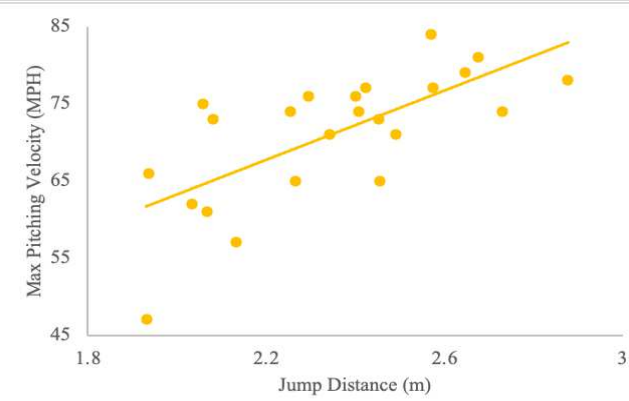

Figure 2: Bilateral Broad Jump Distance and Maximal Pitching Velocity

CONCLUSIONS

These findings indicate that global performance measures (e.g., jump distance) might be more predictive of pitch velocity, while asymmetries are most detectable in reactive strength rather than isolated mechanical variables.

REFERENCES

1. Atwater AE, et al (1979). *Exerc Sport Sci Rev*. **7(1)**:43-85
2. Kageyama, M., et al (2014) *J Sports Sci Med* **13(4)**:742–750.
3. Kline, D., et al (2024). *ASMAR* **7(2)**:101037
4. MacWilliams, BA., et al (1998). *Am. J. Sports Med.* **26(1)**:66–71

Effect of Outdoor Terrain on Foot Strike and Running Economy in Recreational Runners

Doerr, CB, Kietzmann, ME, and Brown, TN
School of Kinesiology
Boise State University, Boise, ID, USA
Email: Calvindoerr@u.boisestate.edu

INTRODUCTION

Running with a prominent heel strike may increase impact forces and elevate musculoskeletal injury risk for recreational runners. During recreational running, individuals reportedly alter leg stiffness and produce greater muscular work to successfully traverse uneven terrain [1]. Although runners commonly encounter uneven terrain, such as dirt trails, on recreational runs, it is unknown if this terrain leads to heel strike or running economy changes that may accelerate muscular fatigue and injury risk. This study sought to determine the effect of outdoor terrain on foot strike angle and running economy in recreational runners, and whether foot strike and running economy were related.

METHODS

To date, 5 recreational runners have completed a four-mile outdoor run over varying terrain (concrete, asphalt, grass, and uneven trail) at a comfortable pace. Prior to the outdoor run, each participant completed a 5-minute treadmill warm-up where speed was adjusted until a "comfortable" pace was reached. Participants wore a Garmin GPS watch that notified them of their speed to ensure they were within 2% of their comfortable pace throughout the run. During the run, participants wore pressure-sensing insoles in each shoe, and a portable metabolic analyzer and heart-rate monitor.

Custom MATLAB code was used to time sync insole, metabolic, and heart rate data, and use latitude and longitude from Garmin to segment terrain. Then, stride rate (strides/min), heart rate (beats/min), foot strike angle and index, and running economy were calculated for each segment. Foot strike index was determined as center of pressure location at initial contact as a percentage of foot length, and then used to estimate foot strike angle according to [2]. Running Economy was calculated as absolute VO2, normalized to participant's weight divided by segment distance (ml/kg/km).

Each dependent variable was submitted to repeated measures ANOVA to determine the effect of surface (Concrete, Uneven Trail, Grass, vs Asphalt). Correlation coefficients (r) determined relation between stride rate and strike index with running economy and heart rate. Alpha level was set at 0.05.

RESULTS AND DISCUSSION

Contrary to our expectations, running terrain did not impact any dependent measure ($p>0.05$). This lack of significance may be expected as the current sample is limited to 5 participants, and preliminary power analysis assuming a small to moderate effect (ES = 0.25) indicates approximately 36 participants are needed to achieve appropriate statistical power between terrain. Considering the narrow range of strike index (~ 52 to 54.5 % of foot length), foot strike angle (~6 to 7°), and stride rate (~ 83 to 84 strides per minute) currently observed on the trail and grass terrain, it may be feasible to expect recreational runners do not alter stride when encountering new terrain (Fig 1A). However, current participants exhibited a strike index and angle that corresponds with midfoot strike and a high level of experience [3]. Expanding the data set may diversify foot strike and running experience, which may potentially lead to terrain changes.

Traversing the softer trail and grass surfaces increased physiological strain, with a 5 to 6 beat per minute increase in heart rate and a 2 to 3 increase in ml/kg/km in running economy compared to harder surfaces (Fig 1B). When runners encounter softer, more compliant surfaces, like the trail or grass, they stiffen the lower limb, increasing required muscular work and are potentially less economical [1]. Considering stride rate and strike index exhibited a strong, positive ($r = 0.611$) and negative relation ($r = -0.829$) with running economy, shifting towards a heel strike may be riskier, and less economical. Yet, it appears that a significant linear relation exists between biomechanical and physiologic variables (r: 0.251 to 0.829), and future work is needed to determine the magnitude of changes in lower limb biomechanics that alter the energetic cost of running.

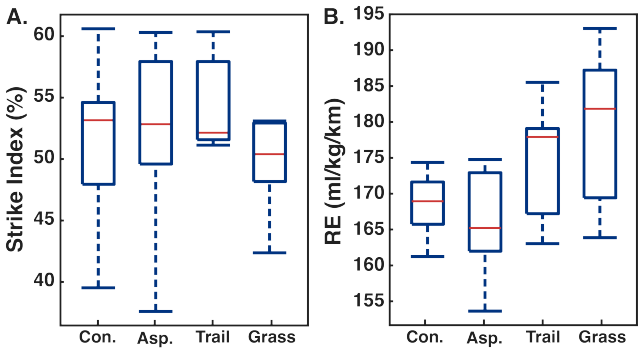

Figure 1: Depicts a box plot for strike index (A) and running economy (B) over each surface of the outdoor run.

CONCLUSIONS

Terrain did not impact stride or foot strike biomechanics during outdoor run from the current results. But, traversing the softer trail and grass surface led to less economical running. Shifting towards a heel strike was less economical and may also increase injury risk. Recreational runners may need to monitor the terrain they traverse to reduce injury risk.

REFERENCES

1. Voloshina AS, and Ferris DP. *J of Exp. Bio* **5**, 711-719, 2005.
2. Altman AR, and Davis IS. *Gait Posture* **35**, 298-300, 2012.
3. Larson P et al. *J Sports Sci* **29**, 1665-73, 2011

ACKNOWLEDGEMENTS

NIH NIGMS (P20GM109095, P20GM148321, P20GM103408) supported this work.

Validation of OpenCap-Based Estimates of Peak Knee Abduction Moments during a Drop Vertical Jump

Gaston L[2], Lynch A[1], Stemler S[2], Larson J[1], Aflatounian F[1] and Monfort S[1]
[1]Department of Mechanical and Industrial Engineering, [2]Biomedical Engineering Program
Montana State University, Bozeman, MT USA
Email: lucas.gaston@student.montana.edu

INTRODUCTION

Large peak external knee abduction moments (pKAbM) have been linked to anterior cruciate ligament (ACL) injury risk [1]. However, monitoring knee kinetics using motion capture (MoCap) requires expensive equipment and is often impractical in clinical settings. OpenCap offers an affordable and easy-to-use alternative, requiring only iOS devices to collect motion data, making it more feasible for clinicians [2]. However, OpenCap-based estimates of pKAbM have scarcely been validated against MoCap data. This study aims to address this gap by simultaneously collecting MoCap and OpenCap data during the clinically significant double limb drop vertical jump (DLDJ). We hypothesized that OpenCap-based pKAbM would strongly correlate with MoCap-based pKAbM.

METHODS

Eight participants (4F/4M; 22.5 ± 3.5 yrs; 1.72 ± 0.08 m; 69.5 ± 14 kg; Tegner: 4.57 ± 1.27; Marx: 6.25 ± 3.69) completed five DLDJ trials. Three iOS devices running OpenCap and an 8-camera Qualisys MoCap system recorded data. MoCap data were processed in Theia3D, and OpenCap kinetics were estimated using torque-driven OpenSim algorithmic differentiation simulations [3]. Right leg pKAbM during the first 100ms following landing were estimated and normalized by height and weight. The simulations did not converge for eight of the total collected trials, leaving 32 trials for analysis. Each participant's OpenCap and MoCap estimates were averaged. Pearson correlations between the two were used to assess associations between methods, and Bland-Altman plots were used to provide further insight into the agreement in pKAbM from the two approaches.

RESULTS AND DISCUSSION

OpenCap and MoCap pKAbM values demonstrated a nonsignificant, moderate-strength correlation (r = 0.68; p = 0.061; Fig. 1). The nonsignificant correlation is weaker than prior reports for kinematics, although agreement in kinematics has varied [4]. The correlation for pKAbM is also weaker than our ongoing work comparing knee extensor moments when landing from a single limb vertical jump (r = 0.88). This lessened correlation may highlight the difficulty of estimating frontal plane kinetics, particularly with open-source software and limited specialized equipment. However, the moderate strength correlation coefficient may indicate an association that can be more definitively detected with a larger sample size. The Bland-Altman analysis (Fig. 2) revealed a small negative mean bias (-0.00388 %BW-HT), suggesting OpenCap tends to, on average, slightly overestimate pKAbM relative to MoCap.

Ongoing data collection efforts will help to adequately power the detection of this relationship. Notably, the wide 95% confidence interval for the correlation coefficient [-0.04, 0.937] reflects the small current sample size and indicates substantial uncertainty around the true correlation. This means that while a meaningful correlation between methods is plausible, it cannot be confirmed with the current data.

We are currently collecting additional data using a 16-camera hybrid setup, which concurrently collects marker-based MoCap data, providing a benchmark against the 'gold-standard' method for both markerless methods.

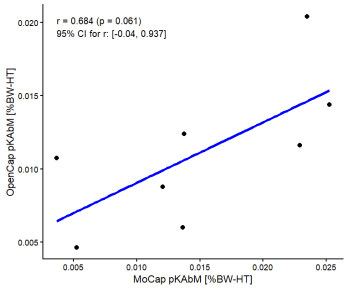

Figure 1: Correlation of pKAbM estimated from MoCap vs OpenCap plus simulation. Values were averaged for each participant and are presented in units of %BW-HT: percent bodyweight-height.

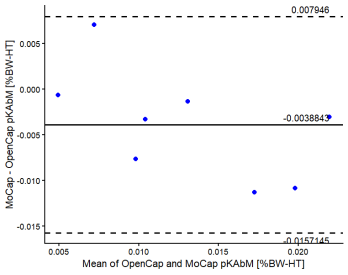

Figure 2: Bland-Altman plot depicting the mean values vs. the differences between the pKAbM estimates from OpenCap and MoCap. Lines represent the mean difference and limits of agreement (95%).

CONCLUSIONS

This preliminary dataset indicates moderate-strength, nonsignificant associations between OpenCap and MoCap pKAbM estimates during the DLDJ task. The wide 95% confidence interval suggests the current sample is underpowered to draw definitive conclusions about the true relationship between methods. Further investigation with a larger sample is warranted given the clinical importance of accurate and affordable motion analysis systems, and the additional comparison with marker-based MoCap.

REFERENCES

1. Hewett TE, et al. *Am J Sports Med* **33**, 492-501, 2005.
2. Turner JA, et al. *J Biomech* **171**, 112200, 2024.
3. Falisse A, et al. *PLoS One* **14**(10), e0217730, 2019.
4. Lima YL, et al. *J Sports Sci* **42**, 1-12, 2024.

ACKNOWLEDGEMENTS

This research was supported by M.J. Murdock Charitable Trust grants, MSU USP, and MSU NRT.

SKATE-X BINDINGS INCREASE FOREFOOT PRRESSURRE DURING SKATE SKIING

Haig, W, Becker, J
Department of Food Systems, Nutrition, and Kinesiology
Montana State University, Bozeman, MT USA
email: haigwill@gmail.com, web:https://www.montana.edu/biomechanics/

INTRODUCTION

Since the early 1980s, the skate skiing technique has been fundamental to cross-country skiing. The hinge connecting the boot to the ski plays a central role in skating mechanics. Given that forward lean and forefoot pressure are key metrics of good technique, hinge position may be an important but poorly understood factor in skiing biomechanics. In other sports such as speed skating, hinge position is known to influence mechanics [1]. While a single investigation has shown that changing hinge position in skiing improves physiology, this has not resulted in widespread adoption of new hinge positions [2]. A recently released commercial binding does move the hinge position; however, it is unclear how this influences the biomechanics of skiing. Therefore, the purpose of this study is to compare plantar pressure differences between a traditional NNN binding and the Skate-X (SX) binding.

METHODS

A 21-yr old national level biathlete roller skied on a motorized treadmill at a 5% grade at 14.5 kph using both NNN and SX bindings (Figure 1). Two five-minute trials were conducted with each binding. Plantar pressure was collected using plantar pressure insoles (Xsensor Technology Corp, Calgary, Canada) sampling at 120 Hz. Each stride was divided into three phases: gliding, preloading, and pushing based on the total force curve. Peak pressures under the hind and forefoot were calculated for each phase, along with the total time spent in each phase. Since the V2 technique is symmetric, data from left and right feet were averaged. A 2 x 2 repeated measures ANOVA was used to evaluate differences in peak pressures between binding and foot regions. Paired t-tests were used to evaluate time spent gliding, preloading, and pushing with different bindings.

RESULTS AND DISCUSSION

There were significant binding x region interactions for the gliding ($F_{1,40} = 47.3$, $p < .001$), preloading ($F_{1,40} = 44.2$, $p < .001$), and pushing (($F_{1,40} = 36.2$, $p < .001$) phases. In the gliding and preloading phases, the SX binding increased pressure under the forefoot while decreasing pressure under the rearfoot (Figure 2). Glide time was not different between bindings ($p = .242$, $d = .186$). However, preload time was longer ($p = .037$, $d = .337$) and push time was shorter ($p = .012$, $d = .412$).

The posteriorly located binding hinge of SX increases forefoot loading and reduces rearfoot loading across all phases, indicating a more forward body position. This is consistent with the forward body position emphasized in efficient skate skiing technique. The longer preload and shorter push phases suggest more time is spent positioning the body over the ski, with the resulting forward position enabling more rapid force production during push-off.

CONCLUSIONS

The SX binding shifts plantar pressure in a way which appears advantageous for skiing mechanics. Additional research is required to see if these changes result in performance benefits during competition.

Figure 1: Skate-X and NNN (trad) binding location

REFERENCES

1. Houdijk, H. et al. (2002). J Applied Biomech. 18, 292-205.
2. Bolger, C.M. et al. (2016). PLoS ONE. 11(5), e01

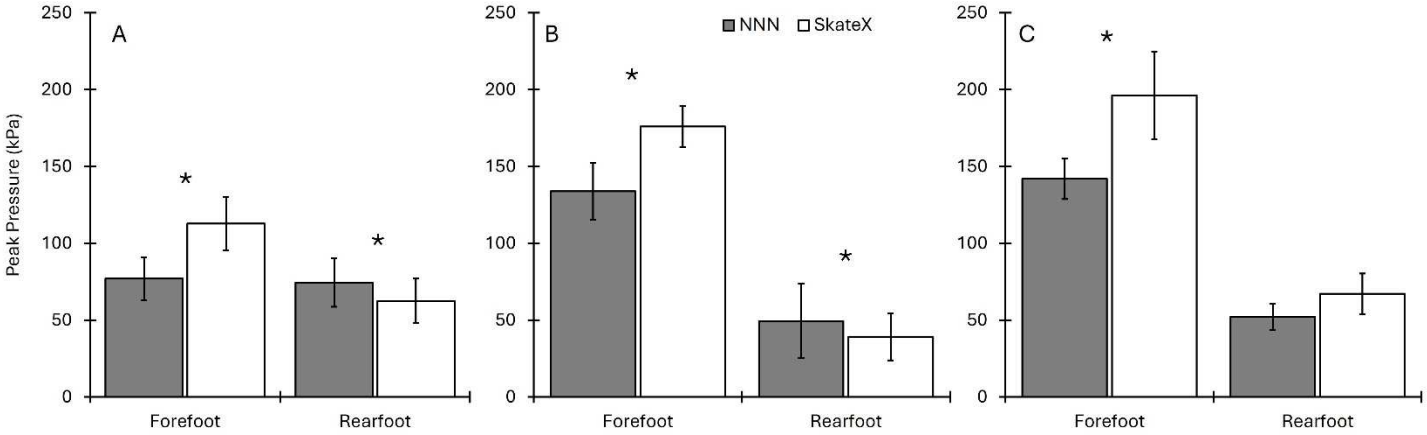

Figure 2. Mean peak pressure values for the two bindings and foot regions in the gliding (A), preloading (B), and pushing (C)

CENTER OF MASS DISPLACMENT AS A PREDICTOR OF BONE ADAPTATION IN FIRST-TIME MARATHON RUNNERS

Massarat, A[1], Hugard, S[1], Hahn, M[1]
[1] Bowerman Sports Science Center, Department of Hyman Physiology, University of Oregon, Eugene, OR
email: aryam@uoregon.edu

INTRODUCTION

Bone stress injuries (BSIs) are common overuse injuries among distance runners and often result in substantial time lost from training and competition. Studies estimate that between one-third and two-thirds of competitive cross-country and long-distance runners report a history of BSI, with annual incidence rates ranging from 4.9% to 21.1% in competitive runners [1]. Recent work suggests that running mechanics may contribute to BSI development. In collegiate runners, greater vertical center of mass (COM) displacement during running has been associated with increased risk of BSI [2]. Previous work examining this relationship has used BSI incidence as the sole outcome measure. The current study uses high-resolution peripheral quantitative computed tomography (HR-pQCT) to further understand the relationship between running vertical COM displacement and tibial bone adaptation in response to marathon training. It is hypothesized that athletes with a greater vertical COM displacement during running will experience greater increases in total volumetric bone mineral density (Tt.vBMD) at the tibia.

METHODS

Data collection for this ongoing study includes recreational first-time marathon runners (n = 6; 5 M, 1 F; age 18–30 yr) currently completing 16 weeks of standardized marathon training. This is a preliminary subset of an ongoing study with a projected sample size of 28. Bone density, geometry, and strength are being assessed using HR-pQCT scans collected at the distal tibial metaphysis at baseline and subsequently every 2-4 weeks throughout marathon training. Running gait analysis was performed in the Brooks Launch 10 for all participants at baseline. Marker position data were collected (200 Hz) using an eight-camera motion capture system (Motion Analysis Corp, Rohnert Park, CA) during treadmill running trials. Participants ran at 105% of their speed at lactate turn point. Joint kinematics and kinetics were calculated using an inverse dynamics model in Visual3D (HAS Motion, Ontario, CA). Location of the whole-body COM was estimated using the pelvis center location derived in Visual3D. Bone adaptation was quantified as the change in metaphyseal Tt.vBMD measured between baseline and week 8 using HR-pQCT. This represents a preliminary metric, as the primary outcome for the completed study will be the change in tibial Tt.vBMD from baseline to week 16 of training. A linear regression analysis was performed to assess the relationship between vertical COM displacement during running and 8-wk change in tibial Tt.vBMD.

RESULTS AND DISCUSSION

Vertical COM displacement demonstrated a non-significant positive association with change in tibial metaphyseal Tt.vBMD, with greater COM displacement corresponding to a greater increase in Tt.vBMD (R^2 = 0.2462, p=0.32). Greater COM displacement may increase ground reaction forces as well as internal muscle-on-bone contractile forces. Increasing mechanical stimuli leads to adaptive bone formation modeling and targeted remodeling, both of which result in net increases in bone mineral density. Importantly, vertical COM displacement has been shown to be a modifiable metric through training, suggesting that this may represent a potential target for interventions aiming to optimize bone adaptations during endurance training. However, given the small sample size and the preliminary nature of the data, additional participants and analysis through week 16 will be necessary to further evaluate the strength of this relationship.

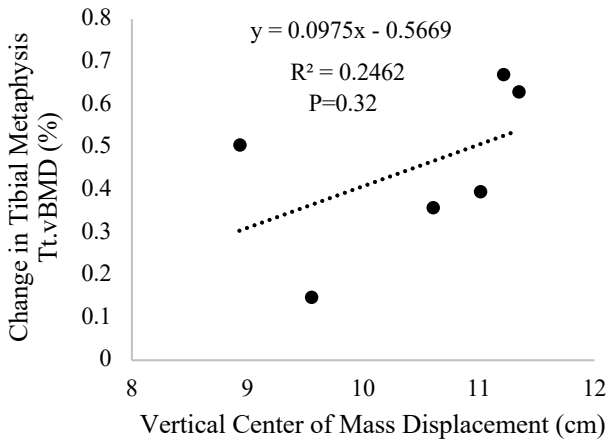

Figure 1. Average vertical center of mass displacement during running vs change in tibial metaphyseal total volumetric bone mineral density after 8 weeks of marathon training (n = 6).

CONCLUSIONS

This study highlights a non-significant positive relationship between vertical COM displacement during running and changes in tibial bone mineral density during marathon training. These preliminary findings suggest that vertical COM displacement is not significantly associated with bone adaptation. However, a greater sample size is needed to further investigate this relationship.

REFERENCES

1. Warden S. J. et al., *J Orthop Sports Phys Ther,* 44(10), 2014
2. Joachim M R. et al., *J Orthop Sports Phys Ther,* 53(12), 2023

ACKNOWLEDGEMENTS

This work was supported by the Wu Tsai Human Performance Alliance and the Joe and Clara Tsai Foundation. Footwear was provided by Brooks Running.

BRIDGING BIOMECHANICS AND MENSTRUAL HEALTH: A SYSTEMATIC REVIEW

Hiler, AM[1], Olvera, HL[1], Havens, KL[2], Fitzpatrick, CK[1], Silverman, AK[3], and Mannen, EM[1]
[1]Boise State University, Boise, ID USA, [2]University of Southern California, Los Angeles, CA USA, [3]Colorado School of Mines, Golden, CO USA
email: arihiler@u.boisestate.edu, web: https://www.boisestate.edu/coen-babi/

INTRODUCTION

Intravaginal menstrual products are integral to menstrual care for millions of women worldwide. Despite the widespread use of tampons, cups, and discs, the biomechanical interactions between these products and female pelvic tissues remain largely unquantified. Understanding how these devices load, displace, or interact with vaginal tissue is essential for improving product design, enhancing comfort, and supporting long-term use. The purpose of this systematic review is to synthesize existing research on biomechanical effects of intravaginal products on female pelvic anatomy and to identify current gaps in literature that warrant further investigation.

METHODS

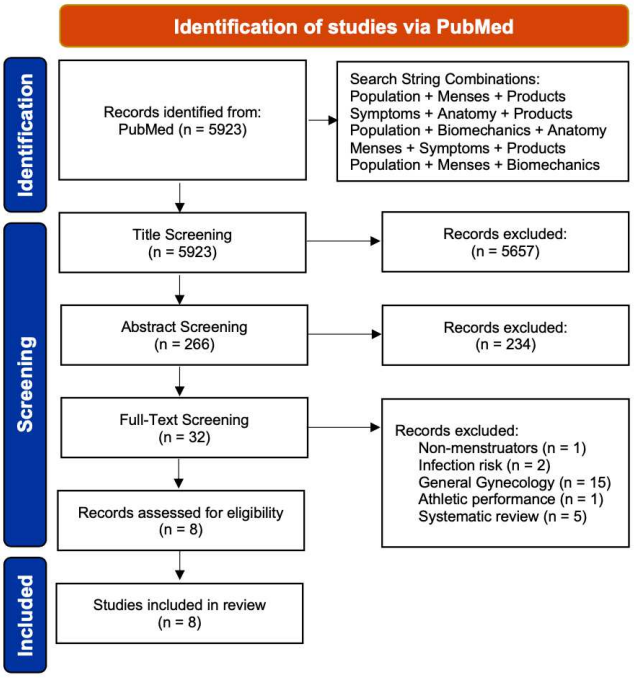

Figure 1: PRISMA flow diagram of study selection. A PubMed search was conducted using six concept groups. Of 5,923 records screened by independent reviewers (HLO, AMH), 8 studies were included [1].

A systematic search of PubMed was conducted in September 2025 using combined keywords related to menstruation, products, biomechanics, symptoms, and anatomy (Figure 1). Two independent reviewers (HLO, AMH) screened articles by title, abstract, and full text. Studies were excluded if they exclusively focused on non-menstruating individuals, external products, infection risk, general gynecology, mental health, period poverty, or athletic performance. Methodological quality of potentially relevant studies was assessed using the Joanna Briggs Institute (JBI) critical appraisal checklists.

RESULTS AND DISCUSSION

A total of 5,923 records were returned from PubMed. Following title, abstract, and full text screening, 8 studies were deemed relevant and assessed for eligibility. All 8 studies were included in the final review.

Evidence indicates intravaginal menstrual products can mechanically interact with pelvic structures. Case-control studies suggest menstrual cup (MC) use may increase the risk of intrauterine device (IUD) displacement, likely due to suction forces upon cup removal [2,3]. Several case reports describe hydronephrosis and urinary tract obstruction due to incorrectly positioned MCs [5,6]. Pelvic floor function may also be affected, as one study reported several participants with hypertonic pelvic floor muscles shifted to normal tone after three menstrual cycles using a MC, potentially improving pelvic floor function [4].

Across all studies, experimental measurements of forces, pressures, and tissue deformation remain scarce. Understanding these biomechanical measures is critical, as excessive forces or tissue deformation could contribute to pain, discomfort, or pelvic disorders, while controlled loading may offer therapeutic benefits [4].

CONCLUSIONS

This review demonstrates how limited and fragmented the biomechanical evidence base is surrounding intravaginal menstrual products, highlighting the novelty of this exploration. We identified significant gaps in biomechanical characterization of intravaginal menstrual products, including limited in vivo assessment and inconsistent test protocols. Quantitative data on forces, pressures, or strain distributions describing how these products load or deform surrounding tissues during wear are needed to inform safer designs. By synthesizing biomechanical parameters across studies, this review highlights the mechanistically informed opportunities to advance the safety, comfort, and anatomical compatibility of intravaginal menstrual products.

REFERENCES

1. Page MJ, et al. *BMJ* **372**, 71, 2021.
2. Madar, J, et al. *Gynecologie, obstetrique, fertilite & senologie*, **52**(12), 683–689, 2024.
3. Claire, J, et al. *Contraception and reproductive medicine*, **10**(1), 33, 2025.
4. Schevchenco, B, et al. *Women & Health*, **63**(1), 35–43, 2023.
5. Stolz, A, et al. *Case Reports in Women's Health*, **22**, e00108, 2019.
6. Prip, CM, et al. *BMJ Case Reports,* **18**(2), 2025.

EFFECTS OF RELATIVE PEAK VERTICAL GROUND REACTION FORCES ON BONE ADAPTATION

Humpries, S[1], Hugard, S[1], Hahn, M[1]
[1]Bowerman Sports Science Center, Department of Human Physiology, University of Oregon, Eugene OR USA
email: sam5humphries@gmail.com

INTRODUCTION

Bone adaptation is stimulated by mechanical loading, as bones structurally remodel in response to the stress placed on them [1]. Bone stress injuries occur as a result of repeated mechanical overloading disrupting the delicate balance between the body's microdamage-induced bone remodeling and repair processes [2]. Previous retrospective work has found that bone strength (failure load in compression per unit area) relative to mechanical loading in the form of mean peak vertical ground reaction forces (vGRF) is significantly lower at the mid-tibia (diaphysis) in runners with previous stress fracture history [3]. However, it is unknown if relative peak vGRF influences tibial bone adaptation. Therefore, the purpose of this study is to prospectively investigate the influence of relative peak vGRF on tibial bone adaptation during marathon training. It is hypothesized that individuals with greater relative peak vGRF will experience greater increases in total volumetric bone mineral density (Tt.vBMD), which reflects the amount of mineralized bone per unit volume, as a result of marathon training.

METHODS

Data collection for this study is ongoing. Six participants (5M/1F) ages 18-30 are currently undergoing 16 weeks of standardized marathon training. This is a preliminary subset of an ongoing study with a projected sample size of 28. High-resolution peripheral quantitative computed tomography (HR-pQCT) scans at the tibial diaphysis and distal metaphysis on the participants' non-dominant leg were collected throughout training. A baseline HR-pQCT scan was performed at the tibial diaphysis (45% of tibial length) and metaphysis (7.3% of tibial length) at week 0. Metaphyseal scans were repeated every 2-4 weeks to assess adaptation while diaphyseal adaptation will be assessed at 16 weeks. Adaptation was measured as the percent change in Tt.vBMD. A running kinematic and kinetic analysis was performed for all participants at baseline. Vertical ground reaction forces were collected at 1000 Hz using a force-instrumented treadmill (Bertec, Columbus, OH). Participants ran at 105% of their lactate turnpoint until volitional exhaustion. Microfinite element analysis was used to estimate failure load in compression at the tibial metaphysis. Average peak vGRF for the non-dominant leg was determined over the final 30 seconds of the running trial. Relative peak vGRF was calculated using the following equation:

$$Relative\ peak\ vGRF = \frac{Avg\ peak\ vGRF\ (N)}{Estimated\ failure\ load\ (N)} \times 100$$

The relationship between relative peak vGRF and change in Tt.vBMD was assessed using linear regression analysis.

RESULTS AND DISCUSSION

Linear regression analysis revealed a non-significant positive relationship between relative peak vGRF and change in metaphyseal Tt.vBMD (R^2=0.198, p=0.38) (Figure 1). Although the relationship was not statistically significant, the regression trend suggests that participants experiencing higher relative peak vGRF tended to show greater increases in tibial metaphyseal Tt.vBMD (Figure 1). However, the large variability among participants limited the strength of this relationship and the low sample size reduces the statistical power of the analysis. Data collection is ongoing, however, and additional weeks of adaptation as well as an increased sample size may strengthen this relationship.

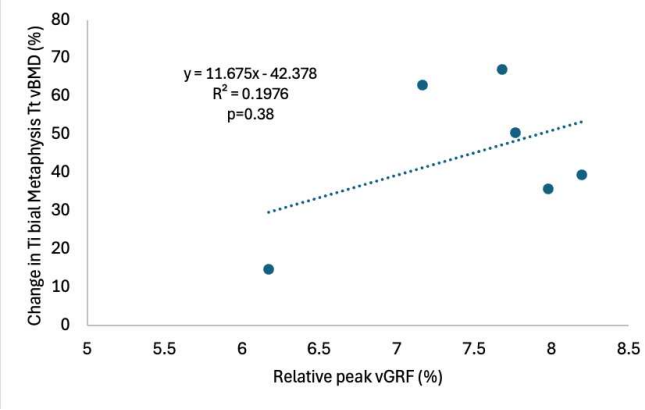

Figure 1: Relationship between relative peak vGRF (%) and change in tibial metaphysis Tt.vBMD (%) after 8 weeks of marathon training.

CONCLUSIONS

Preliminary results indicate a non-significant positive relationship between bone relative peak vGRF and adaptation at the distal tibial metaphysis. Further data collection is ongoing and may further clarify this relationship.

REFERENCES

[1] Bergman et al. *Bone Reports* 10, 100195, 2019.
[2] Evans et al. *Medicine & Science in Sports & Exercise* 40, S660-S670, 2008.
[3] McDermott et al. *Bone* 94, 22-28, 2017.

ACKNOWLEDGEMENTS

This work was supported by the Wu Tsai Human Performance Alliance and the Joe and Clara Tsai Foundation.

Pressure Sensing Insoles Estimate Vertical GRFs Across Various Running Surfaces

Kietzmann, ME, Doerr, CB, and Brown, TN
Department of Kinesiology
Boise State University, Boise, ID
email: madelynkietzmann@u.boisestate.edu

INTRODUCTION

Each year, 50% of runners sustain a musculoskeletal injury. These injuries are reportedly caused by rapid transmission of large vertical GRFs to the musculoskeletal system during recreational runs [1] Throughout a run, individuals commonly encounter various surfaces (e.g. asphalt, concrete, and grass). Recent advances in pressure-sensing insoles make it feasible to estimate vertical GRFs during outdoor recreational running. But it is unknown whether insoles accurately estimate vertical GRFs on various surface encountered during recreational runs. This study aims to determine effect of surface on magnitude (peak and impact peak) and speed (loading rate) of vertical GRF, and compare insoles and force platform derived vertical GRFs.

METHODS

10 recreational runners had vertical GRFs recorded while they ran at a self-selected comfortable pace over 2 different surfaces (hard and foam). To determine each participant's self-selected pace, treadmill speed was adjusted during a 5-minute warm-up until a "comfortable" run pace was achieved. The hard and foam surfaces consisted on a flat particle board panel and high-density foam (indention Load Deflection 44 values) secured atop a force platform, respectively. Each participant completed 5 good trials over each surface. During each trial, participants wore a pressure sensing insole in each shoe and were required to contact an in-ground force platform with their dominant limb.

Custom Matlab code was used to calculate force platform derived vertical GRF measures. First, the GRF data was filtered and normalized to body weight for the participant. Then, peak stance phase vertical GRF and impact peak (defined as magnitude at 13% of the stance), and loading rate (determined as vertical GRF slope between 20% and 80% of heel strike and impact peak) [2]. Custom python code was used to calculate pressure-sensing insole derived force measures. First, plantar pressure data was filtered and converted to force (pressure multiplied by area for each sensel). Then total vertical force obtained (each sesnsel force summed) and normalized to body weight. Using the normalized force data, peak vertical force, impact peak, and loading rate were calculated with the same procedures as force platform data.

Correlation coefficients (r) were calculated between force platform and insole vertical GRF measures for each surface and mean absolute error (MAE) and root mean squared error (RMSE) determined the magnitude of error between force platform and insole derived vertical GRF measures.

RESULTS AND DISCUSSION

During the run, insole derived vertical GRF measures exhibited moderate to strong relation with force platform derived measures. Pressure-sensing insoles appear to be a practical tool for estimating peak vertical GRF during running. Specifically, insole derived measures exhibited a significant, strong linear relation with force platform derived peak vertical GRF on the hard ($p < 0.001$, $r = 0.923$) and soft, grasslike surface ($p = 0.003$, $r = 0.825$). Yet, impact or rate dependent GRF measures derived from the pressure-sensing insole may not exhibit similar accuracy, as impact peak and loading rate derived from the insole exhibited insignificant, moderate relation with force platform derived measures ($p > 0.085$, $r < 0.571$).

Pressure-insoles consistently underestimated vertical GRF measures, regardless of hard and soft, grasslike surface (Fig. 1). For example, the MAE and RMSE were 0.54 and 0.62 BW and .56 and 0.66 BW for peak vertical GRF and 53.3 and 92.8 BW/sand 56.0 and 96.7 BW/s for loading rate on the hard and grass-like surface, respectively. Although pressure-sensing insoles may be useful for relative comparisons, such as an individual running over different surfaces, they consistently underestimate GRF magnitudes compared to the gold-standard force platform. As such, researchers may need to use caution when quantifying GRF magnitudes with insoles.

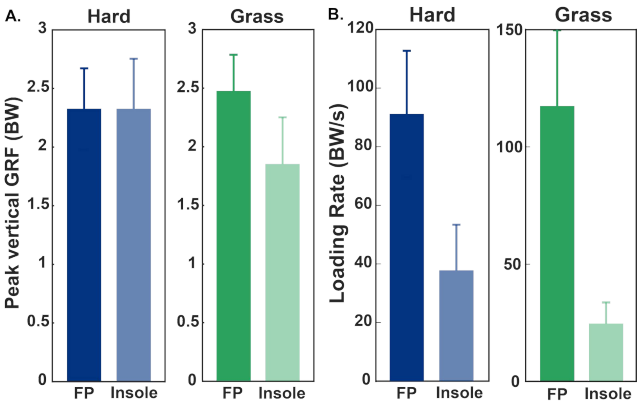

Figure 1: Depicts mean (SD) for peak vertical GRF (A) and loading rate (B) derived from the force platform and insoles for both hard (blue) and soft, grass (green) surfaces.

CONCLUSIONS

Pressure-sensing insoles may be a practical tool for estimating GRFs, as they exhibited strong agreement with force plate derived measures for peak GRF. But insoles may have less utility to estimate rate dependent measures and the fact they consistently under-estimated vertical GRF measures may limit their usefulness to quantify GRF magnitudes.

REFERENCES

1. Warden, SJ et al., *Curr Osteoporos Rep* 4, 2006.
2. Crowell, HP and Davis IS, *Clin Biomech* 26, 2011.

ACKNOWLEDGEMENTS

We would like to thank Aden Harrison for his assistance and NIH NIGMS (P20GM109095, P20GM148321, P20GM103408) for their support.

METABOLIC PERFORMANCE EFFECTS OF RUNNING SHOE MIDSOLE COMPLIANCE

Knowles, RC[1], Robinson, RM[1], Denton, AN[1,2], and Hahn, ME[1]
[1]Bowerman Sports Science Center, Department of Human Physiology, University of Oregon, Eugene, OR USA
[2]Knight Campus for Accelerating Scientific Impact, Department of Bioengineering, University of Oregon, Eugene, OR USA
email: rknowles@uoregon.edu, web: https://bssc.uoregon.edu/neuromechlabs/

INTRODUCTION

Modern running shoe parameters can enhance an athlete's biomechanical and physiological performance [1]; however, the independent and collective effects of midsole stiffness and bending stiffness remain unclear. Midsole stiffness alone [2] or the combined effect of midsole stiffness and longitudinal bending stiffness [3] can enhance running performance by improving running economy through the storage and return of elastic strain energy during ground contact.

Recent experimental work attempting to isolate the effect of compliance suggests that greater midsole compliance may improve running economy while altering lower-limb joint mechanics, particularly at the knee [4]. At the same time, only a limited number of modeling studies have examined how changes in shoe compliance influence joint-level mechanics and metabolic energy cost, despite the potential of computational simulations to isolate these effects in a controlled manner.

Thus, the purpose of this study was to examine the impact of running shoe midsole stiffness on running mechanics and metabolic cost of transport (MCOT) using musculoskeletal modeling and computer simulation. It was hypothesized that a more compliant midsole, relative to the baseline parameter, would lower MCOT.

METHODS

Preliminary predictive simulations of a running stride at 3.16 m/s were generated in Opensim Moco [5] using a sagittal plane musculoskeletal model [6]. Simulations were formulated as an optimal control problem where the objective was to minimize the sum of cubed muscle excitations. Shoe-ground contact elements were calibrated to a neutral running shoe (Brooks Launch 10) and varied from −75 to +100 percent of baseline stiffness, with load-displacement parameters tuned to match the manufacturer's 5J impact test. Three simulations for each stiffness were generated using different starting points, and the simulation with the lowest objective function value for each stiffness was retained for further analysis. For each condition, whole-body and muscle-specific metabolic cost of transport (MCOT) were estimated using a muscle energy expenditure model [7]. A second-order polynomial was then fit to the MCOT data, allowing this framework to characterize the relationship between midsole stiffness, running MCOT, and lower-limb mechanical demand.

RESULTS AND DISCUSSION

The data displayed a U-shaped relationship between midsole stiffness and MCOT ($R^2 = 0.88$) (Figure 1). A midsole stiffness 50% below baseline minimized whole-body MCOT, resulting in a 1% reduction relative to baseline. Reduced whole-body MCOT was driven by lower hip (2.7% decrease) and knee (1.6% decrease) extensor muscle-specific costs, suggesting that a relatively compliant midsole may improve running economy by reducing demand on more metabolically expensive muscle groups while having little effect on more economical muscle groups such as the plantar flexors. The U-shaped trend further suggests that both overly stiff and overly compliant midsoles may be energetically unfavorable, with the main benefits occurring within an intermediate range of compliance.

These findings indicate that compliant midsoles may be beneficial for endurance performance, but future work is needed to better characterize individual responses to midsole stiffness. This work is currently being expanded using a 3-D musculoskeletal model paired with experimental kinematics and kinetic data from a cohort of 21 distance runners. This will allow for determination of the optimal midsole stiffness both across the cohort and for individual runners.

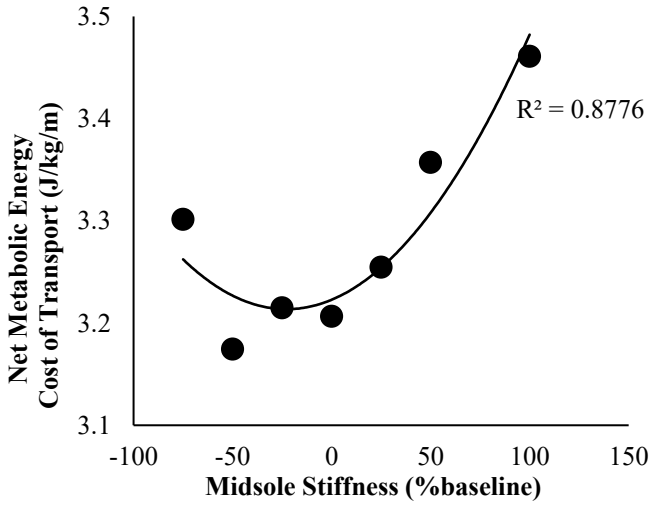

Figure 1: The net metabolic energy cost of transport during running with variable midsole stiffness (-75% to +100%) relative to the baseline condition (0%).

CONCLUSION

A more compliant midsole minimized metabolic cost of transport (MCOT) by reducing hip and knee energetic demand, suggesting performance benefits for endurance running.

REFERENCES

1. Hoogkamer W, et al. *Sports Med* **48**, 1009–1019, 2018.
2. Healey LA, and Hoogkamer W. *J Sport Health Sci* **11**, 285–292, 2022.
3. Stephen CHN, et al. *J Sport Health Sci* **14**, 101069, 2025.
4. Petrella D, et al. *Med Sci Sports Exerc* **58**, 310–320, 2026.
5. Dembia CL, et al. *PLoS Comput Biol* **16**, e1008493, 2020.
6. Nguyen VQ, et al. *IEEE Trans Neural Syst Rehabil Eng* **27**, 1426–1435, 2019.
7. Bhargava LJ, et al. *J Biomech* **37**, 81–88, 2004.

MARATHON TRAINING INFLUENCE ON FATIGUED RUNNING MECHANICS

Goldcamp, N[1], Hugard, S[1], Hahn, ME[1]
[1]Bowerman Sports Science Center, Department of Human Physiology, University of Oregon, Eugene, USA
Email: goldcamp@uoregon.edu

INTRODUCTION

Novice runners experience running-related injuries at a disproportionate rate compared to their trained counterparts. One factor thought to contribute to the increased injury risk is altered running mechanics after fatigue. Previous work has shown that novice runners exhibit greater center of mass (CoM) displacement after fatigue, whereas experienced runners do not. Fatigue has also been shown to increase knee flexion at initial contact (IC) and decrease vertical stiffness revealing an increased compliance in the lower extremity while running, which may be influenced by experience level as well [1]. Additionally, novice runners have been shown to alter running mechanics after a training program [2]. However, little is known about how a training program influences the ability to resist biomechanical changes from fatigue, defined as fatigue resistance. This study aims to examine the effect marathon training has on fatigued running mechanics. It is hypothesized that marathon training will improve fatigue resistance, as demonstrated by a smaller percent change in biomechanical metrics following fatigue when comparing pre- and post-training.

METHODS

Five novice marathon runners (2F, 3M; height: 176.3 ± 11.7 cm; mass: 72.6 ± 11.3 kg) completed a 16-week marathon training plan. This work is part of an on-going study that aims to include a total of 28 participants. All participants provided written informed consent per the requirements of the University of Oregon Institutional Review Board (STUDY00001624). Prior to beginning the training plan (week 0), participants completed a biomechanical analysis consisting of three running trials. For all data collection visits, footwear was standardized to the Brooks Launch 10 (Brooks Running). The first and third trials consisted of a 10-minute submaximal run at 80% of their speed at lactate turn point, as determined by a previously administered lactate threshold test. The second trial served as the fatiguing element, consisting of a run at 105% of the participants' speed at lactate turn point until volitional exhaustion. Lower-extremity biomechanics data were collected using a force-instrumented treadmill (Bertec, 1000 Hz) and an 8-camera motion capture system recorded marker trajectories (Motion Analysis Corp., 200 Hz) using a common marker set. An inverse dynamics model was used to calculate joint kinematics and kinetics. Vertical stiffness was defined as the ratio between peak vertical ground reaction force and max CoM displacement during stance [3]. Running trials were repeated during week 14 of marathon training. Fatigue resistance was quantified as the percent change in biomechanical variables from pre- to post-fatigue trials. Paired comparisons were used to assess differences in fatigue responses before and after marathon training ($\alpha = 0.05$).

RESULTS AND DISCUSSION

Percent changes in knee angle at IC, CoM displacement, and vertical stiffness after fatigue before and after training are reported below in Table 1. Paired t-test comparisons revealed no statistically significant ($p > 0.05$) differences in fatigue resistance metrics between pre- and post- marathon training. Mean differences in percent change are also presented and reflect the change in fatigue-induced mechanics following training. Thus, an increase indicates a larger change in fatigued mechanics after training, while a negative number represents a smaller change. Given the sample size ($n = 5$), substantial variability was observed in the responses of novice runners to marathon training.

CONCLUSIONS

This preliminary analysis currently indicates marathon training may not alter fatigued running mechanics or improve fatigue resistance. However, no final conclusions can be made with the current sample size. Furthermore, the variability in response to the training highlights the need for a more thorough analysis with a larger sample size.

REFERENCES

1. Zandbergen et al. *Gait & Posture* **99**, 60-75, 2023.
2. Moore et al. *Med. Sci. Sports Exerc.* **44**, 1756–63, 2012.
3. McMahon and George *J Biomech* **23**, 65-78, 1990.

ACKNOWLEDGEMENTS

This work was supported by the Wu Tsai Human Performance Alliance and the Joe and Clara Tsai Foundation. Footwear was provided by Brooks Running.

Table 1: Fatigue-induced percent changes before and after marathon training (mean ± SD), with paired comparisons used to assess changes in fatigue resistance.

Variable	Pre-Training %Δ (Mean ± SD)	Post-Training %Δ (Mean ± SD)	Mean Difference in Percent Change	*p-value*
Knee Angle at IC	**-1.50 ± 15.54**	**6.16 ± 29.06**	**7.66**	**0.707**
CoM Displacement	**-3.54 ± 3.64**	**-0.53 ± 5.69**	**1.96**	**0.193**
Vertical Stiffness	**4.31 ± 5.90**	**0.55 ± 2.77**	**-3.61**	**0.166**

MODELING THE INFANT HEAD-NECK COMPLEX TO INVESTIGATE POSITIONAL ASPHYXIA RISK IN INCLINED ENVIRONMENTS

Bossert, A.[1], Anderson, D., PhD[2], Fitzpatrick, C., PhD[1], Mannen, E., PhD[1]
[1]Department of Mechanical and Biomedical Engineering, Boise State University, Boise, ID
[2]Beth Israel Deaconess Medical Center, Harvard Medical School, Boston, MA
email: drewbossert@u.boisestate.edu

INTRODUCTION

Of the 3600 sudden infant death cases in the United States each year, nearly 1/3 are caused by asphyxia [1]. Chin-to-chest positioning increases risk of asphyxia, and an infant's ability to achieve and self-correct from this posture in common inclined environments is poorly understood. It is unethical to expose living infants to dangerous experiments; thus, robust computational models are critical to elucidate the mechanics of positional asphyxia. This study developed a novel computational musculoskeletal model to understand the risks associated with chin-to-chest posture.

METHODS

Experimental data in the form of neck kinematics were generated using a physical surrogate (Figure 1) of an infant allowing neck flexion and extension. A custom motion capture marker set was created to capture the unique scaling parameters of infant populations. An 8-camera Qualisys motion capture system was used to collect kinematic data for four distinct supine laying conditions. At body incline angles of 0°, 15°, 30°, and 45° - representing incline angles of common infant products – starting from a chin-to-chest position, the neck was extended to contact the inclined surface, and then flexed to return to the chin-to-chest position.

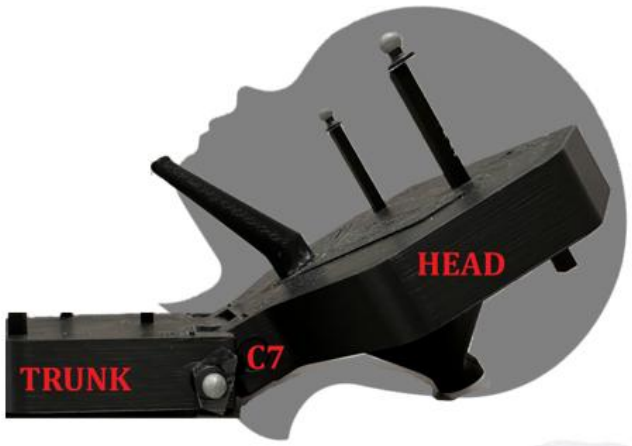

Figure 2: Physical surrogate used to represent sagittal plane neck flexion with markers and necessary geometry.

This kinematic data was used as in input to an existing OpenSim model [2]. This model was adapted to replicate the experimental setup and scaled to infant proportions. Muscle parameters were adjusted to represent realistic infant anatomy and ground reaction forces at the head were simulated based on estimated head mass of a 4-month infant. The Static Optimization tool packaged with OpenSim was used to determine the muscle forces at the neck during each prescribed motion profile.

RESULTS AND DISCUSSION

Muscle forces were grouped by function into flexor and extensor categories. The muscle forces in each group were summed across the motion profile to determine their total contribution to the movement. Figure 2 shows the sum of the flexor forces across the four inclined conditions. As incline angle increased, peak force necessary to lift the head decreased in sinusoidal proportion. At 45° body incline, 65.7% less force was required to lift the head off of the platform compared to the 0° condition.

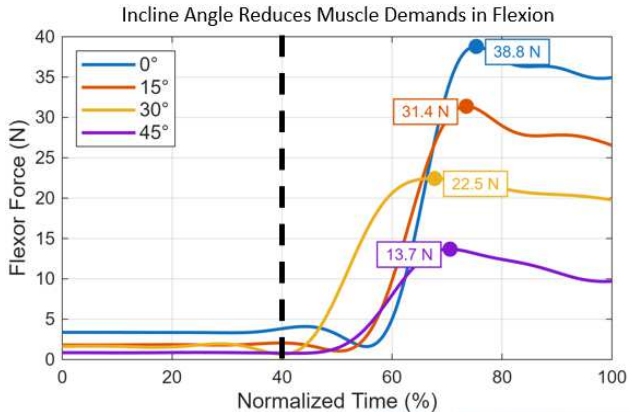

Figure 1: Results of Static Optimization showing the reduced muscular demand of the flexors when body incline is increased.

The lower force required to achieve a chin-to-chest posture at greater body inclines demonstrates an inherent vulnerability for infants to assume positions associated with elevated asphyxia risk. Notably, many infant products currently on the market feature back-rest incline angles between 15°-45° [3], placing infants in situations where chin-to-chest postures are more easily achieved. This computational model provides a framework for comparing how positional changes contribute to asphyxia risk across product designs. Future work incorporating CT derived anthropometric data may be used to further refine model geometry, muscle definitions, and other model parameters, ultimately informing design features that prioritize infant safety.

REFERENCES

1. Shapiro-Mendoza, et al. *Pediatrics* **151**, 2023.
2. Mortensen, et al. *PLoS ONE*, **13**(6), 2018.
3. Arya, et al. *Arch. Dis. Child. Fetal Neonatal Ed.*, **102**, F136-F141, 2016.

ACKNOWLEDGEMENTS

This research is supported by the NICHD, NIH Grant No. 1R01HD113921. EMM owns Mannen Bio, LLC, an expert and engineering consulting company.

THE EFFECTS OF PUSH-UP TECHNIQUE ON KINEMATICS AND MUSCLE ACTIVATION IN HEALTHY MEN

Ferrari, A[1], Gibin, C[1], Zedler, M[1], and Potthast, W[1]
Institute of Biomechanics and Orthopaedics, German Sport University Cologne, Cologne, Germany[1]

INTRODUCTION

Push-ups are a very popular exercise, commonly done to strengthen the upper-body. Push-ups involve mainly two phases: flexion of the elbows (descending phase) and extension of the elbows (ascending phase). In conventional push-ups the pectoralis major (PM) and the triceps brachii (TB) are the primary working muscles [2]. Previous studies have shown that performing push-ups on unstable or dynamic surfaces can alter neuromuscular demand, often increasing activation of stabilizing muscles compared to stable conditions [3]. In recent years, a bar with movable handles (thePure^{TM}) has been developed to allow a more dynamic push-up movement, which was expected to increase muscular response and calorie consumption [4]. The purpose of this study was to perform a biomechanical analysis to compare conventional push-ups with thePure bar push-ups. The initial hypothesis was that utilizing thePure^{TM} bar will result in a higher activation of both the PM and TB muscles, with potential changes in joint kinematics.

METHODS

The study took place at the Institute of Biomechanics and Orthopaedics of the German Sport University Cologne. Twelve healthy male participants (age: 25 ± 4.4 years, height: 182.2 ± 7.9 cm, body mass: 81.0 ± 9.4 kg) who had the ability to perform at least ten consecutive conventional push-ups took part in the study. All subjects were asked to perform a 5 minutes upper body warm up, followed by a familiarization period to try thePure^{TM} bar. The participants were then asked to perform 5 conventional push-ups and 5 bar push-ups in a randomized order, with 5 minutes rest period between trials. The push-up speed was standardized to a metronome at 30 beats per minute (bpm), signaling the beginning of each descending and ascending phase. Twenty spherical retro-reflective markers were placed on upper body anatomic reference points on each subject. Markers trajectories were recorded using a 3D motion capture system (Qualisys AB, Gothenburg, Sweden) consisting of fourteen infrared cameras (Oqus 7+ series). Furthermore, two Bipolar Electromyography (EMG) (myon 320, myon AG, Schwarzenberg, Switzerland) sensors were placed on PM and TB muscles to record muscle activation. Statistical analysis was performed on both kinematics and EMG data through Statistics Parametric Mapping (SPM). Furthermore, a paired t-test was performed to analyse differences between conditions' Area Under the Curve (AUC) of EMG data.

RESULTS AND DISCUSSION

In the elbow kinematics analysis, a statistically significant difference was found between the conventional and bar trials in all three planes of movement ($p < 0.01$). Specifically, elbow flexion was significantly lower during 12.9 - 24.4% and 30.8 - 55.7% of the push-up cycle in the bar condition compared to conventional condition. The shoulder axial rotation significantly increased during 25.5 - 64.2% of the push-up cycle in the bar trial compared to the conventional trial ($p < 0.01$). Such findings suggest that the instability, given by the movable handles of the bar, primarily shifts demand toward horizontal stabilization rather than vertical movement of the upper body. Furthermore, the bar condition led to a ~25% increase in PM activation and significantly higher PM total effort (AUC) during the ascending phase of the push-up (Figure 1). However, TB activation did not show any statistically significant difference (Figure 1). Because the bar handles slide laterally, PM muscles have to maintain a high level of isometric tension while simultaneously performing the dynamic shortening (concentric contraction) required to push the body upward in the ascending phase. This dual-role demand likely explains the significantly higher AUC found in the PM muscle. Furthermore, using a wide hand base of support results in significant changes in the neural activation of the primary movers of PM [1], which is likely the main reason why the bar push-ups further increase PM activation.

CONCLUSIONS

These findings suggest that thePure^{TM} bar may be an effective tool for increasing pectoralis major time-under-tension and challenging the motor control strategies required for upper-body stability. To fully map the neural response to this device, further research is required to include the rotator cuff and deltoid muscles in the EMG analysis. Such research would clarify the specific co-activation patterns required to manage the "sliding" degrees of freedom introduced by the bar.

REFERENCES

1. Allen, C.C., et al. *International Journal of Exercise Science* **6**(4), 278-288, 2013.
2. Degirmen, Y.B., et al. *Biomechanics Human Kinetics* **14**, 75-85, 2022.
3. Torres, R. J. B., et al. *Journal of sport rehabilitation,* **26**(4), 281–286, 2017.
4. The Pure. *The PushUpREvolution.*

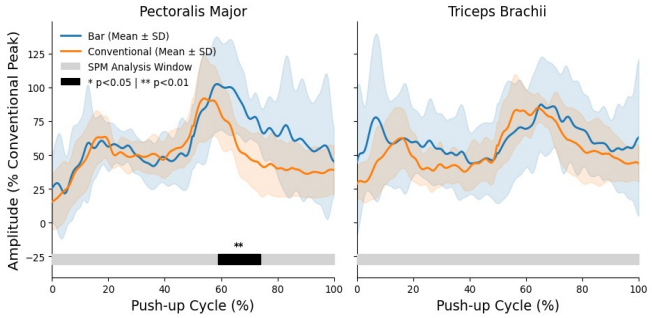

Figure 1: Mean pectoralis major (left) and triceps brachii (right) EMG amplitudes (thick) and standard deviation (shaded) of all subjects, with SPM analysis (grey) of the push-up cycle to show the statistically significant difference (black) between bar and conventional push-ups.

Poster Session B

Saturday, May 23rd 1:20 – 2:20 PM

THE BAYESIAN KNEE: RELIANCE ON SENSORY PRIORS INCREASES WITH IMPAIRED SENSORY FEEDBACK WHEN ESTIMATING KNEE POSITION

Smith, C, Morse, T, Mueller, L, Whittier, TT
Department of Food Systems, Nutrition and Kinesiology
Montana State University, Bozeman, MT USA
email: tyler.whittier@montana.edu

INTRODUCTION

Despite efforts to understand risk factors for knee injuries, these injuries remain prevalent in athletic, military, and healthy adults of all ages [1]. While traditional rehabilitation has yielded minimal effects at decreasing re-injury rates, a growing body of evidence suggests that ACL injuries result in significant neural damage [2]. One impactful impairment is the loss of crucial sensory receptors that inform the central nervous system (CNS) of vital information regarding the state of the knee during movement. This damage leads to impaired motor control leaving the knee susceptible to additional injury. In this study, we applied a Bayesian model to estimate the degree of uncertainty in the state of knee in healthy individuals during a full body stepping movement. The purpose of this study was to apply the principles of Bayesian motor control to understand knee control in healthy individuals performing an ecologically relevant stepping task.

METHODS

In this ongoing study, 22 healthy young adults (8 Female, M_{age} = 21.4 ± 1.5 years) performed a lower body visuomotor adaptation task in virtual reality (VR) designed to measure Bayesian inference by varying the level of sensory feedback uncertainty [3]. Participants performed 430 trials attempting to move a pink cursor (controlled by their left or right knee) to a virtual target via a single-legged step. In each trial, participants were forced to compensate for a varying shift to the cursor position that was drawn from a normal distribution N(10 cm, 5 cm) while receiving varying qualities of visual feedback. The slope of the linear relationship between the actual cursor shift and the estimated cursor shift was used as a metric to infer the sensorimotor weight placed on sensory input in each visual condition [4].

RESULTS AND DISCUSSION

The results of mixed-effects repeated measures ANOVA indicated a main effect of sensory uncertainty on the weight of sensory input when estimating knee position ($F(2, 42) = 82.21$, $p < 0.001$). Pairwise comparisons indicated a significant decrease in the weight of sensory input as visual feedback became less certain ($p < 0.05$). (Figure 1).

These findings indicate that participants rely on visual sensory input less when the input is not reliable and increase the weight placed on sensory priors, consistent with previous work in Bayesian motor control [3,4].

CONCLUSIONS

This study furthers our understanding of sensorimotor processes within young and healthy individuals. Results of this study highlight Bayesian inference as a valid measure of sensorimotor processing and may lead to future injury rehab or advanced training protocols by optimizing sensory-motor integration to reduce sensorimotor uncertainty.

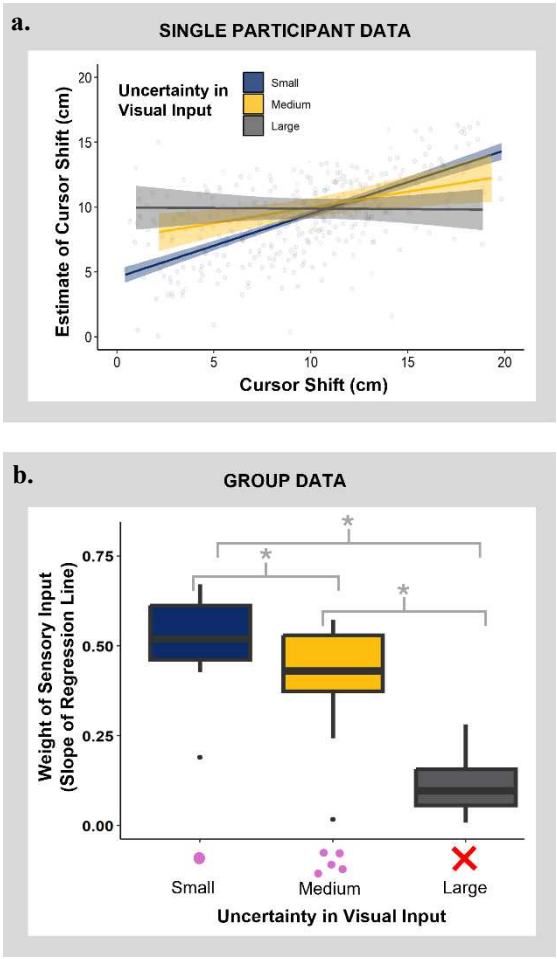

Figure 1. **a**. Individual results from the VR motor learning assessment as participants estimate a shift added to the cursor controlled by their knee while receiving visual feedback at various levels of uncertainty. **b**. Group results indicate a significant decrease in the weight of sensory input when estimating knee position. ★ $p = 0.002$.

REFERENCES

1. Ardern, C.L., et al. *British journal of sports medicine*, *48*(21), 1543-1552, 2014
2. Wiggins, A. J., et al. *The American journal of sports medicine*, *44*(7), 1861-1876, 2016
3. Whittier, T. T., et al. *Neuropsychologia*, *173*, 108310.4. Lohse, K-R et al. *Plos One* **9**, e93318, 2014.
4. Kording, K.P., & Wolpert, D.M. *Nature*, 427(6971),244-247. 2004.

SENSOR EVALUATION FOR INFANT BIOMECHANICS: FORCE SENSITIVE RESISTORS VS. PRESSURE SENSORS IN A PAVLIK HARNESS

Nyelah Smith[1], Ant Lakatos[3], Benjamin Johnson[3], Erin Mannen[2]
Departments of [1]Engineering Plus, [2]Mechanical and Biomedical Engineering, [3]Electrical and Computer Engineering
Boise State University, Boise, ID USA
email: nyelahsmith@u.boisestate.edu, web: https://www.boisestate.edu/coen-babi/

INTRODUCTION

Developmental dysplasia of the hip (DDH) is a common pediatric condition often treated with the Pavlik harness for infants <6 months old (Figure 1A) [1]. Breech presentation is a well-established risk factor for DDH [2], demonstrating that intrauterine leg positioning and loading influence hip development. The Pavlik harness holds the hips in a similar flex-abducted position; however, the kinetic environment inside the harness remains poorly understood. Pavlik harness treatment fails in 20% of cases for unknown reasons. Understanding loading during harness wear may help clarify factors related to treatment success and failure. We hypothesize wear time correlates with the forces transmitted across the hip joint which may accelerate and improve outcomes, but there is currently no available sensor-infused harness to gather these data. Therefore, our objective was to compare a custom force-sensitive resistor (FSR) with commercial pressure sensors to identify a practical and reliable approach for measuring infant kicking force and frequency (Figure 1B).

METHODS

We fabricated custom Velostat-based FSRs (Figure 1B) and characterized them using an Instron testing machine with a 500 N load cell (Figure 1C). We tested four sensors under compressive loads of up to 100 N, which exceeds the expected infant kicking range from prior studies [3,4]. A Teensy microcontroller recorded sensor output concurrently with Instron force measurements. We processed these datasets in MATLAB to generate calibration curves and evaluated linearity, sensitivity, and repeatability across trials.

RESULTS AND DISCUSSION

The updated FSRs showed consistent sensitivity across all four devices, with calibration slopes of 52-54 ADC/N (Sensor 1: 54.3; Sensor 2: 54.2; Sensor 3: 52.8; Sensor 4: 52.3 ADC/N). Linearity also improved compared to the commercial pressure sensor ($R2 = 0.77$), with the revised sensors achieving R2 values of 0.77, 0.84, 0.89, and 0.92 for Sensors 1-4, respectively. Sensor 4 exhibited the highest linearity ($R2 = 0.92$) while maintaining comparable sensitivity (52.3 ADC/N), representing ~19% improvement in linearity compared to the commercial sensor. These results demonstrate improved sensor consistency and linearity across the tested range, indicating that the updated FSR design is suitable for quantifying infant kicking forces during Pavlik harness wear.

CONCLUSIONS

Accurately measuring infant kicking force and frequency is essential for understanding hip biomechanics during Pavlik harness treatment. Reliable sensor measurements will enable future in-harness monitoring of infant movement and loading, which may improve understanding of treatment mechanics and help identify factors contributing to Pavlik harness failure in DDH treatment. Future work includes *in vivo* testing on healthy infants to evaluate kicking force and frequency during wear.

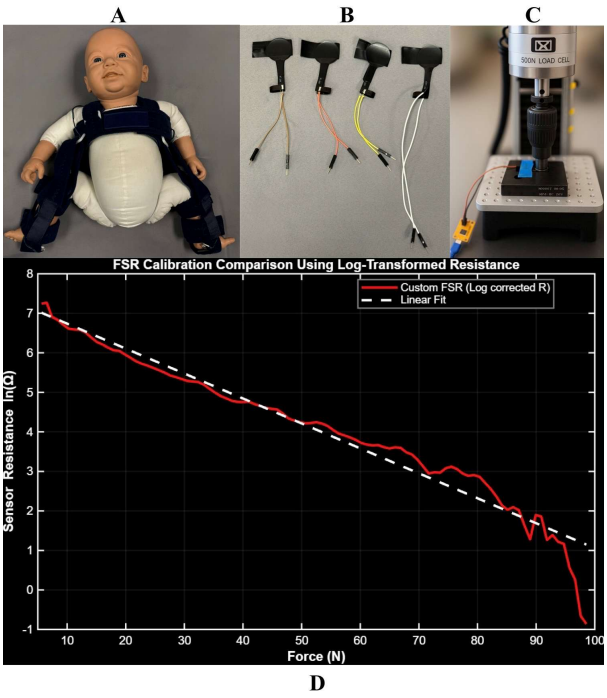

Figure 1: (A) Pavlik harness on a mannequin. (B) Custom fabricated FSRs. (C) Instron compression testing setup in progress. (D) Calibration curves comparing the custom FSRs and commercial pressure sensor.

REFERENCES

1. Gargan K, et al. *J Orthop.* 2016.
2. Lankinen V, et al. *BMC Pediatr.* 2023.
3. Lim Y, et al. *Math Comput Appl.* 2022.
4. Verbruggen SW, et al. *J R Soc Interface.* 2018.

ACKNOWLEDGEMENTS

This research is supported by the National Institutes of Health IDeA INBRE and COBRE Programs, NIH Grants No. 920GM103408, P20GM109095, and P20GM148321 (NIGMS). Harnesses provided by RHINO Pediatric Orthopedic Designs INC. Dr. Erin Mannen owns Mannen Bio, LLC, an engineering and expert consulting company. This project was made possible in part to the Higher Education Research Council Fellowship, funded by the Idaho State Board of Education.

SEMI-AUTOMATED BONE AND SKIN SEGMENTATION FOR DYNAMIC MUSCULOSKELETAL ULTRASOUND

Ozanich, NR[1,2], Telfer, S[1,2,3], Muir, BC[1,2] and Ledoux, WR[1,2,3]
[1]Center for Limb Loss and MoBility (CLiMB), VA Puget Sound Health Care System,
Departments of [2]Mechanical Engineering and [3]Orthopaedic Surgery & Sports Medicine, University of Washington,
email: ozanich@uw.edu

INTRODUCTION

Measuring tissue thickness from dynamic B-mode ultrasound is useful for characterizing musculoskeletal soft tissue mechanics, yet frame-by-frame manual segmentation is prohibitively time-consuming for the thousands of frames typical in dynamic recordings. Here we present a semi-automated segmentation pipeline that predicts bone and skin segmentations, filters them via shape-quality metrics, refines them using a lightweight U-Net [1], and produces per-frame tissue thickness measurements across loading cycles.

METHODS

Dynamic B-mode ultrasound data was collected from two anatomical sites at 45 fps for a cadaveric specimen (heel pad) and in vivo human subject (second metatarsal head). For the calcaneal heel pad, one cadaveric specimen was tested under Instron-applied cyclic loading at three frequencies (0.5, 1.0, and 1.5 Hz), each at three speed-of-sound (SoS) settings (1540, 1600, and 1660 m/s) for 25647 total frames. For the second metatarsal head, one in vivo subject was recorded during walking at the same three SoS settings for 4033 frames total. Regions of interest were drawn for the bone and skin to constrain initial segmentations. Bone segmentation proceeded in two stages. First, pseudo-labels were generated automatically using Gabor filtering, adaptive thresholding, and B-spline contour smoothing. These pseudo-labels were filtered via three shape-quality criteria: minimum contour area, minimum mean mask thickness, and a contour-curvature spike score that penalizes sharp protrusions in the segmented mask. Skin boundaries were detected using a similar Gabor filtering and thresholding approach with parameters tuned to the skin layer.

The filtered pseudo-labels were used to train a lightweight U-Net (4 encoder/decoder blocks, batch normalization, binary cross-entropy (BCE) + Dice similarity coefficient (DSC) loss) to regularize bone masks across all frames. U-Net inference replaced noisy or missing pseudo-labels with smoother, temporally consistent masks. Per-frame tissue thickness was measured as the vertical distance between the skin boundary and bone apex, averaged across a 7-column window centered at the bone apex. Loading/unloading cycles were identified via peak detection on the smoothed ``thickness time series. Segmentation quality was assessed via temporal intersection over union (IoU: overlap between consecutive frames), centroid drift, and thickness time-series smoothness (jitter) before and after U-Net refinement.

RESULTS AND DISCUSSION

For the cadaveric heel pad, U-Net regularization improved temporal IoU from 0.784 ± 0.020 to 0.883 ± 0.022 and reduced centroid drift from 2.3 ± 0.4 to 1.1 ± 0.2 pixels. Thickness jitter (median frame-to-frame change) decreased from 0.041 to 0.003 mm. Shape-quality filtering rejected 82.5 ± 15.2% of pseudo-labels, with higher rejection rates at 1600 and 1660 m/s speed-of-sound settings. Tissue thickness range was 1.10 ± 0.011 mm (Figure 1). For the in vivo metatarsal head, U-Net improved IoU from 0.789 ± 0.003 to 0.821 ± 0.003, reduced drift from 2.1 to 1.9 pixels, and decreased jitter from 0.039 to 0.025 mm. The rejection rate was 47.3 ± 16.5% and tissue thickness range was 2.21 ± 0.24 mm. Unloaded thickness scaled with the configured SoS (~9.5% increase between 1540 and 1660 m/s in cadaver testing), consistent with the distance scaling inherent to the configured SoS.

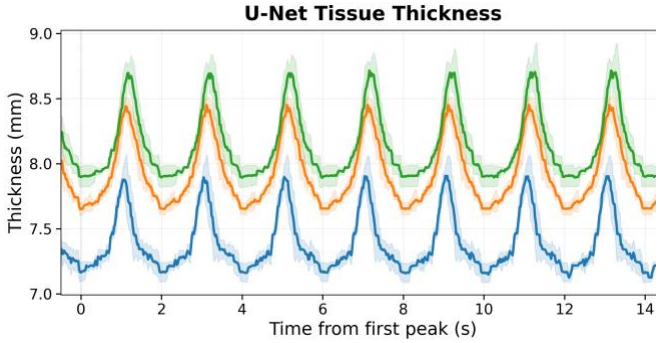

Figure 1: Mean plantar soft tissue thickness above the U-Net segmented bone mask across frames, compared across speed-of-sound settings (blue: 1540 m/s, orange: 1600 m/s, green: 1660 m/s), for cadaveric heel pad specimens under 0.5 Hz cyclic loading.

This methodology is suited for medium-sized, homogeneous dynamic B-mode ultrasound datasets, with preprocessing and shape-filtering parameters tunable for different applications. A limitation is the absence of ground-truth expert segmentations; quality was assessed through temporal consistency metrics rather than direct accuracy measurement.

CONCLUSIONS

This work introduces a semi-automated framework for bone and skin segmentation in dynamic musculoskeletal ultrasound. By generating pseudo-labels from classical image processing, filtering via shape-quality metrics, and refining with a lightweight U-Net, the pipeline produces temporally consistent boundary masks and per-frame tissue thickness measurements with minimal manual input.

REFERENCES

1. Ronneberger O, et al. *Medical Image Computing and Computer-Assisted Intervention – MICCAI 2015*, Lecture Notes in Computer Science, **9351**, 234-241, 2015.

ACKNOWLEDGEMENTS

Funded partially by AR072216 and IK6RX00297.

The Effect of Feeding on Infant Breathing Biomechanics, A Pilot Study

Shameka Kimmel[1], Holly Olvera[1], Chris Wilson MS[1], and Erin Mannen PhD[1, 2]
Departments of [1]Biomedical Engineering and [2]Mechanical Engineering, Boise State University, Boise, ID USA
email: shamekakimmel@u.boisestate.edu

INTRODUCTION

Around 3,600 infants die suddenly in their first year of life, and for poorly understood reasons, most deaths occur between 1 and 4 months of age [1]. Feeding has been linked to lower oxygen saturation and volumetric changes in the thorax of infants. Infant respiratory mechanics differ substantially from those of adults [2]. Their rib cages are more compliant, diaphragms function differently, and abdominal contents occupy proportionally more space. Despite these differences, post-feeding positioning is often treated as biomechanically neutral. Feeding increases gastric volume, which may influence diaphragmatic excursion and thoracoabdominal coordination. However, the direct relationship between feeding and breathing biomechanics remains unknown, and no results have informed best practices for infant care related to respiratory function or Sudden Unexpected Infant Death. The purpose of this study is to, for the first time, determine the effect of feeding on breathing biomechanics in full-term and preterm infants.

METHODS

Three full-term infants, 6 months of age, were included in this pilot study. Using motion capture, a pattern of retro-reflective markers was placed on the infant's chest and abdomen to capture inhalation and exhalation motion of the Belly Band shown in Figure 1. Marker trajectories were recorded using an 8-camera motion capture system at 100 Hz. EMG data were collected from the right and left abdominal muscles, along with heart rate measurements. A respiratory monitor and nasal cannula were used to track CO_2 output, and an oxygen saturation monitor was placed on the foot to ensure adequate oxygen levels during trials. The infant was placed supine on a hard surface within the capture volume. Two pre-feeding trials were collected for baseline data. The infant was then weighed and measured for pre-feeding anthropometrics and fed by the parent using a bottle. The bottle was weighed before and after feeding to measure total food intake. Post-feeding weight and anthropometric measurements were collected within five minutes of feeding. Four post-feeding trials were then recorded to evaluate changes in respiratory rate and breathing biomechanics.

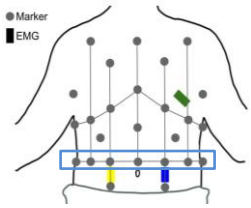

Figure 1: Representing the Belly Band marker placements used in the motion capture system.

RESULTS AND DISCUSSION

Thoracic and abdominal marker displacement were used to quantify respiratory exhalation and breathing frequency. Figure 2 shows and inferior view of the belly, highlighting the maximum inhale and exhale displacement for pre- and post-feeding breaths. The post-feeding graph in Figure 2B exemplifies a stomach protrusion in the frontal plane of the infant. The shape of the belly becomes a wider profile and

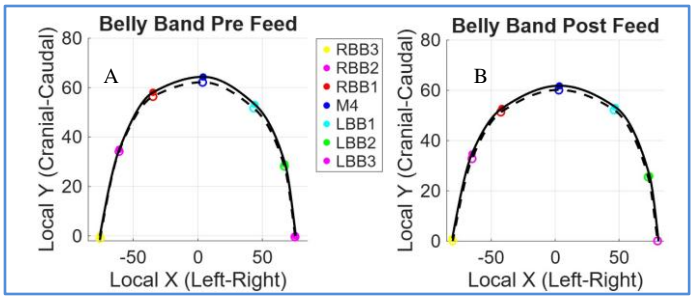

Figure 2: A. Representing motion capture markers at full inhalation(solid) and exhalation(hollow) for pre-feeding. B. Representing the post-feeding breath.

vertical expansion of the breaths change after feeding. Although not shown on these graphs, the overall increase in expansion at full inhalation of the M4 marker, located above the belly button, was between 3 mm and 6 mm post feed, demonstrating the idea of gastric filling.

Although this pilot study includes only three infants, these preliminary methods demonstrate our ability to detect small differences in thoracoabdominal mechanics during respiration before and after feeding. Altered abdominal expansion following feeding may reflect changes in diaphragmatic movement or increased abdominal pressure due to gastric filling. Future analysis will compare respiratory rate, heart rate, and thoracoabdominal expansion patterns between pre- and post-feeding conditions to determine whether feeding alters respiratory biomechanics. CO_2 output will be monitored to evaluate potential ventilatory changes, and oxygen saturation and breathing cycle duration will also be assessed. Understanding how feeding influences breathing mechanics may help identify physiological changes during this period and inform future investigations into infant respiratory regulation.

CONCLUSIONS

Preliminary results from this pilot study demonstrate our ability to detect small differences in thoracoabdominal mechanics during respiration before and after feeding. Future work will expand this protocol to a cohort of 90 infants, including both full-term and preterm infants, with age ranges of 4–8 weeks, 12–16 weeks, and 20–24 weeks. This larger study will examine how feeding influences respiratory rate, heart rate, thoracoabdominal motion, and the time required for respiratory patterns to return to baseline following feeding.

REFERENCES

1. Parks, S. E., et al. *Pediatrics*, 147(5), 2021.
2. Hammerman, C. and Kaplan, M. *Neonatology*, 67(2), 1995.

ACKNOWLEDGEMENTS

This research is supported by the NICHD, NIH Grant No. 1R01HD113921. EMM owns Mannen Bio, LLC, an expert and engineering consulting company.

Repeatability of Segmental Asymmetry Metrics for Telemedicine Amputee Mobility Assessment using Self-Placed IMUS

Redmond J.R., Kennedy C., Nash W., Flynn G., Pew C.A.
Department of Mechanical and Industrial Engineering
Montana State University, Bozeman, MT USA
email: joesph.redmond@montana.edu

INTRODUCTION

Amputees experience gait asymmetries, impacting mobility and quality of life. Clinicians currently assess amputees using Observational Gait Analysis, a subjective measure relying on clinician skill and in-person appointments. For remote populations, assessments can be infrequent and inaccessible. Inertial Measurement Units (IMUs) can provide objective metrics of gait symmetry using segmental metrics of the thigh and shank [1]. Measurements may lose accuracy if IMUs are self-placed in Telemedicine visits. This study aims to evaluate IMU measures of segmental symmetry when sensors are placed by the patient. We hypothesize that self-placed IMUs can produce reliable and repeatable segmental symmetry analysis.

METHODS

Four IMUs with an alignment pin were developed to aid participants in self-placement on the anterior thighs and shanks. Participants were observed on a treadmill walking at 3 different speeds relative to a 2-minute walk test. Optical motion capture (MoCap) generated a control dataset, and markers applied to IMUs quantified misalignment. Sagittal angular velocity measurements were normalized and used to create asymmetry scores for each segment pair, computed by the mean Euclidian difference between paired gait cycles on the left and right [1]. Self-placement was done twice to assess measurement repeatability. Between MoCap and IMU generated scores, a paired t-test evaluated score changes, while a Pitman-Morgan test evaluated intertrial variance.

RESULTS AND DISCUSSION

Shank asymmetry metrics on 9 Healthy Controls (6F; 53±19yrs.) were found to be greater using self-placed IMUs compared to MoCap (11.85 vs 11.12, $p=0.021$) and showed higher variance under with sensor reapplication (Ratio=3.7, $p=0.001$). Net axial misalignment between the left and right sensors correlated with higher asymmetry scores ($\beta=0.09$ pts/deg, $R^2=0.19$, $p=0.001$; Misalignment=11.6±8.1º). Under repeated conditions, motion capture established a minimal detectable change (MDC=2.55) that 29% of IMU score pairings exceeded.

While score bias can be calibrated, IMU noise reduces repeatability of asymmetry measurements. Sensor alignment impacted scores, and variability increased with sensor replacement. While assisted alignment constrained placement of sensors, self-placed IMUs variability sensitivity of measurement.

CONCLUSIONS

In Telehealth visits, increased score variability introduces false-positive detection of change compared to clinical-placed sensors and reduces measurement resolution. Future work will discuss consistency metrics, extend analysis to thigh segments, evaluate amputee populations, and consider noise regression methods.

REFERENCES

1. Sheila Clements et al. *Clinical Biomechanics* 2020.

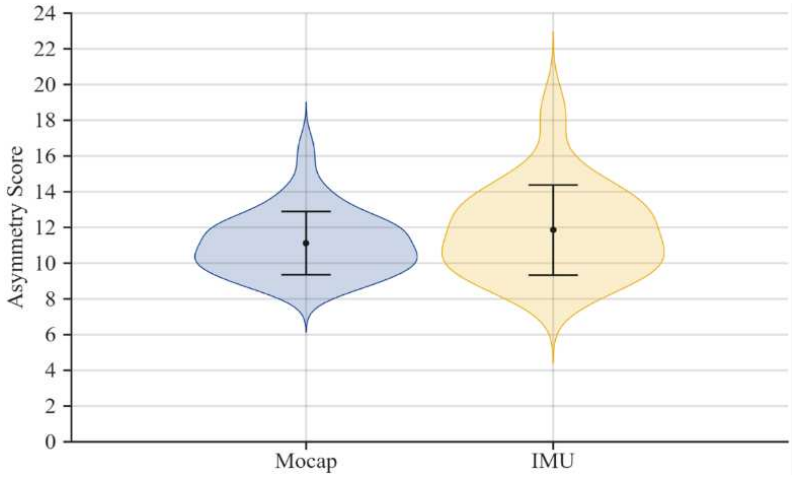

Figure 1: Violin plot of asymmetry score distributions, compared between IMU and Cocap collected data (Mean ± 1 Std. Dev.)

VALIDATION OF OPEN CAP FROM NON-RECOMMENDED VIEWPOINTS

Maya Ansu-Kyeremeh[1], Ishi Arora[1], and Calvin Kuo[1]
[1]School of Biomedical Engineering, University of British Columbia, Vancouver, BC Canada
email: mayasnasu@gmail.com , web: https://humbl.sbme.ubc.ca/

INTRODUCTION

OpenCap is a markerless motion capture technology that utilizes 2D pose estimation algorithms from OpenPose to determine kinematics from two or more synchronized cameras. OpenCap recommends a two-camera setup at a 30-45° angle off the participant's frontal line [1]. However, following these recommendations may not always be possible outside a controlled motion capture laboratory.

In efforts to make motion capture more accessible, we therefore need to understand how changes in camera angle could result in discrepancies in the OpenCap's 3D reconstruction algorithm and its ability to accurately quantify joint angles.

METHODS

To assess OpenCap with different camera angles, we collected videos from 24 participants performing various sport-related movements. Data from 2 participants (24 y.o., 1F) were analyzed for this study. The movements were captured by 8 synchronized Sony RX0II cameras (60Hz) arranged around the participant at 45° increments. From these cameras, we tested OpenCap with all 28 different pairs of cameras with separations of 45, 90, 135, and 180 degrees. A localized version of OpenCap was used to compute knee joint angles across triple crossover jump trials, where we compared the peak knee joint angle during the third crossover jump against a ground-truth 3D marker-based motion capture system (8-camera 960Hz PhaseSpace with 50 markers). The first and last peak in the time-series data (Figure 1) correspond to synchronization stomps to align the different conditions.

The knee joint angles from the maker-based data were calculated using inverse kinematics based on marker clusters placed on the thigh and shank, with segment coordinate systems defined relative to anatomical landmarks at the hip, knee, and ankle.

RESULTS AND DISCUSSION

Out of the 28 different camera configurations, only nine of the camera configurations were able to produce 3D key points and successful kinematic outputs from the OpenCap pipeline. The peak knee joint angle error ranged from 6.87° to 34.88° (Table 1). The lowest error was observed for the CAM5–CAM6 configuration (45° separation), which is consistent with the OpenCap recommendation, with both cameras placed forward from the participant. In contrast, the highest error was observed for the CAM1–CAM4 configuration (135° separation). This configuration includes a camera positioned behind the subject and may have increased occlusion.

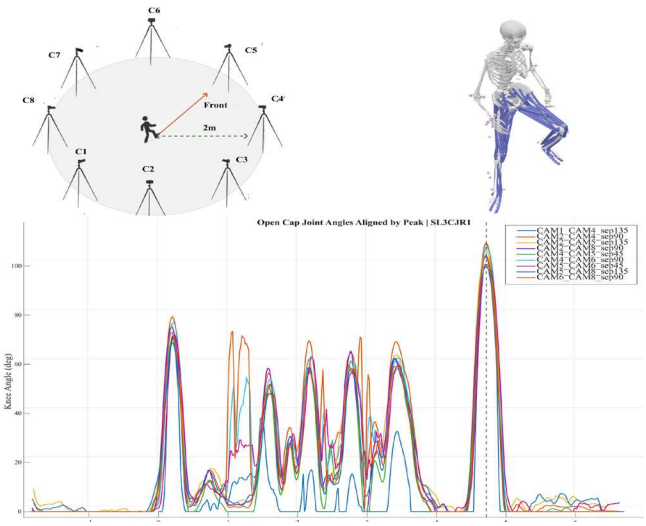

Figure 1: Effect of camera configuration on OpenCap knee joint angle reconstruction

The results indicate that camera configuration has a significant impact on the accuracy and reliability of OpenCap. Although angular separation between cameras is often considered a primary factor in multi-view reconstruction, the results indicate that separation alone does not fully determine accuracy. While 45° configurations consistently produced low errors, 135° configurations yielded both some of the best and worst results. This suggests that relative viewpoint with respect to the movement plane is more critical than separation angle alone. As an example, none of the configurations that included cameras positioned at 90° (C3) or 270° (C7) resulted in successful OpenCap reconstructions. This could be a result of an additional increased occlusion of lower limb join from later orientations and OpenCap not being able to see the same key points from both camera angles.

CONCLUSIONS

This study showed that camera configuration has an impact on the success and accuracy of OpenCap. While OpenCap recommends specific camera positions for their system, our work shows that OpenCap can reconstruct 3D motion biomechanics across a larger range of camera configurations, but care must still be taken to avoid certain camera angles such as the 90° and 270° positions.

REFERENCES

1. Uhlrich S. (2023). PloS Comput Biol

Table 1: Peak knee joint angle error across successful camera configurations

Camera Configuration	C5C6	C2C5	C5C8	C4C5	C4C6	C2C4	C2C8	C6C8	C1C4
Separation (°)	45	135	135	45	90	90	90	90	135
Peak Error (°)	6.87	7.36	7.69	10.69	11.08	14.42	15.01	20.70	34.88

TURN-CYCLE HIP AND KNEE JOINT MECHANICS IN A BELOW-KNEE ADAPTIVE SKIER USING TWO PROSTHETIC FOOT DEVICES

Malakian, A, Wilson, C, and Seifert, J
Department of Food Systems, Nutrition and Kinesiology
Montana State University, Bozeman, MT USA
Email: alique.malakian@montana.edu

INTRODUCTION

Adaptive skiing is a growing sport that is constantly changing with the development of modern and specialized equipment. In particular, the development of lower-limb sport-specific prosthetic devices has allowed a large population of people to enjoy the benefits of skiing regardless of physical disabilities of the lower limb.

Two main types of skiing prostheses are an articulated 'ankle' that attaches to the prosthesis and clamps directly into the ski binding. The other type is a rigid, non-articulating prosthesis that has a rigid foot at the distal end that inserts into the ski boot. These prosthetic devices differ in construction and function and may theoretically alter skiing mechanics. The purpose of this study was to compare how hip and knee sagittal plane joint kinematics differed throughout an alpine turn cycle between a non-articulating prosthetic limb and an articulating ski foot. It was hypothesized that the articulating ski foot would allow the skier to assume a more dynamic position throughout a turn, exhibited by increased outside leg (OL) hip and knee extension and inside leg (IL) hip and knee flexion.

METHODS

One experienced below-the-knee prosthetic skier (female, 24 years old, right leg prosthetic) completed 68 total left and right alpine ski turns with a non-articulating prosthetic limb and 52 left and right turns with an articulating ski foot (Alpine Foot, Fresno, CA). All turns were collected on the same ski run at Bridger Bowl Ski Area (Bozeman, MT). Brush gates were used to standardize turns. The same skis were used under both conditions. Full-body 3D kinematics were collected using the Xsens Link IMU body suit at 240 Hz. Turns were normalized to 100% for each limb and condition. Joint kinematics were calculated using a YXZ Cardan sequence. A statistical parametric mapping paired t-test was conducted between the subject's mean non-articulating prosthetic and articulating ski boot turns. Left and right OL turns were differentiated for each joint.

RESULTS AND DISCUSSION

Contrary to the hypothesis, the articulating ski foot primarily enhanced dynamic joint characteristics for the control limb OL turns as opposed to both control and prosthetic limb OL turns. While performing OL turns on the control limb (left leg), the articulating ski foot allowed the participant to exhibit significantly greater prosthetic limb hip and knee flexion compared to the non-articulating prosthetic. To compliment this, the control OL displayed significantly greater hip extension in the latter half of the turn cycle and significantly greater knee extension throughout the entire turn cycle duration. However, while performing OL turns on the prosthetic limb (right leg), the articulating ski foot exhibited significantly greater prosthetic limb hip and knee flexion; notably, the joint movement strategy for the control limb as the IL did not differ for either prosthetic condition throughout a majority of the turn cycle (Figure 1).

It was unexpected to mainly observe dynamic joint kinematics for the control limb outside turns but not for the prosthetic limb outside turns, even though the prosthetic limb was the varying component between conditions. The knee movement pattern with the articulating ski foot, characterized by greater control OL extension and prosthetic IL flexion, aligns with PSIA-described high-level skiing mechanics for non-adaptive skiers [1]. Additionally, significantly greater control IL knee extension at the end of the turn cycle suggests that the articulating ski foot facilitated the transition from IL to OL for the control limb better than the non-articulating prosthetic (Figure 1).

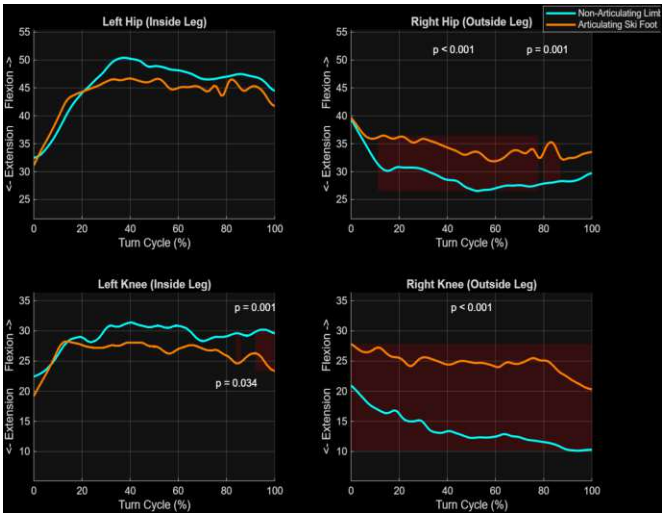

Figure 1: Sagittal plane mean joint angles (°) of prosthetic OL alpine ski turns with SPM results. Significant clusters are shaded with the respective p-values reported.

REFERENCES

1. Professional Ski Instructors of America. *Alpine Technical Manual*. (2015).

THE ROLE OF ACHILLES TENDINOPATHY ON THE TORQUE-ANGLE RELATIONSHIP DURING ISOKINETIC PLANTAR FLEXION

Hayashi, H[1], Whalen, C[1], Hahn, ME[1]
[1]Bowerman Sports Science Center, Department of Human Physiology,
University of Oregon, Eugene, Oregon, USA
Email: hhayash7@uoregon.edu

INTRODUCTION

Achilles tendinopathy (AT) is a degenerative pathology associated with increased cross-sectional area and decreased stiffness [1]. Previous work showed that a shift in peak torque angle to a more extended position occurs with increasing joint angular velocity during isokinetic knee extension, and that this shift can be attributed to tendon compliance [2]. While it is known that AT alters tendon compliance, the effect of such pathology on the ankle joint angle-peak torque relationship is unclear. Therefore, the purpose of this study was to elucidate the effect of AT on the ankle joint angle-peak torque relationship during a concentric isokinetic plantar flexion task.

METHODS

Five participants with symptoms of AT and 5 healthy age and sex matched controls provided informed consent to participate in this IRB approved study. The inclusion criteria for the AT group included being 18-45 years of age, have had self-reported symptoms of AT for at least the past 4 weeks prior to data collection, score <80 on the Victorian Institute of Sport Assessment-Achilles questionnaire, have no history of Achilles tendon rupture, and have no other current lower extremity injury.

Participants were positioned on an isokinetic dynamometer with their thigh-trunk angle at 110 degrees (180 degrees = full extension), knee fully extended, and the foot firmly fixed to the footplate. After a warm-up consisting of a series of submaximal concentric plantar flexion contractions, participants performed 2 sets of 5 maximal concentric plantar flexion contractions at pre-set angular velocities of 30, 60, and 90 deg/sec. Isokinetic torque and angular position data were sampled at 1kHz. The trial with the highest torque output was used for analysis and was analyzed in the range of 5 degrees of dorsiflexion to 15 degrees of plantar flexion. A mixed model ANOVA (group x angular velocity) was used to test for the effect of independent variables on the joint position at peak torque.

RESULTS AND DISCUSSION

There was a significant interaction between group and angular velocity ($p < .05$, fig.1). Simple main effect analysis revealed a main effect of angular velocity, with significant difference between the 30 and 90 deg/sec as well as between the 60 and 90 deg/sec conditions ($p < .05$). There was no main effect of group ($0 = .487$). While the effect of angular velocity on the shift in peak torque angle towards a more plantar flexed position is consistent with previous findings for the knee extensors [2], the significant interaction effect suggests altered velocity dependent modulation of the torque-angle relationship in individuals with AT.

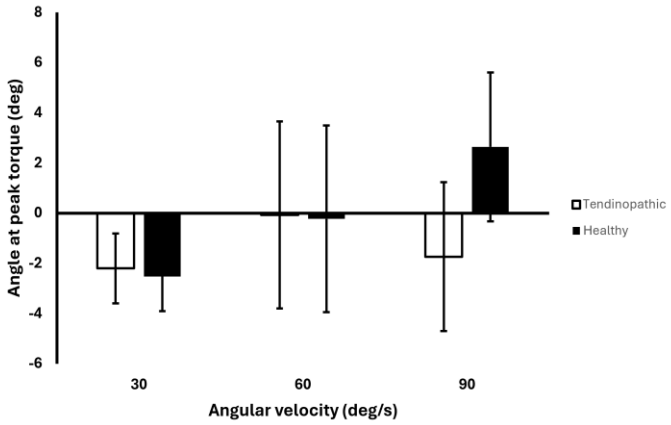

Figure 1: Ankle joint angle at peak torque as a function of joint angular velocity during isokinetic plantar flexion

CONCLUSIONS

A shift in peak torque angle towards a more plantar flexed position was observed, which is consistent with previous studies [2]. Further, the significant interaction effect may suggest that AT alters muscle-tendon unit function at higher joint angular velocities. Further analysis of fascicle behavior and muscle activation patterns may reveal the mechanisms in which AT may alter torque output during isokinetic plantar flexion movement.

REFERENCES

[1] Arya S and Kulig K (2010). *J Appl Physiol,* **108**: 670-675
[2] Kawakami et al., (2002). *Eur J Appl Physiol,* **87**: 381-387

ACKNOWLEDGEMENTS

This work was supported by the Wu Tsai Human Performance Alliance and the Joe and Clara Tsai Foundation.

VALIDATION OF OPENCAP KINETIC ESTIMATION DURING THE SINGLE-LEG VERTICAL JUMP TASK

Stemler S[2], Lynch A[1], Gaston L[2], Larson J[1], Aflatounian F[1] and Monfort S[1]
Department of [1]Mechanical and Industrial Engineering
[2]Montana State University, Bozeman, MT USA
Email: sophia.stemler@student.montana.edu

INTRODUCTION

Assessing asymmetries in the knee extension moment (KEM) can identify unresolved compensatory strategies following anterior cruciate ligament reconstruction (ACLR) [1]. However, collection of kinetic data typically requires costly lab-based motion capture (MoCap). OpenCap is an affordable alternative that uses 2+ iOS devices for motion capture, automated cloud-based kinematic estimation, and estimation of kinetics through additional simulation [2]. OpenCap kinematics can be comparable to MoCap, though OpenCap kinetics remain largely unexplored [3]. This study addresses that knowledge gap by comparing kinetics estimated from OpenCap with simultaneously collected MoCap data during the single-leg vertical jump (SLVJ) task [1]. We hypothesized that OpenCap+simulation KEM estimates would strongly correlate with MoCap.

METHODS

Eight participants (4F/4M, 22.5±3.5yrs, 1.72±0.08m, 69.5±14kg) completed 3 SLVJ trials on their right leg. Trials were recorded with a laboratory motion capture system (Qualisys) and a 3-device OpenCap setup. MoCap data were processed in Theia3D, and MoCap kinetics were estimated using inverse kinematics in Visual3D. OpenCap kinetics were estimated with a torque-driven simulation through the OpenSim algorithmic differentiation workflow [4]. Peak KEM (pKEM) values for propulsion (0.4s before takeoff to takeoff) and landing (takeoff to peak knee flexion) were normalized by height and averaged for each individual. Pearson correlations between MoCap and OpenCap pKEM values were evaluated.

RESULTS AND DISCUSSION

A significant strong correlation was found between MoCap and OpenCap pKEM estimates in the landing phase ($r=0.875$, $p=0.004$), while no significant correlation was found in the propulsion phase ($r=0.435$, $p=0.282$) of the SLVJ (Figure 1).

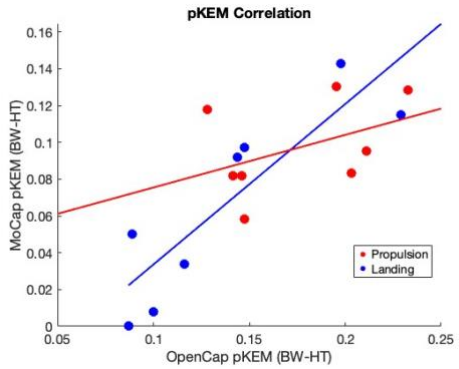

Figure 1: Scatterplot depicting normalized pKEM estimates from OpenCap and MoCap in the SLVJ.

OpenCap-based estimation of pKEM via torque-driven simulation displayed similarities to laboratory grade kinetics, though small systematic bias (~0.07 %BW-HT) remains (Figure 2). These findings may support the use of OpenCap+simulation to identify KEM asymmetries following ACLR as an alternative to more expensive MoCap systems. The additional field of view from the third camera and the marker-enhancement software update in OpenCap [5] likely improved kinematic and kinetic estimates from prior comparisons [6]. However, the lack of significant correlation in the propulsion phase may indicate underlying limitations in OpenCap kinetic estimation. Ground reaction force (GRF) estimation from video-based data collection techniques remains difficult and may impede kinetic estimation with OpenCap data. These data are part of an ongoing study with additional comparison to marker-based MoCap using a 16-camera hybrid setup. Additional participants may affect overall outcomes. Future work should address other dynamic tasks and kinetic measures that were not investigated in this study.

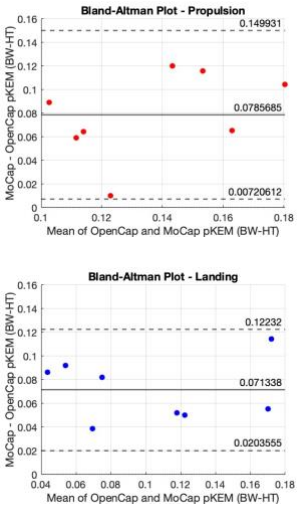

Figure 2: Bland-Altman plot depicting the mean values vs. the differences between pKEM estimates from OpenCap and MoCap. Lines represent the mean difference and limits of agreement (95%), which is larger for propulsion than landing. Data show natural variability about the average difference line, with OpenCap systematically underestimating KEM relative to MoCap.

CONCLUSIONS

This preliminary dataset indicates agreement between OpenCap and MoCap KEM estimates during landing in the SLVJ task. Further investigation is necessary due to the important clinical relevance of an accurate, affordable motion analysis system.

REFERENCES

1. Kotsifaki, A, et al. *Br J Sports Med* **56**(9), 490-498, 2022.
2. Uhlrich, S, et al. *PLoS Comput Biol* **19**(10), e1011462, 2023.
3. Turner, J, et al. *J Biomech* **171,** 112200, 2024.
4. Falisse, A, et al. *PLoS One* **14**(10), e0217730, 2019.
5. Falisse, A, et al. *IEEE Trans Biomed Eng* **72**(6), 2013-2020. 2025
6. Stemler, S, et al. *ASB Abstract*, 2025.

ACKNOWLEDGEMENTS

Supported by the MSU Undergraduate Scholars Program.

INTER-JOINT COORDINATION DIFFERS ACROSS ABILITY LEVELS IN CROSS-COUNTRY SKATE SKIING

Whitcomb, C, Becker, J
Department of Food Systems, Nutrition and Kinesiology
Montana State University, Bozeman, MT USA
email: charlotte.whitcomb@msu.montana.edu, web: https://www.montana.edu/biomechanics/people/becker.htlm

INTRODUCTION

Skate cross-country skiing requires complex full-body simultaneous movement of multiple joints and segments. Vector coding analysis quantifies inter-joint coordination and multi-joint movements patterns through angle-angle presentations, as opposed to classic joint angles versus time presentations [1]. A common method for running technique analyses, vector coding provides a measure of relative timing and magnitude of motion between segments [2]. This method has never been applied to cross-country skiing and thus the purpose of the study was to characterize coordination patterns during V2 skiing. Secondly, we compared coordination patterns between junior-caliber, national-caliber, and world-class athletes.

METHODS

Nine junior-caliber (JC) (18 ± 1.06 years; 4M, 4F), seven national-caliber (NC) (26 ± 3.95 years; 4M, 3F), and eight world-class (WC) biathletes (27.63 ± 4.50 years; 5M, 3F) skied at race intensity on a rollerski treadmill while whole-body kinematics were captured via a hybrid markerless motion-capture system. Three joint couplings were analyzed: torso flexion/extension and pole angle (torso-pole), shoulder flexion/extension and elbow flexion/extension (shoulder-elbow), and hip flexion/extension and knee flexion/extension (hip-knee). Each coupling was assessed across the full ski cycle, defined based on consecutive pole plants. For each coupling, coordination was calculated using angle-angle plots and modified vector coding [3]. Coordination was "binned" into four different patterns: in-phase, anti-phase, distal dominant, and proximal dominant. A 3 (group) x 4 (coordination pattern) ANOVA was used to compare differences in coordination patterns across groups.

RESULTS AND DISCUSSION

Figure 1 displays mean coupling angle for ability groups over the normalized cycle for each joint coupling pair. Patterns were categorized by equal amounts of in-phase, anti-phase, proximal, and distal dominant coordination. No differences were observed for torso-pole, or shoulder-elbow. However, a significant group x coordination pattern was observed for hip-knee ($F(6,63) = 3.123$, p-value = 0.010). JC athletes showed more distal dominant coordination than NC athletes ($p = 0.14$). JC and WC athletes utilize more proximal dominant coordination and less anti-phase coordination than NC athletes ($p = 0.037$, $p = 0.044$, $p = 0.014$, $p = 0.012$).

The results may support the "intermediate effect" demonstrated by the U-shaped pattern function, where performance decreases with intermediate levels of training compared to performance of novice and elite level athletes [4].

CONCLUSIONS

NC athletes used less proximal dominant coordination and more anti-phase coordination within the hip-knee joint coupling than JC and WC athletes.

REFERENCES

1. Khuyagbaatar B, et al. *Proc Inst Mech Eng H*, 2017.
2. Hafer J, et al. *Elsevier*, Amherst, Ma, 2016.
3. Chang R, et al. *J Biomech*, 2008.
4. Patel V, et al., *The Oxford Handbook of Thinking and Reasoning,* 2017.

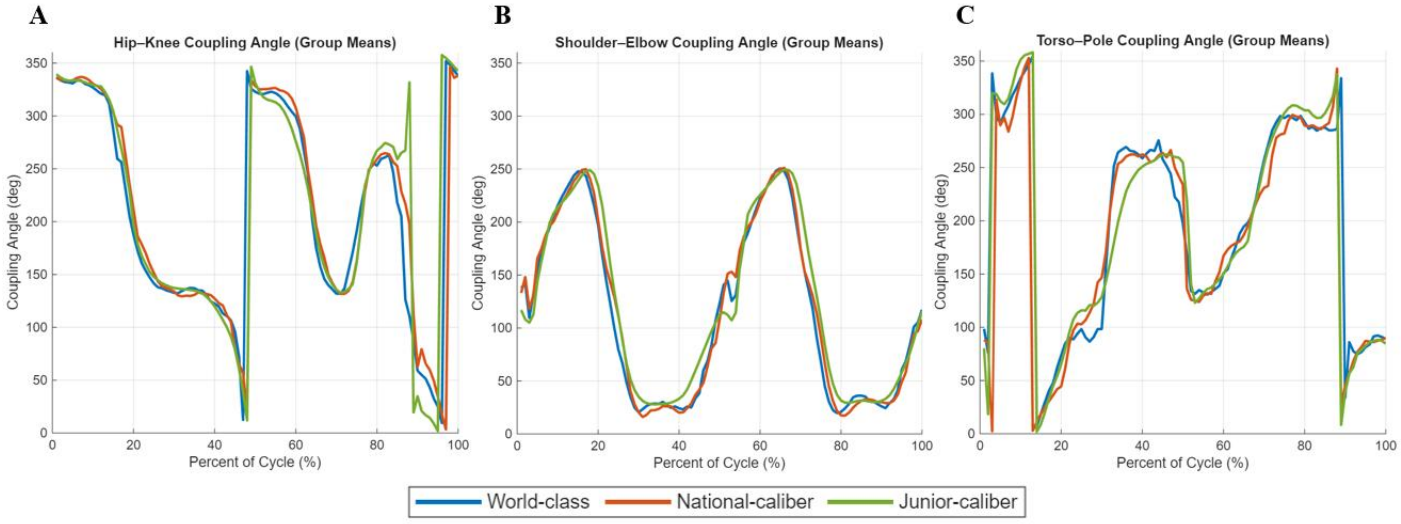

Figure 1. Group mean coupling angle over cycle for (A) hip-knee, (B) shoulder-elbow, and (C) torso-pole coupling pairs between world-class, national-caliber, and junior-caliber ability groups.

THE EFFECTS OF SPEED AND FATIGUE ON PEAK VERTICAL GROUND REACTION FORCES DURING RUNNING

Williams E[1], Hugard S[1], and Hahn M[1]
[1]Neuromechanics Lab, Department of Human Physiology, University of Oregon, Eugene, OR
email: ewillia8@uoregon.edu

INTRODUCTION

Vertical ground reaction force is the largest component of surface contact force acting on the body during gait [1]. Previous retrospective analysis has found a significant correlation between peak vertical ground reaction force (vGRF) and increased risk of running-related injuries such as bone stress injury (BSI) [2]. Most previous work has investigated the effects of vGRF under a single speed condition, or in a non-fatigued state, which might not represent true running conditions and running experience. Previous investigations on the effects of speed or fatigue on peak vGRF during running have shown varying results. The purpose of this study is to investigate whether vGRF changes significantly with different speed or fatigue conditions during running. It is hypothesized that both speed and fatigue state will significantly change peak vGRF during running.

METHODS

Six healthy, recreational runners (5 males, 1 female, ages 18-30) provided informed consent to engage in this IRB-approved study. This is a preliminary subset of an ongoing study with a projected sample size of 28. Participants completed 3 running trials using the Brooks Launch 10. During the first trial (low-speed, low-fatigue) and third trial (low-speed, high-fatigue) participants ran for 10 minutes at 80% of their lactate turnpoint (LTP). Thirty seconds of vGRF data were collected at minute 8 for trials 1 and 3. During the second trial (high-speed, low-fatigue), participants ran at 105% of their LTP and vGRF data were collected for 30 seconds at minute 2. Ground reaction force data were collected at 1000 Hz using a force-instrumented treadmill (Bertec, Columbus, OH). Peak vGRF data were averaged and normalized to body mass in Matlab (Mathworks, Natick, MA). Paired t-tests were used to compare average peak vGRF values between the two speed and fatigue conditions ($\alpha = 0.05$). To assess the effect of speed, we compared vGRF in the low-speed, low-fatigue trial to the high-speed, low-fatigue trial. To assess the effects of fatigue, we compared vGRF in the low-speed, low-fatigue trial to the low-speed, high-fatigue trial.

Results and Discussion

Peak vGRF was significantly different during running at different speeds ($p < 0.05$) but was not affected by fatigue state ($p = 0.45$). Participants were found to have significantly higher vGRF at higher speeds compared to lower speeds. This may be because with faster speeds we see a decrease in contact time, which requires greater force application within a shorter ground contact period. Additionally, during higher speeds, a higher vGRF is needed to propel the body forward more quickly. We expected to see an effect of fatigue on vGRF, but participants' vGRF were not influenced by fatigue. Our hypothesis was partially supported, as we saw that speed significantly changed vGRF, but fatigue state did not.

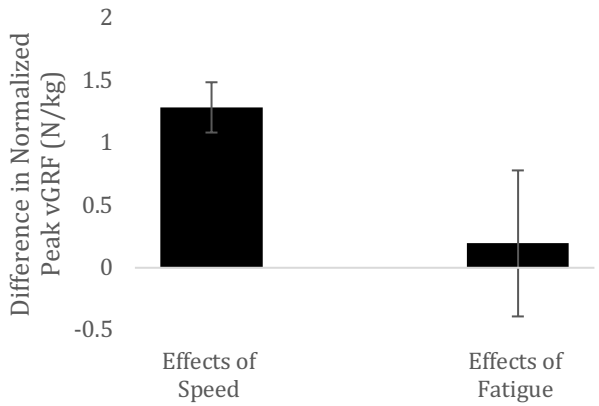

Figure 1: Differences in normalized peak vGRF as a result of increased speed (high-speed – low-speed) and fatigue (high-fatigue – low-fatigue) during running.

CONCLUSIONS

It is important to understand the effect of running speed and fatigue on peak vertical ground reaction forces when designing biomechanical experiments investigating the effects of vGRF. This study looked at the effects of fatigue and speed on vGRF during running. Our results showed that speed significantly impacts a runner's vGRF while fatigue does not. However, this is a preliminary result, and additional data collection is ongoing to further clarify this relationship. Future work could examine changes in vGRF at additional speed and fatigue states.

REFERENCES

[1] Fineberg DB, et al., *J Spinal Cord Med. 2013*
[2] Popp K, et al. *Bone.* 2016

ACKNOWLEDGEMENTS

This work was supported by the Wu Tsai Human Performance Alliance and the Joe and Clara Tsai Foundation. Footwear was provided by Brooks Running.

CENTER-OF-MASS INCLINATION ANGLE AND SKI EDGE ANGLE INFLUENCE GLIDE LENGTH ON ROLLERSKIS

Cabaniss, B, Burgess, I, Livingood, E, Becker, J
Department of Food Science, Nutrition, and Kinesiology, Montana State University, Bozeman, MT, USA

email: Brandoncabaniss2@gmail.com

INTRODUCTION

Glide length is a critical determinant of cross-country skiing performance, with longer glide length consistently linked to faster V2 ski speed [1]. On-snow studies show that mediolateral plantar-pressure balance, but not ski edge angle, is strongly correlated with glide time [2]. However, this relationship has not been examined on rollerskis despite rollerskiing accounting for over half of yearly training volume [3]. Additionally, coaches regularly refer to the importance of maintaining a stacked body position over the gliding ski, however research has not examined this concept. Thus, the purpose of this study was to investigate the relationship between glide length and plantar-pressure balance, ski edge angle, and mediolateral center of mass - ankle inclination angles during rollerskiing.

METHODS

Elite biathletes from the U.S. National (n = 12), Development (n = 8) and Junior National (n = 9) teams (15M/14F, 24±5 years) skied on a roller ski treadmill at race intensities. Ski, pole, and whole-body kinematics were collected using hybrid markerless motion capture, while forces applied to the ski were measured using in-boot plantar-pressure insoles. The gliding phase of each ski cycle was identified from ski on to peak unloading (Figure 1A; [4]). Glide length (GL), mean mediolateral center of mass - ankle inclination angle (θML) [5], mean asymmetry in mediolateral pressure distribution (ASI) [2], and average ski edging angle (θski) during the gliding phase were then calculated. Multiple linear regression was used to evaluate whether θML, ASI, and θski predicted GL.

RESULTS AND DISCUSSION

Multiple regression analysis demonstrated that ASI, θski, and θML explained 30% of the variance in GL ($F_{3,52}$=7.393, p<0.001). While ASI, not θski, is a strong predictor of GL on snow, our findings suggest the same may not be true on rollerskis. One explanation may be differences between gliding on an actual flat ski base versus a wheel on rollerskis. Less evenly distributed ASI on snow may increase ski friction and thus decrease GL. However, the same may not hold true on rollerskis, as changing ski orientation may not have as large an impact on the ski's rolling speed. On a roller ski, a skier's ability to dynamically balance on the wheels, as measured by θski and θML, appears to be more influential than plantar-pressure balance. Supporting this idea, national level skiers maintain a smaller edge angle (Figure 1C) and stack their bodyweight better over the ski (Figure 1D) compared to development and junior groups, while ASI remains similar across all groups (Figure 1B).

Table 1: Mean data for *GL*, θ_{ski}, θ_{ML} and *ASI* across the glide phase. Beta-coefficients *(ß)* and significance for each variable in the multiple regression are shown.

Variable	Mean ± SD	*ß*	*p-value*
GL (m)	3.1 ± 0.7	4.16	<0.001
ASI (%)	4.0 ± 2.9	-0.02	0.155
θ_{ski} (°)	12.9 ± 8.2	-0.07	0.025
θ_{ML} (°)	5.7 ± 1.8	-0.05	0.049

CONCLUSIONS

Skiers who maintain a more stacked body position and flatter ski across the gliding phase may glide further on rollerskis.

REFERENCES

[1] Smith et al. J Appl Biomech. 1996; 12(1)
[2] Pavailler et al. Front Sports Act Living. 2020; 2.
[3] Sandbakk & Holmberg. IJSPP. 2014; 9(1)
[4] Stöggl et al. Scand J Med Sci Sports. 2011; 21(6)
[5] Chen & Chou. Gait & Posture. 2010; 31(3)

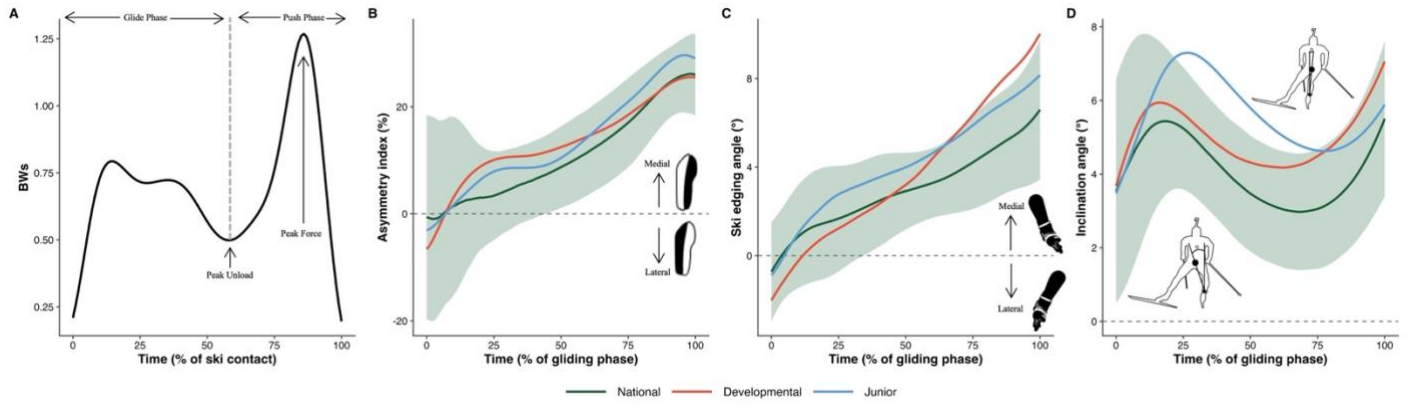

Figure 1. Kinetic and kinematic profiles during the gliding phase across three performance levels (A) Normalized vertical ground reaction force expressed in body weights (BWs) [4]. (B) Asymmetry index (%) throughout the glide. (C) Ski edging angle (°) and (D) CoM inclination angle (°). Solid lines represent group means, and the shaded region illustrates the 1-SD confidence interval for the National group.

An Explainable Automated Deep Learning Framework for Biomechanical Time-series Analysis and User Education

Mojtaba Mohasel[1], Corey A. Pew[1]
Email:*Corey.Pew@montana.edu

Introduction

The adoption of deep learning (DL) in biomechanics is often hindered by the "black-box" nature of automated tools and the specialized knowledge required for temporal data preprocessing. While Automated Deep Learning (AutoDL) can simplify model development, existing frameworks often lack domain-specific features like sliding window optimization and fail to educate the user on the underlying decision-making process [1]. This study introduces *xAutoGA* (Explainable AutoDL based on Genetic Algorithms), a software designed to bridge the gap between high-performance automation and user education. The primary goal is to empower non-expert researchers by providing an interpretable, end-to-end pipeline that explains *how* and *why* specific model hyperparameters are selected.

Methods

The xAutoGA framework was developed as a Python-based application using Keras and TensorFlow. It automates a multi-stage pipeline: subject-wise data splitting, joint optimization of sliding window parameters, and Neural Architecture Search (NAS) across time and frequency domains. A Genetic Algorithm (GA) serves as the optimization engine, evolving a population of 50 models over 30 generations to maximize F1-scores while addressing class imbalance common in movement disorder datasets [2].

The educational component is integrated through a multi-tiered explainability approach. First, the software employs a natural selection analogy to visualize the optimization trajectory. Similar to the evolution of giraffe neck lengths, users can observe "gene domination" plots where superior hyperparameters (e.g., specific batch sizes or window lengths) gradually outcompete less fit configurations. Second, a rule-extraction method identifies deterministic if-then patterns that contribute to top-performing models. Finally, a locally deployed Large Language Model (LLM), Qwen3-4B, synthesizes these rules and dataset characteristics into human-readable educational insights, providing contextual rationales for model choices (Figure 1).

The software's usability and educational value were evaluated through a survey of 19 university students and two machine learning experts. Participants used a 5-point Likert scale to rate trust and effectiveness and completed the System Usability Scale (SUS) [3].

Results and Discussion

Statistical benchmarks against existing tools (McFly) demonstrated that xAutoGA achieved superior performance on three out of five public biomechanical datasets ($p < 0.05$) (Figure 2). Specifically, on the AReM and WISDM datasets, the automated optimization of window size and dual-stream architectures led to significantly higher macro-averaged F1-scores.

Regarding the educational aspect, 73% of survey participants reported that the natural selection visualization "very much" or "completely" increased their trust in the AutoML process. The gene domination plots (Figure 1) were identified as the most intuitive feature, helping users understand how the population converged toward an optimal 64-sample batch size. Qualitative feedback from the "think-aloud" protocol indicated that the LLM-generated rationales successfully translated abstract machine rules into actionable design principles. However, some users noted a steep initial learning curve, reflected in the SUS scores, suggesting a need for more interactive onboarding tutorials in future iterations.

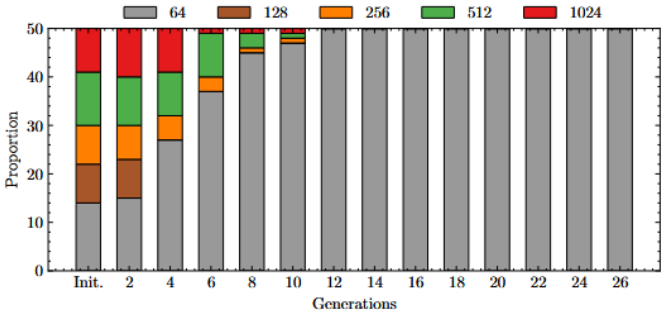

Figure 1: *Gene domination plot. The x-axis represents generations, starting from the initialization phase (Init.), while the y-axis shows the proportion of batch sizes. The population consists of 50trained neural networks with different batch sizes, with colors representing their proportions in the population*

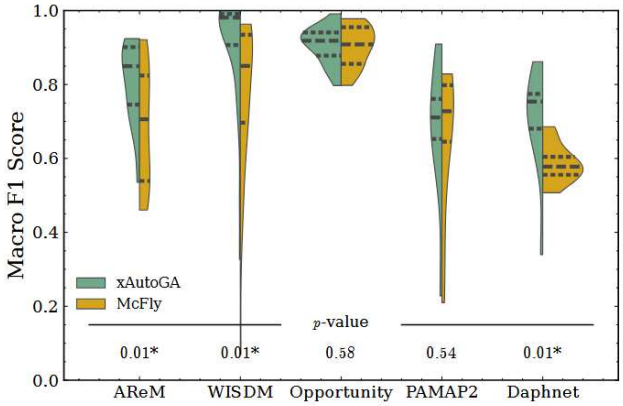

Figure 2: *Comparison of F1-score performance between AutoML systems across five datasets.*

Conclusions

xAutoGA demonstrates that AutoDL can be transformed from an opaque optimization tool into a transparent educational asset. By combining GA-based optimization with LLM-driven explanations, the software enables biomechanics researchers to develop high-performance models while simultaneously gaining a deeper understanding of deep learning fundamentals.

Acknowledgements

Computational efforts were performed on the Tempest HPC at Montana State University.

References

[1] Dong X, et al. Foundations and Trends in ML, 17(5), 767-920, 2024. [2] Halilaj E, et al. Journal of Biomechanics, 81, 1-11, 2018. [3] Brooke J. Usability Evaluation in Industry, 189-194, 1996.